

DOKTORI (PhD) ÉRTEKEZÉS

SPATIO-TEMPORAL ANALYSIS OF VEGETATION
HABITATS IN RIPARIAN WETLANDS
(HULLÁMTÉRI VIZES ÉLŐHELYEK VEGETÁCIÓJÁNAK
TÉRBELI ÉS IDŐBELI VIZSGÁLATA)

Kollár Szilvia

Nyugat-magyarországi Egyetem (Sopron)
Erdőmérnöki Kar
Kitaibel Pál Környezettudományi Doktori Iskola
K4 Geoinformatikai Program

Témavezetők:

Dr.Vekerdy Zoltán
Faculty of Geo-Information Science and Earth Observation
University of Twente, Enschede, Hollandia

Prof.Dr.habil Márkus Béla
Nyugat-magyarországi Egyetem
Geoinformatikai Kar, Székesfehérvár

Sopron
2014

SPATIO-TEMPORAL ANALYSIS OF VEGETATION HABITATS
IN RIPARIAN WETLANDS
(HULLÁMTÉRI VIZES ÉLŐHELYEK VEGETÁCIÓJÁNAK
TÉRBELI ÉS IDŐBELI VIZSGÁLATA)

című értekezés doktori (PhD) fokozat elnyerése érdekében készült
a Nyugat-magyarországi Egyetem Kitaibel Pál Környezettudományi Doktori Iskolája
K4 Geoinformatikai Programja keretében.

Írta: Kollár Szilvia

Témavezetők:

Dr.Vekerdy Zoltán

Elfogadásra javaslom (igen / nem)

(aláírás)

Prof.Dr.habil Márkus Béla

Elfogadásra javaslom (igen / nem)

(aláírás)

A jelölt a doktori szigorlaton%-ot ért el.

Sopron,

a Szigorlati Bizottság elnöke

Az értekezést bírálóként elfogadásra javaslom (igen / nem)

Első bíráló (Dr.) igen / nem

(aláírás)

Második bíráló (Dr.) igen / nem

(aláírás)

Esetleg harmadik bíráló (Dr.) igen / nem

(aláírás)

A jelölt az értekezés nyilvános vitáján%-ot ért el.

Sopron,

a Bírálóbizottság elnöke

A doktori (PhD) oklevél minősítése

Az EDT elnöke

“Blessed be the LORD God, Who alone works wonders.”

Psalms 72:18

Abstract / Kivonat

The dissertation demonstrates automated image classification techniques applied to recent high resolution (<5 m/pixel) aerial imagery for vegetation classification purposes. It was proved based on a riparian wetland site for different years that the application of a combined spectral-textural feature set in the supervised class description based fuzzy algorithm significantly enhances the classification performance compared to the use of spectral or textural features only. The best classification results gave 87-88% overall accuracies with a simple and an extended classification scheme, defined after botanical and silvicultural reference data. Furthermore, classification algorithm transfer was considered for automated applications in space and time. It was proved that the automated mapping of poplar stands is feasible by transferred decision tree classification approach, under those conditions that the samples selected in the training site only include the hybrid poplar forest stand type. By systematic Jeffries-Matusita class separability analysis, the GLCM (Grey Level Co-occurrence Matrix) standard deviation (STDEV) was found as a significant and stable textural parameter for the analysis of vegetation pattern differences in colour-infrared aerial images. For the most recent CIR imagery it was proved that a decision tree classifier with GLCM STDEV and vegetation index applied to the separation of high and low vegetation, is automatically transferable to former CIR images. Based on the supervised classification of NIR-R-G images GLCM STDEV was found as a single descriptor without the use of vegetation index for the detection of high and low vegetation. Decision tree transferability was proved for further classification automation in space and time, with the above mentioned generalized classification scheme applied to the separation of forested and non-forested wetlands. These classification methods help in the effective processing of large aerial image archives and their application is proposed for silvicultural and botanical inventories.

A disszertáció témája nagy felbontású (<5 m/pixel) légifelvételekre alkalmazott automatikus képosztályozási eljárások kidolgozása vegetációtérképezés céljából. A szerző hullámtéri tesztterület különböző időpontból származó felvételeire bebizonyította, hogy az osztályjellemzésen alapuló (class description based) fuzzy algoritmus mint tanítóterületekkel végzett objektum alapú osztályozás akkor adja a legjobb vegetációosztályozási eredményt, ha az osztályozó bemeneti paramétereinek spektrális és texturális jellemzőket is tartalmaznak, ellentétben a kizárólag spektrális vagy texturális paraméterek alkalmazásával. A legjobb osztályozási eredmények 87-88%-os átlagos megbízhatóságot eredményeztek egy botanikai és erdészeti adatokon alapuló egyszerű és kibővített osztályozási rendszerrel. A szerző vizsgálta az osztályozási algoritmus térbeli és időbeli átvitelét. Bebizonyította, hogy a nyáras osztály automatikusan térképezhető a döntési fa képosztályozó átvitelével azon feltételek mellett, hogy a tanítóképen kiválasztott minták első faállományának típusa kizárólag nemes nyáras lehet. A szerző szisztematikus Jeffries-Matusita elválaszthatósági elemzés alkalmazásával kimutatta, hogy a GLCM (Grey Level Co-occurrence Matrix) szórás (standard deviation, STDEV) jellemzője szignifikáns és stabil paraméter a vegetációs mintázatok változásának elemzésére infraszínes légifelvételeken. Az elérhető legújabb CIR felvételekre létezik olyan döntési fa képosztályozó algoritmus GLCM STDEV és vegetációs index felhasználásával alacsony és magas vegetáció elkülönítésére, mely a mintaképen való tesztelést követően automatikusan alkalmazható korábbi infraszínes légifotókra. NIR-R-G spektrális felbontású felvétel tanítóterületekkel való osztályozása alapján a szerző bebizonyította a GLCM STDEV paraméter kizárólagos alkalmazhatóságát a vegetációs index nélkül, alacsony és magas vegetáció szétválasztására. Az osztályozás további automatizálására vonatkozóan bizonyításra került, hogy adott tesztképre kidolgozott döntési fa képosztályozó térben és időben egyaránt átvihető, a fent említett generalizált osztályozási rendszerrel, erdős és nem erdős hullámtér automatikus elkülönítésére. Ezen módszerek alapján nagy méretű légifelvétel-adatbázisok hatékony és gyors feldolgozása lehetővé válik, melynek botanikai és erdészeti alkalmazása nagy jelentőséggel bír.

Acknowledgements

First of all, I would like to thank for the great support of my supervisors over the past five and a half years. Dr.Zoltán Vekerdy, assistant professor at the Department of Water Resources, ITC (Faculty of Geo-Information Science and Earth Observation, University of Twente, Enschede, the Netherlands), honorary associate professor at the Department of Geoinformation Science, Faculty of Geoinformatics, University of West Hungary (Székesfehérvár) and visiting professor at the Department of Water and Waste Management, Faculty of Agricultural and Environmental Sciences, Szent István University (Gödöllő, Hungary) who has been my second father in that period believing in my research often more than me and his continuous encouragement helped me going through difficult periods. Prof.Dr.habil Béla Márkus, the head of the Land and GI Knowledge Center and professor at the Department of Geoinformation Science, Faculty of Geoinformatics, University of West Hungary who has supported me from the very first beginning with my application for the PhD grant at the University of West Hungary and for a 3-month research stay at the Department of Geoinformatics in the University of Salzburg.

I wish to express my sincerely gratitude to the University of West Hungary, Faculty of Forestry (Sopron, Hungary) for the provided PhD grant between 2008–2011 and my special thanks to all the staff members of the Faculty of Geoinformatics (Székesfehérvár) and specially to my colleagues at the Department of Geoinformation Science and at the Department of Photogrammetry and Remote Sensing, where I have done the main part of my research in a caring and supporting environment. I am grateful to the “Central European Exchange Program for University Studies” (CEEPUS) providing me a research grant for three months at the Department of Geoinformatics in the University of Salzburg, where I focused on the application of advanced remote sensing methods (including object-based image analysis), which became the backbone of my further investigations. I convey my thanks to Dr.László Martinovich who helped me organising a short research (3 months) at the Institute of Geodesy, Cartography and Remote Sensing (FÖMI, Budapest) in 2009. I highly appreciate the support of Trimble Geospatial Munich (Germany) for providing me the eCognition Developer software for my research, after I spent a fruitful internship period at the company in 2010. Concerning my shorter stays (3-14 days) in Enschede for research discussions with my supervisor, I am specially grateful to Marcsi Vekerdy, the wonderful wife of my supervisor, who has been always so caring and hospitable at their house, and thus, during my work at the Technical University of Dortmund a small “Hungarian island” was not so far from me geographically.

I also thank to the Fertő-Hanság National Park (Gábor Takács) in Sarród and to the Forestry Directorate (Judit Péter) in Szombathely (Hungary) for giving me access to the botanical

and silvicultural data, and to István Hahn (Eötvös Loránd University, Department of Plant Taxonomy and Ecology, Budapest) for his guidance during the field investigations and for his support regarding the botanical aspects of the study.

As a research staff member at the Department of RIM (Spatial Data Analysis) at the Faculty of Spatial Planning, in the Technical University of Dortmund (Germany) since 2012, I would like to express my sincere thanks to the Head of the Department, Univ.-Prof.Dr.habil Nguyen Xuan Tinh for his support and understanding especially concerning the most intensive periods of finishing the dissertation.

I am so grateful for my family, parents, two sisters and brother, my grandparents and friends geographically close and far and my loved husband, who believed in me and gave encouragement always.

Contents

Abstract / Kivonat	iii
Acknowledgements	v
Contents	vii
List of Figures	x
List of Tables	xii
Abbreviations	xiii
1 Introduction	1
1.1 General introduction	1
1.2 Aims & structure of the research	3
2 Riparian vegetation mapping based on remote sensing: a review	4
2.1 Wetlands and vegetation mapping	4
2.2 The remote sensing perspective	5
2.3 Analysis of high spatial resolution optical imagery	6
2.3.1 Availability of imagery	6
2.3.2 Applications	8
2.3.3 Spectral characterization of images	9
2.3.4 Visual image interpretation	10
2.3.5 Pixel- versus object-based image analysis	11
3 Materials	15
3.1 Study area	15
3.1.1 Effects of hydrological changes on the vegetation	16
3.1.2 Botanical mapping	18
3.1.3 Remote sensing analysis	20
3.2 Applied imagery	21
3.3 Botanical and silvicultural maps	22
4 Methods	24
4.1 Image segmentation	24
4.2 Spectral characterization	25
4.3 Geostatistical characterization	26
4.3.1 Texture analysis based on GLCM	27

4.3.2	The semivariogram	30
4.4	Class separability analysis	31
4.5	Supervised classification algorithms	33
4.5.1	Class description based fuzzy (CDBF) algorithm	34
4.5.2	Decision tree classification	36
4.6	Accuracy assessment	38
5	Spectral-textural classification	41
5.1	Sample application to the study site of Dunaremete	41
5.1.1	Separation of water bodies	44
5.1.2	Classifying vegetation	46
5.1.3	Application of geostatistics	48
5.1.4	Feature selection	50
5.1.5	Classification algorithm	51
5.1.6	Results	52
5.1.7	Discussion	54
5.2	Classification scheme	56
5.2.1	Extending the classification scheme	57
5.2.2	Result & discussion	59
6	Classification transferability	61
6.1	Necessity for an objective approach	62
6.2	Classification transferability in the spatial dimension	62
6.2.1	Adequacy of the principal test site	63
6.2.2	Applied classification scheme	63
6.2.3	Expected results	65
6.2.4	Difficulties with the CDBF classification algorithm	66
6.2.5	Decision tree approach	68
6.2.5.1	Application to the main test site	68
6.2.5.2	Analysis of classification algorithm transfer	70
6.2.6	Results and discussion	73
6.3	Classification transferability in the temporal dimension	78
6.3.1	Separation of water bodies	79
6.3.2	Transfer of classification algorithms	80
6.3.3	Class separability analysis	82
6.3.3.1	Detecting a stable parameter for temporal vegetation analysis	83
6.3.3.2	Detecting vegetation with structural differences	86
6.3.4	Transferring a generalized classification scheme	87
6.3.5	Results	90
6.4	Spatio-temporal classification transferability	91
7	Summary	94
8	Conclusions & future research	96
8.1	Conclusions	96
8.2	Future research	97
9	Theses	99

A Aerial Images (1999-2008)	101
B Ancillary Data	103
C Feature separability analysis	106
Bibliography	110

List of Figures

2.1	Reflectance curve of vegetation	10
2.2	Comparison of pixel- and object-based approaches	14
3.1	Map of the Szigetköz Danubian floodplain	17
3.2	Willow and poplar forests in the Szigetköz	18
3.3	Test sites in the Szigetköz	21
4.1	Semivariogram	30
4.2	Problem of class separability	32
4.3	Example for class description	35
4.4	Example for membership function	35
4.5	Example for a decision tree	37
5.1	The study site of Dunaremete (DR)	42
5.2	Analysis steps applied to DR test site	43
5.3	Segmentation and classification of water bodies (DR,2008)	45
5.5	Willow species in the test site of Dunaremete (2010)	47
5.4	Hybrid poplar stand in the Szigetköz (2010)	47
5.6	Target vegetation classes by square segments from 2008	48
5.7	Semivariogram analysis of vegetation classes in 2008	49
5.8	Classification results with the simple classification scheme for DR site (2008-1999)	54
5.9	Comparing chessboard and multi-resolution segments	55
5.10	Hierarchical classification scheme applied to image DR, 2008	58
5.11	Classification with the complemented scheme for DR, 2008	59
6.1	A unique classification scheme for the test sites of DK, DR and ASV in 2008, based on separate classification results	64
6.2	Transferred CDBF classification algorithm to DK, 2008	67
6.3	Comparison of classification results applying CDBF and DT algorithms to DR, 2008	69
6.4	Structure of the decision tree regarding the extended classification scheme for DR, 2008	70
6.5	Methods applied for the analysis of decision tree transfer	71
6.6	Classification result after transferring DT algorithm to the scene of DK, 2008	72
6.7	Decision tree computed from DK, 2008	75
6.8	Transferring decision tree from DK to DR and ASV	76
6.9	Modified decision tree based on DK (2008) focusing on the separation of HP	78

6.10	Class description of water bodies applied to the 2008 and 1999 image scene (DR)	79
6.11	Classification results after transferring CDBF and DT algorithms to the former (1999) scene of DR	80
6.12	Structure of the decision tree with the simple classification scheme, DR, 2008	81
6.13	Stable parameter assessment	84
6.14	DT1 structure for the separation of HV and LV based on DR(2008)	88
6.15	DT2 structure for the separation of HV and LV based on DR(2008)	89
6.16	Comparison of DT-based classification results with a generalized classification scheme for DR (2008,1999)	90
6.17	Transferred DT-based classification results with a generalized classification scheme for DK (2008)	93
A.1	Orthophoto 1999, DR	101
A.2	Orthophoto 2005, DR	102
A.3	Orthophoto 2008, DR	102
B.1	Botanical habitat map	103
B.2	Subsets of habitat maps for DR test site	104
B.3	Silvicultural data (Forest Stand Type) about the test sites	105

List of Tables

3.1	Detailed information on the applied imagery	22
4.1	The most important textural parameters of GLCM and GLDV	29
5.1	Comparing textures for different geometric resolutions	44
5.2	Vegetation indices applied to aerial images (2008,2005,1999)	45
5.3	Statistical separability analysis for the originally chosen target vegetation classes in DR, 2008	51
5.4	Accuracy assessment of the first classification results (DR, 2008-1999)	52
5.5	Error matrix for DR, 2008 (best classification result)	53
5.6	Comparing results from different segmentation approaches based on accuracy calculation.	55
5.7	Class separability analysis by the merge of certain vegetation classes	56
5.8	Comparison of accuracy measures concerning the use of different VIs for DR, 2008	60
6.1	Comparison of two-level classification scheme for the 3 test sites	65
6.2	Comparing accuracy measures related to CDBF and DT classification algorithms, DR, 2008	68
6.3	Error matrix for the result of transferred decision tree for DK, 2008	73
6.4	Accuracy measures for HP class based on different DT transfers	77
6.5	Accuracy comparison for the 3 test sites based on the modified DT	77
6.6	Accuracy of Low vegetation classification in DT-transfer	81
6.7	Separability analysis for class-pairs with Reed (DR, 1999, 2008)	84
6.8	Similarity test for Reed (1999-2008) by class separability analysis in DR site.	85
6.9	Separability test for Reed (2008) and other vegetation classes (1999) by class separability analysis in DR site.	86
6.10	Separability analysis for class pairs with HP (DR, 1999, 2008)	86
6.11	Separability test of Willow (2008) and other vegetation classes (1999) by class separability analysis in DR site.	87
6.12	Separability test of Willow & poplar (2008) and other vegetation classes (1999) by class separability analysis in DR site.	87
6.13	Accuracies for spatio-temporal transferability	92
C.1	Feature separability analysis for DR, 1999	107
C.2	Feature separability analysis for DR, 2005	108
C.3	Feature separability analysis for DR, 2008	109

Abbreviations

Á-NÉR	<i>Hu.</i> Á ltalános N emzeti É lőhelyosztályozási R endszer
ASV	Á sványráló test site
B	B lue band
BlueNDVI	B lue N ormalized D ifference V egetation I ndex
BSG	B are S oil mixed with G rass
CDBF	C lass D escription B ased F uzzy (algorithm)
DK	D unakiliti test site
DN	D igital n umbers (radiometric values)
DP	D omestic P oplar
DP-R	D omestic P oplar- R obinia
DR	D unaremete test site
DT	D ecision T ree (classification algorithm)
FAFK	<i>Hu.</i> F afaj kód (code of tree species)
FATI1	<i>Hu.</i> Az 1. faállomány típus kódja (forest stand type)
FÖMI	F öldmérési és Távérzékelési I ntézet (<i>En.</i> Institute of Geodesy, Cartography and Remote Sensing, Budapest)
FST	F orest S tand T ype
G	G reen band
GLCM	G rey L evel C o-occurrence M atrix
GLDV	G rey L evel D ifference V ector
GreenNDVI	G reen N ormalized D ifference V egetation I ndex
HP	H ybrid P oplar
HR	H igh resolution
HV	H igh V egetation
JM	J effries- M atusita (statistical separability analysis)

LV	L ow V egetation
mNDVI	m odified N ormalized D ifference V egetation I ndex
MR	M ulti- r esolution
MS	M ultispectral
NDVI	N ormalized D ifference V egetation I ndex
NFI	N ational F orest I nventry
NIR	N ear i nfrared band
OA	O verall a ccuracy
OBIA	O bject- B ased I mage A nalysis
PC1	The first p incipal c omponent
R	R ed band
RD	R ee D
RS	R emote sensing
UWH	U niversity of W est H ungary
VED	V egetation on E dges and D ams
VHR	V ery h igh resolution
W	W illow
WP	W illow & P oplar

Chapter 1

Introduction

1.1 General introduction

Over the past 50 years, the rapid and extensive change of ecosystems induced a significant decrease in the biological diversity (MEA, 2005) and in this regard the sixth great extinction wave is already occurring in the Earth's biota (Mendenhall et al., 2012). Therefore, in the European Union the "EU 2020 biodiversity strategy" has been developed related to the European Habitats and Birds Directive, in order to halt the loss of biodiversity and ecosystem services in the EU by 2020 (European Commission, 2011). Besides a policy framework, an appropriate technology is needed for the monitoring of ecosystems, where remote sensing methods are representing objective and time-effective techniques for the continuous observation of ecosystems from above (Lang et al., 2013). Beyond satellite imagery, archive aerial photography provides the basis for the historical characterization of the variability within ecosystems as well as for strategy development related to the management of ecological integrity (Landres et al., 1999).

Wetland ecosystems are among the most productive ecosystems in the world, but they have reached a vulnerable status, wherefore a conservation and sustainable development strategy has been formulated in the Ramsar Convention on Wetlands (1971) (Maltby and Barker, 2009). The main drivers of the degradation and loss of inland wetlands are infrastructure development (such as dams, dikes and levees), land conversion, water withdrawals, pollution, overharvesting and the introduction of invasive alien species. Furthermore, it has been

projected, that global climate change and nutrient loading have become an important factor for the next 50 years (MEA, 2005).

Detailed monitoring of riparian floodplains is vital for an effective restoration management, which requires large scale inventory, often carried out by traditional systematic field surveys. However, traditional field observation cannot provide a synoptic and systematic overview about recent changes because of its limitations in space and time. Under extreme flooding conditions it could be often impossible to carry out field investigations in a certain time frame. Beyond that, due to high personal costs and possible inconsistencies in the experiences of different surveyors, the application of remotely sensed images with high geometric resolution came in the focus of interest. Aerial photo archives contain images from earlier periods than the first satellite images, providing a challenging opportunity for analysing vegetation habitat changes over several decades.

Visual interpretation of aerial photography has been extensively applied for decades for fine-scale vegetation habitat mapping and forest inventories (Morgan et al., 2010). Since an ever increasing amount of remote sensing data is being produced nowadays in a broad range of spatial, spectral, radiometric and temporal resolutions, automated information extraction methods came into the focus of interest, which can also compete with the subjective nature of human interpretation. With the increasing computation power in the recent years, automated approaches have gone through a rapid development and can provide objective analysis methods for larger areas.

In the analysis of high spatial resolution (under 5 m/pixel) imagery traditional pixel-based image classification methods often fail due to the wide range of spectral responses related to certain target classes, e.g., a given forest stand in a complex riparian vegetation environment. A potential solution is applying object-based (segmentation-based) image analysis (OBIA) methods, where, instead of individual pixels, image segments as group of pixels become the focus of the image analysis and the classification.

Beyond the automated analysis of separate image scenes, a harmonized automation in the spatial and temporal domain is essential when large areas are covered by time series of several images (e.g., aerial photos).

1.2 Aims & structure of the research

Based on the above-described problems, the present research is aiming at developing a vegetation habitat mapping method based on high spatial resolution aerial imagery, using automated digital image analysis techniques.

In the *first step* an automated classification method is to be found for an appropriate separation of vegetation habitat classes, based on a selected test site in the Szigetköz floodplain, using aerial images from the recent years.

The *second step* is to extend the vegetation habitat classification method developed for one image to other areas in the same riparian wetland.

In the *third step* an appropriate analysis and classification method is sought for the detection of similar vegetation habitats in distinct years, concentrating on a selected test site.

The *fourth step* is related to the spatio-temporal transferability of the classification, where it is aimed at finding a universal classification algorithm to automatically classify forested and non-forested wetlands based on a principal training site (image scene), where the algorithm is applicable to aerial images scenes covering the same wetland and having the same spatial resolution, but potentially coming from different times.

In the main chapters of the dissertation firstly wetland and vegetation mapping is described briefly, followed by fine-scale riparian vegetation mapping techniques using remote sensing (Chapter 2). Chapter 3 addresses the study area and the data used in the analysis. Chapter 4 describes the applied methods in detail. The applications of the methods, their further development and the scientific findings are demonstrated in Chapter 5 and Chapter 6. The closing chapters are Chapter 7 with the summary, Chapter 8 with conclusions and future prospects and in the end scientific results (theses) are presented (Chapter 9).

Chapter 2

Riparian vegetation mapping based on remote sensing: a review

2.1 Wetlands and vegetation mapping

Wetlands have been listed among the world's most productive ecosystems ([Maltby and Barker, 2009](#)). Out of them floodplain environments in their natural state are of particular importance due to their high biodiversity providing critical habitats for many plants and animals and further on being a natural element in the maintenance of water quality ([Andersen, 2004](#)). During the last decades wetlands have become the most vulnerable ecosystems. An intergovernmental treaty called Ramsar Convention on Wetlands (1971) is aiming at the wise use of wetlands by improving their management and developing a comprehensive information base on the status and trends of wetlands, their values and the major drivers of adverse change ([Maltby and Barker, 2009](#)).

Since vegetation in general provides a base for all living beings and plays an essential role in affecting global climate change, with an influence on terrestrial CO₂ by the net ecosystem exchange of CO₂ between the atmosphere and forest ecosystems ([Xiao et al., 2004](#)), its classification and mapping has been an important task for managing natural resources ([Xie et al., 2008](#)). Analysing vegetation structure is important for the characterization of wildlife habitat quality, where animal species both within and among habitats are partitioned according to the vegetation composition ([Wood et al., 2012](#)). Changes in vegetation are evidence of

environmental impacts which are important for the functioning of the ecosystem and for biodiversity maintenance (Ihse, 2007).

Vegetation and land cover maps for a certain reference time or over a continuous period at different scales are essential instruments for the global climate modelling and for ecological and biodiversity studies (Millington and Alexander, 2000) and provide valuable information for understanding natural and man-made environments (Xie et al., 2008). Obtaining current states of vegetation is essential for the planning of vegetation (habitat) protection and restoration. Millington and Alexander (2000) summarized the need for vegetation maps in two crucial points: firstly to communicate a complex set of information about vegetation in a simplified and spatially referenced form, secondly to provide spatially referenced numerical data about vegetation that can be used for analyses.

2.2 The remote sensing perspective

Traditional methods for vegetation analysis, like field surveys, map interpretation and ancillary data analysis are often not effective enough, since they are time consuming, often provide information about lagged dates and have high expenses (Xie et al., 2008). Although ground based field monitoring can provide highly detailed information about the vegetation cover, it is very time intensive and could be only feasible over small spatial extents (Levick and Rogers, 2008). Davidson and Finlayson (2007) emphasized the essential role of Earth observation (remote sensing) techniques adopted by the Ramsar Convention on Wetlands for the inventory, assessment, monitoring and management of wetland ecosystems at widely differing spatial scales.

Remote sensing is a promising analysis method where the Earth surface is sensed from above, without touching or accessing it. Remote sensing can provide the basis for vegetation classifications in different ground spatial resolutions from global (e.g., for climate and biogeochemical models) through regional scale (e.g., for habitat mapping or watershed modelling) to species level. Spatial scale or resolution, commonly referred to as ‘pixel size’ in digital images, is a key element of remote sensing. At the global and continental scales the 1-km-spatial resolution has been commonly applied, e.g., based on AVHRR (Advanced Very High Resolution Radiometer) (Running et al., 1995), SPOT4-VEGETATION (SPOT, French: *Satellite Pour l’Observation de la Terre*) or MODIS (Moderate Resolution Imaging

Spectroradiometer) satellite imagery (Xie et al., 2008). Medium ground spatial resolution about 30 m/pixel e.g., in case of the Landsat-system, is suitable for regional satellite mapping, applied for instance to biodiversity assessment and conservation planning in the study of Fuller et al. (1998). In the study of Ozesmi and Bauer (2002) remote sensing techniques are applied for different types of wetlands from global (AVHRR, 1 km/pixel) to medium scale (SPOT, 20 m/pixel) and concluded that satellite-based remote sensing is especially appropriate for initial reconnaissance mapping and continued monitoring of wetlands over large geographical areas. General information on water regime and vegetation productivity can be well-detected, however, they cannot provide the detailed information available from high geometric resolution imagery included aerial photography. Several studies (e.g., Yu et al., 2006; Johansen et al., 2007) emphasized the advantage of using high spatial resolution remote sensing images for the analysis of riparian zones with restoration purposes due to a decrease in valuable ecological functions (e.g., vegetation structure) provided by riparian forests to streams (Gergel et al., 2007). This kind of imagery is described in detail in the next section.

The analysis of remotely sensed imagery brings another perspective to vegetation studies, by means of being capable of detecting patterns at different spatial scales which may not be obvious from the ground and this kind of analysis helps in the characterization of ecosystems in larger spatial extents. Beyond that, a great advantage of remotely sensed data is the potential for systematic observations at various scales through the extension of possible data archives from present time to over several decades back (Xie et al., 2008).

2.3 Analysis of high spatial resolution optical imagery

2.3.1 Availability of imagery

Satellite and aerial images in various spatial scales are able to capture the spectral reflectance of different land cover types in distinct wavelength intervals of the electromagnetic spectrum. The optical wavelength interval originally means the range between 400 nm (violet) to 2500 nm (shortwave infrared) (Lefsky and Cohen, 2003), however, in the current study we have been concentrating on the interval between 450 nm and 900 nm including blue, green, red and near-infrared bands, discussed commonly in multispectral remote sensing applications.

Although medium resolution satellite imagery (e.g., Landsat with 30 m/pixel) have been effective in mapping seasonal characteristics of the vegetation for larger extents since 1972, their spatial resolution has been too low for the analysis of those riparian units which can vary in composition and form below that scale (Davis et al., 2002).

In Lefsky and Cohen (2003) analogue aerial photography has been stated as the oldest, most frequently used and best understood form of remote sensing. For mapping small ecosystems, fine-scale landscape features and successional pathways aerial imagery has proved to be effective due to the often present high spatial resolution, radiometric (tonal) detail and historic availability, dating already from the early 1930s in some cases (Green and Hartley, 2000; Morgan et al., 2010). With higher ground spatial resolutions, often less than 1 m/pixel, and with slowly declining costs the use of airborne sensors is reasonable for the improvement of vegetation mapping accuracies (Davis et al., 2002). The spatial scale for airphotos is a function of camera focal length and aircraft flying altitude and also depends on the film's halide crystal grain size, where a moderate resolution photo would have a 1:12000 scale, equivalent to a spatial resolution of about 0.4 m (Lefsky and Cohen, 2003) and hereby, provides very high resolution (VHR) imagery, under 1 m/pixel.

For the digitalisation of hard-copy photographs it is suggested to use a pixel size which is approximately 20% of the output size of the object of interest (Hall, 2003) which is followed by orthophoto-production with an appropriate rectification process. Considering digital aerial photographs directly obtained from digital cameras, a single CCD (charge-coupled device) sensor with mosaic optical filtering and near-infrared airborne camera systems can produce images at very high spatial resolutions (under 0.25 m/pixel) (Wulder et al., 2004).

Beyond analogue and digital aerial photography, the increasing availability of commercially operated high spatial resolution (defined as under 5 m/pixel in Johansen et al., 2010a; Blaschke et al., 2011) multispectral satellite imagery (e.g., IKONOS with ~ 3.28 m/pixel from 1999; QuickBird with ~ 2.44 m/pixel from 2001; GeoEye-1 with 1.65 m/pixel from 2008; WorldView-2 with ~ 1.84 m/pixel from 2009) vegetation mapping and monitoring can operationally develop focusing on narrow riparian zones and certain stand parameters such as height, age and foliage projective cover (Blaschke et al., 2011). It is essential that in case of satellite-borne high-resolution sensors the collection of data is ensured from a stable platform, at regular time intervals, with a relatively large footprint size (Wulder et al., 2004).

2.3.2 Applications

Numerous studies analysed high resolution imagery for conservation and restoration planning issues. In the European Union it often means the monitoring of Natura 2000 territories as part of an effective assessment of biodiversity. Natura 2000 is a European Directive, which was designed to ensure the conservation of the most seriously threatened habitats and species covering almost 20% of the EU territory. In the context of Natura 2000 and nature conservation the so-called SPIN project (“Spatial Indicators for European Nature Conservation”) emphasized the advantage of applying high resolution stereo camera airborne scanner data in a German case study for the classification of phytosociological communities (Bock et al., 2005). In the study of Förster and Kleinschmit (2008) forest types have been delineated at three different levels (forest habitats, crown combinations, crown types of single-tree species) based on a QuickBird scene of the Bavarian submontane area, where the forest habitat level was similar in size to the terrestrially mapped Natura 2000 areas. Langanke et al. (2007) aimed at assessing the mire conservation status of a raised bog in Austria as a single Natura 2000 site and analysed different types of aerial photographs (black & white, colour infrared and true colour) dating back to 1953 (regarding the oldest airphoto) with two interpretation techniques: a standard aerial photo-interpretation and a multi-scale object-based classification, which are described in detail in the next sections. A comprehensive review on colour infrared (CIR) aerial photography concerning several decades of vegetation mapping in Sweden emphasized the significance of CIR aerial imagery as a fundamental tool in nature conservation and environmental planning (Ihse, 2007). Outside Europe Gergel et al. (2007) have mapped harvested and intact forests for riparian restoration planning in coastal British Columbia, Canada at different spatial resolutions and found a significantly better classification performance using high geometric resolution.

Beyond the general vegetation mapping methods with restoration purposes, the application of high spatial resolution imagery has been essential for the assessment of forest resources, concerning forest structure analysis and the measurements of forest biophysical data (e.g., LAI, leaf area index, above-ground biomass and NPP, net primary production) (Wulder et al., 2004). Research studies related to the HR multispectral imagery based estimation of forest structure listed the forest structural parameters. Franklin et al. (2000) analysed airborne multispectral video images and airborne spectrographic images (the highest resolution was 0.3 m) for the classification of pure and mixed-wood forest stands from ecoregions

in Alberta and New Brunswick, Canada and proved the advantages of using images with high spatial resolution. The analysis of digitized CIR aerial photographs at 0.5 m/pixel resolution provided promising results for forest attribute estimation in the study of a boreal forest in southern Finland (Tuominen and Pekkarinen, 2005). Hájek (2008) applied medium-format digital aerial images (resampled to 0.5 m) for the purpose of automated updating of an existing GIS forest management database in southern Moravia, Czech Republic and highlighted the significance of CIR aerial images as an alternative to traditional aerial photos and HR satellite data. Concerning the analysis of high resolution satellite imagery, Wezyk et al. (2004) applied QuickBird imagery for the mapping of forest canopies in south Poland and presented the potential of classifying the development stage (aging) of the forest stands. Kim et al. (2009) presented the application of IKONOS images to delineate forest types (deciduous, evergreen, mixed) in North Carolina, US and proved that the incorporation of textures (discussed later in Chapter 4.3.1) resulted in a classification agreeable with manually interpreted forest types. In the forest structure study of Kayitakire et al. (2006) the estimation of coniferous forest variables (age, top height, circumference and basal area) in eastern Belgium based on 1-m resolution IKONOS-2 imagery gave promising results for the application in forest planning. For the analysis of similar forest structural parameters Ozdemir and Karnieli (2011) presented the potential of World-View-2 multispectral imagery applied to a dryland plantation forest in Israel. Concerning financial issues Hájek (2008) emphasized, that although the radiometry of the 8-bit/pixel aerial imagery (used in his study) can hardly compete with the 11-bit IKONOS satellite image data (the geometric resolution in the multispectral mode is lower there: 3.28 m/pixel) or with a 12-bit/pixel data from the Digital Mapping Camera (DMC), the cost of analogue images and hereby, the lower primary investment plays an important role in the management of forestry. Although, it is not in the scope of this study, the potential of combining HR (aerial/satellite) imagery with LiDAR (Light Detection and Ranging, also called as laser scanning) data has been emphasized in various research studies recently, where the identification of individual trees (tree crowns) and other forest parameters can be significantly improved (Király and Brolly, 2006; Levick and Rogers, 2008; Morgan et al., 2010; Blaschke et al., 2011).

2.3.3 Spectral characterization of images

Looking back to the history of digital image analysis techniques in remote sensing applications spectral approaches have formed the backbone of multispectral (MS) classification

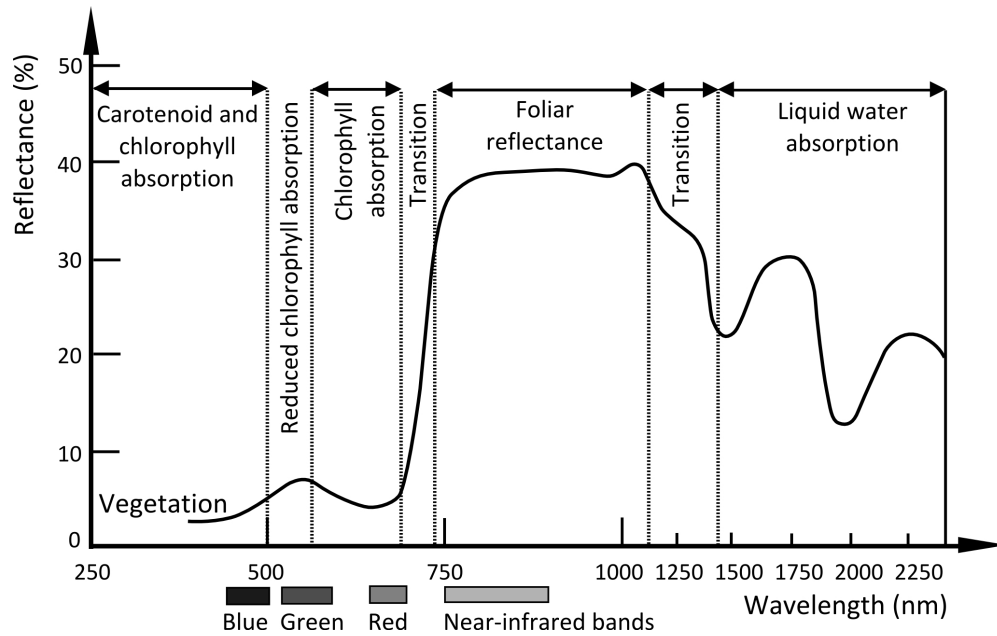


FIGURE 2.1: Reflectance curve of vegetation after [Jensen \(2014\)](#).

methods. According to the spectral resolution of the MS imagery, digital numbers (DN) are captured for different wavelength intervals which are associated with a certain band. In case of analogue aerial photography the available spectral bandwidths depend on the spectral sensitivity of the film, where the normal colour film (now not considering the black & white film with only one panchromatic layer) includes blue (B), green (G) and red (R) sensitive layers, whereas a colour-infrared film has the near-infrared (NIR) layer besides G and R ([Jensen, 2014](#)). The development of colour-IR film is related to World War II, where they were applied to detect painted targets that were camouflaged to look like vegetation ([Lillesand et al., 2008](#)). According to the unique spectral characteristics (high reflectances) of vegetation in the near-infrared region of the spectrum (see in [Figure 2.1](#)) the false colour composite of bands (with NIR,R,G generally) is often applied for visualisation purposes, emphasizing the vitality of the vegetation in reddish colours (see an aerial image example with the B-G-NIR band combination representing a part of the latter analysed test site in [Figure 2.2](#)).

2.3.4 Visual image interpretation

After establishing a relationship between the vegetation structural characteristics and the reflectance (spectral) characteristics of the vegetation, visual image interpretation or image

classification algorithms are used to identify areas with similar reflectance characteristics for the same vegetation structural class (Lymburner, 2005). The traditional analysis of aerial photography has been based on human visual interpretation with manual digitalisation of thematic units complemented with ground truth data from the field inventory, which results in a very time- and labour-intensive approach (Mathieu et al., 2007). Visual interpretation can address a high level of detail, since the human mind is amazingly good at recognizing and associating complex elements in an image like gray-scale tone, colour, height (depth), size, shape, texture, pattern, shadow, site, association and arrangement (Jensen, 2014). Nevertheless, manual interpretation is subjective and vulnerable to inconsistency and error due to personal experiences, knowledge and expectation of the interpreter for a given site (Morgan et al., 2010).

2.3.5 Pixel- versus object-based image analysis

Contrary to the visually-based, solely manual interpretation of imagery, automated digital image analysis techniques provide a time-saving solution and eliminate the influence of the interpreter's subjectivity in land cover/land use, more specifically in vegetation delineation. However, the appropriate use of these methods requires proper experiences in theory and practice. In general digital image analysis techniques aim at (semi-)automated information extraction, where the optimal approach depends primarily on the definition of the output products (e.g., the type of the maps) and is influenced by spatial resolution and inter-pixel variance (Wulder et al., 2004). In traditional image classification methods the pixels of an image are examined in order to give particular class labels to them. The application of pixel-based approaches has been well-accepted at low or moderate spatial resolution (Ozesmi and Bauer, 2002), whereas at high spatial resolution it could be problematic, since an individual feature could often be classified in distinct categories because of consisting multiple pixels with variable spectral reflectance characteristics (Johansen et al., 2010b).

Several remote sensing studies (e.g., Addink et al., 2007; Levick and Rogers, 2008; Kamagata et al., 2008; Johansen et al., 2010a) showed that due to the heterogeneous nature of the target vegetation habitats in high spatial resolution, traditional pixel-based digital image classifiers do not give satisfactory results. Instead of that the analysis of object-based methods came to the focus of interest.

During the analysis of high spatial resolution imagery the target features are generally larger than pixel size (Johansen et al., 2010b), which makes it very much reasonable to analyse the images based on objects like groups of pixels, instead of analysing the pixels individually. This special type of analysis method named object-based image analysis (OBIA) - also called elsewhere as object-oriented image analysis (OOIA) - applies actually the first law of geography (Tobler, 1970), which says: “Everything is related to everything else, but near things are more related than distant things”. In that sense certain image pixels situated next to each other could be merged beforehand and be handled together. With the increasing amount of data with high spatial resolution and the development of automated digital image analysis techniques the principle of grouping pixels into meaningful objects before the classification has become crucial. This need triggered the release of the first commercially available OBIA software (eCognition, from 2000).

Object-based classifiers can use spectral and spatial patterns together for the image analysis and thereby involving contextual information (Lillesand et al., 2008) and overcoming the so-called “salt and pepper effect” (Blaschke, 2010). OBIA consists of image segmentation (clustering of pixels into homogeneous objects), classification (or labelling objects) and modelling based on the characteristics of objects (Johansen et al., 2010b). The following methods, e.g., edge-detection, feature extraction and classification involved in OBIA have already been used in remote sensing image analysis for decades, whereas the image segmentation itself was not applied extensively in geospatial applications between 1980 and 2000, although it has not been a new concept coming originally from industrial image processing (Blaschke et al., 2011). Segmentation approaches currently applied in the present research are discussed in Chapter 4.1, for a more detailed review on the available segmentation methods applied in the eCognition object-based software environment the reader is referred to Dezső et al. (2012).

Due to the capability of building a logical hierarchical structure between different scales of image objects (Benz et al., 2004), OBIA has a high potential in multiscale landscape analysis, where semantically significant regions are found at different spatial scales (Burnett and Blaschke, 2003). The characteristics of meaningful objects can be assessed through spatial, spectral and temporal scales to generate new spatial information in GIS-ready formats representing its compatibility with vector GIS-software (Johansen et al., 2010b).

OBIA is becoming a standard image analysis approach for the analysis and extraction of

GIS-ready spatial information from VHR/HR imagery and its significance has been revealed through biennial conferences (GEOBIA 2006, 2008, 2010, 2012, 2014), the establishment of specific teaching activities in academia, special journal issues and beyond that, private and government agencies adopted OBIA-technique as an integral part of GI Science and spatial information generation (Johansen et al., 2010b).

The comparison of pixel- and object-based analysis of vegetation emphasizing the improvement of accuracies for the OBIA-method has been presented in various research studies applied to HR imagery (Yu et al., 2006; Yan et al., 2006; Addink et al., 2007; Levick and Rogers, 2008; Kamagata et al., 2008; Johansen et al., 2010a). For a general visual comparison of pixel-based and object-based classification results an example is presented in Figure 2.2, based on an aerial photo from the Szigetköz floodplain, which was latter used in the present research. Both types of supervised classifications (maximum likelihood for the pixel-based and class description based fuzzy algorithm for the object-based method, see later in Chapter 4.5) were based on the original bands complemented with the bands for the first principal component and for the vegetation index, after the selection of the same training samples.

Yu et al. (2006) presented improved vegetation classification results in Northern California for the object-based method based on the imagery of Digital Airborne Imaging System (a 12-bit multispectral imaging sensor system) with 1-m spatial resolution in comparison to the pixel-based analysis, overcoming the problem of salt-and-pepper effects often found in the traditional pixel-based approaches. In the study of Levick and Rogers (2008) classification accuracy improvements by OBIA have been presented for the analysis of woody vegetation in a heterogeneous savanna system in South Africa based on black & white aerial photographs. Johansen et al. (2010a) highlighted the advantage of geo-object-based classification in the analysis of temporal changes concerning riparian land-cover classes based on QuickBird images (under 3 m/pixel) in Central Queensland, Australia. Nevertheless, Blaschke et al. (2011) have stated that an optimal use of object-based image classification and mapping for vegetation-related analysis is still under consideration regarding consistency and time-efficiency. Besides that, concerning the general concept of vegetation mapping Xie et al. (2008) emphasized that the search for improved image classification algorithms presents an actual research field in the remote sensing applications because of the lack of those classification methods which could be universally applicable.

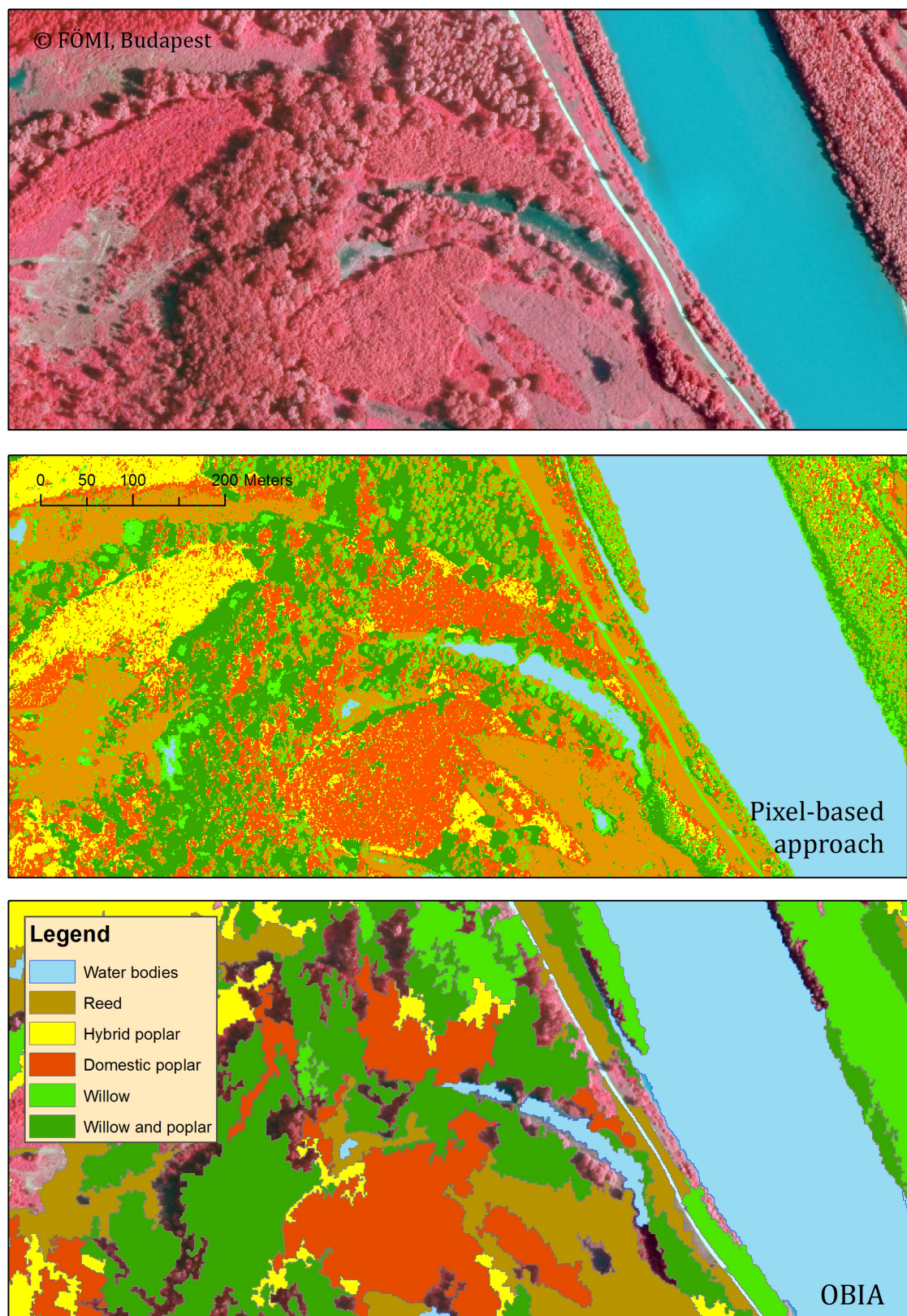


FIGURE 2.2: Comparison of pixel- and object-based classification approaches based on the latter applied aerial image scene of the Dunaremete test site, from 2008, with a spatial resolution of 1.25 m/pixel.

Chapter 3

Materials

3.1 Study area

The present study is focusing on a Hungarian Danubian floodplain ecosystem: the Szigetköz wetland which is located in Northwest Hungary, in the interfluvium of the Danube and Mosoni Danube rivers (Figure 3.1). This floodplain together with the Slovakian Csallóköz is the most extended riparian wetland in the Upper-Danube region characterized by high biodiversity (Illés and Szabados, 2008; Smith et al., 2000). The Szigetköz covers an area of approximately 375 km², its length is about 50 km with an average width of 7 km, however, the regularly inundated area is much smaller. A part of that with around 9682 ha became landscape protected area in 1987 belonging to the Directorate of Fertő-Hanság National Park and nowadays including Natura 2000 SCI (sites of community interest), SPA (special protected area) and IBA (important bird areas)(Szabó, 2005).

In the 19th century significant environmental changes occurred due to the regularization of rivers, which meant that at the end of the century most of the forests on the protected side of the dams were felled and replaced by arable land, hay meadows and pastures (Hahn et al., 2011). In 1992 further changes have happened in the region with severe impact due to the Danube-diversion, conveying approximately 80% of the discharge into the 29 km long bypass canal of the Gabčíkovo Hydropower Plant in Slovakia, between Dunacsúny and Szap (Ijjas et al., 2010). The changed flow and sediment regime has significantly affected the unique diverse pattern of habitat types, which have been altered from aquatic or aquatic-related forms to more terrestrial species (Ijjas et al., 2010). Dried out river branches with a general

decrease in ground water level characterized the changed environment in the Szigetköz, however, the degree of ground water level change have been influenced by the location and the actual amount of water in the Danube (Hahn et al., 2011).

Water was one of the main landscape-forming factors in the Szigetköz by playing a key role in building and maintaining a highly diverse terrain. Most of the continuously carried plant propagules from the Alps established and colonized the slow water tributaries of the Szigetköz. The limitation of the dispersal of propagules by water negatively influences the share of montane species in the flora. Contrary to the general drying of the environment nowadays, regular flooding not only provided favourable water supply, but brought external nutrients into the soil and prevented intolerant terrestrial species establishing on the floodplain (Hahn et al., 2011).

3.1.1 Effects of hydrological changes on the vegetation

The unique value of vegetation in the region refers to the richness of species compositions, where montane and lowland species often grow next to each other. Before the Danube-diversion, 1013 vascular plant species were known to occur in the Szigetköz, which comprises 46% of the total vascular flora of Hungary (Hahn et al., 2011). As it has been mentioned before, areas beyond flood protection dikes are covered mostly by arable land, while forests and meadows are present in the inundation region. Native forests appear particularly on small islands. On the lower wetland sites patches of the original reed, marsh or tall sedge vegetation are preserved, which react to the water regime modifications much faster than forests, due to their shallower rooting depths. Forests in the Szigetköz have nationwide significance and especially high natural value in the field of nature conservation concerning the problem of alien species spread in softwood gallery forests (Hahn et al., 2011).

The state of naturalness varies at the different parts of the Szigetköz, ranging from completely anthropogenic agricultural fields to natural plant communities worth of special protection (Simon et al., 1993). However, due to the higher proportion of alien species in the softwood (willow-poplar) gallery forests (Figure 3.2) the degree of naturalness is lower here than in the hardwood forests (oak-elm-ash). Softwood gallery forests are rich in soil nutrients and receiving floods frequently which provide better habitat for nutrient demanding invasive species. Nevertheless, the naturalness of species composition for almost each layer is higher in the Szigetköz than elsewhere in the country due to the lower proportion of alien

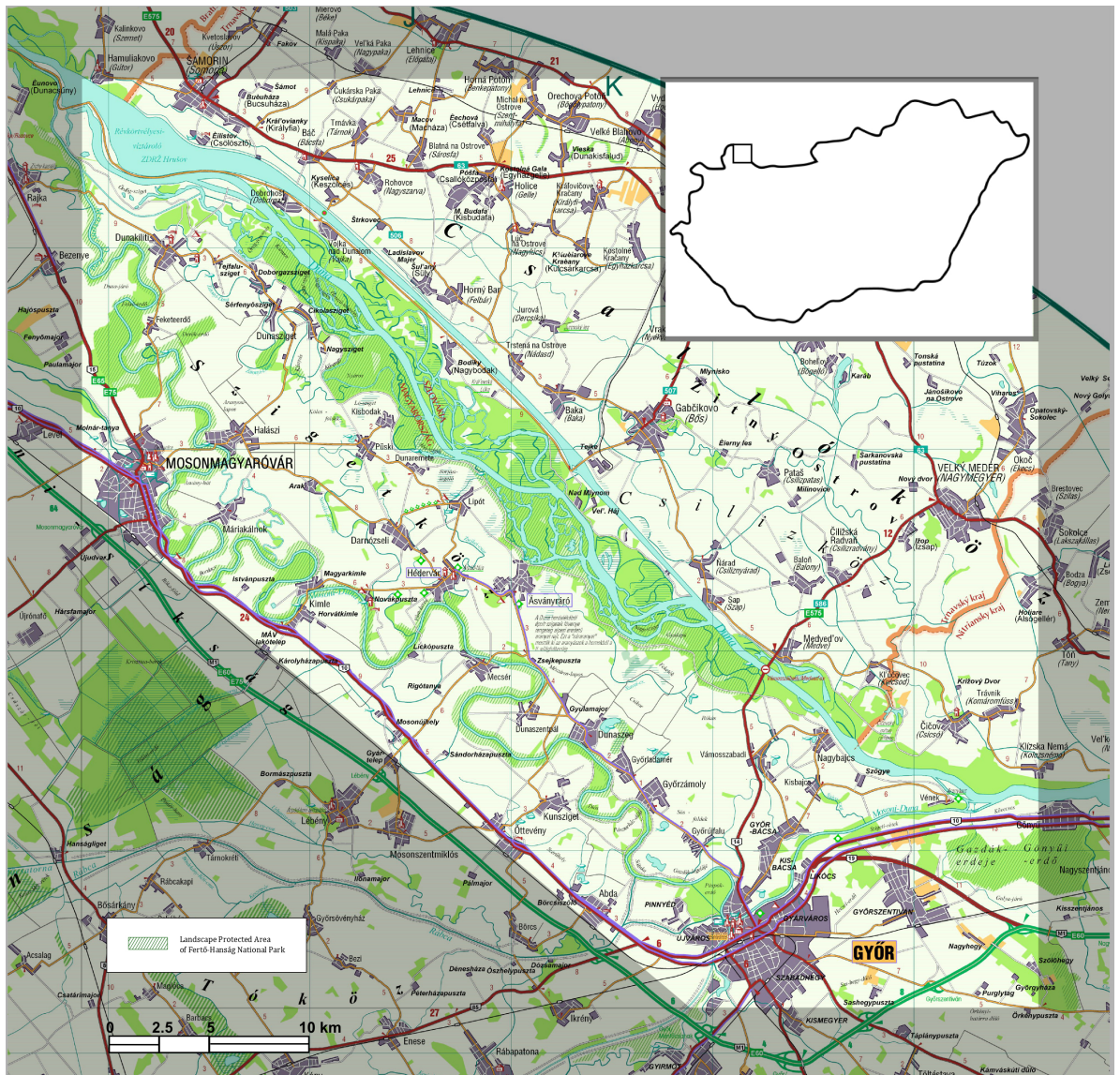


FIGURE 3.1: Map of the Szigetköz Danubian floodplain. Subset from the map of Győr-Moson-Sopron (Hungary), by Imre Bába (Paulus Mapdesign Office).

species, higher amount of natural accompanying species and the lower predominance of disturbance tolerant species. By the abundance of old trees and the amount of dead wood the value of naturalness is greatly improved as well. In addition to that softwood gallery forests are favoured nesting sites for large-bodied birds (Hahn et al., 2011).

After the Danube-alteration, a water recharging system provides the water in the Old-Danube channel and side arms, which is artificially regulated. The Danube diversion effected the various forest communities differently, whereby the most severe influences revealed on the low floodplain, where the sharp drop in the gradient in the depth of groundwater (Vekery and Meijerink, 1998) had a serious impact on forests near to the main Danube riverbed.



FIGURE 3.2: Willow (on the left) and hybrid poplar forests (on the right-hand side) in the Szigetköz, near to Gombóc. The photo has been taken on the field work (06.11.2010).

Despite increasing water levels in the tributaries due to the bottom dike, with the current water recharge system it is not possible to simulate floods. Related to the missing inundations vegetation undergoes significant changes and hereby loses its special character (Hahn et al., 2011).

3.1.2 Botanical mapping

History of botanical surveying

The report of Zólyomi (1937) described that the phytocoenological survey of forest communities started in the late 1920s and provided detailed descriptions of willow woods, oak hardwood gallery forests, relict oak-hornbeam woods and swamp alder woods, where the forest stands were considered as remnants of former extensive natural woodlands. Regarding the proportion of forests to fields it was 60 to 40 in the 1920s (where hybrid poplar plantations accounted for 12.5% of forest area), nevertheless, it went through a remarkable change with the extension of agricultural land until the 1980s, which means that the mentioned ratio became 20 to 80. The share of hybrid poplar plantations within forests increased as well to 81% by that time, whilst seminatural forests covered 19% of the area only (Hahn et al., 2011).

Recent surveying methods

In 1997 a new national project, the National Biodiversity Monitoring System (*Hu.* NBmR: Nemzeti Biodiverzitás-monitorozó Rendszer) has been started in its test phase defining 124 squares of 5×5 km² (covering around 3.2% of Hungary), where the habitats are classified after the so-called Á-NÉR classification system at the scale of 1:25 000 (Török et al., 2007). The Á-NÉR (*Hu.* Általános Nemzeti Élőhelyosztályozási Rendszer) Hungarian habitat mapping method concentrates on the joint observation of physiognomy, species composition, vegetation dynamics and habitat quality based on naturalness in its non-hierarchical, two-dimensional (including vegetation type and habitat quality) categorization (Bölöni et al., 2008). The scale (1:25 000) and the number of categories (116) were both exceeded the CORINE Land Cover classification system (with the scale of 1:100 000 and 44 categories in total: <http://www.eea.europa.eu/publications/COR0-landcover>) and were less than the traditional vegetation mapping system (current phytocoenology applies the scale of 1:10 000 - 1:5 000 and maps beyond 400 classes)(Fekete et al., 1997). This type of biodiversity monitoring aims at the characterization of a concrete site, also in comparison with other sites and analysing changes for the certain test area.

Questions and uncertainties

Botanical mapping has a subjective nature, since it depends much on the surveyor's mapping concepts and experiences, therefore, the current surveyors have to take into account carefully how their predecessors had mapped the area (Takács and Molnár, 2009). During the mapping of thematic data, e.g., vegetation habitats without administrative borders, it is a common question, whether we are able to do hard or smooth classification regarding the vegetation boundaries, where the geometric resolution and the definition of target classes play an essential role.

Considering the "classification rule" of the botanists (e.g., Á-NÉR), there are some classes where the distinction or delimitation between them is very difficult and subjective to the botanist's personal judgement. Examples are spontaneous successions, e.g., distinction between riverine willow shrubs ("J3" code in Á-NÉR) and willow mire shrubs ("J1a" in Á-NÉR, generally *Salix cinerea*).

3.1.3 Remote sensing analysis

Medium resolution Landsat satellite image analysis showed a decrease in the normalized difference vegetation index in short-term (1992-1993) (Smith et al., 2000), which was caused by dropping groundwater levels, documented and modelled in the region, e.g., by Vekerdy and Meijerink (1998). Similarly to that, negative changes were detected in the wetness values based on the Tasseled Cap transformation of Landsat, however, from 1997 a continuous regeneration is experienced, except for older willow species (Kristóf, 2005).

Focusing on detailed vegetation analysis, advanced image interpretation techniques have been commonly applied to remote sensing studies in the recent years (Blaschke et al., 2011), however, in the test site of the current research, botanical vegetation habitat classifications have been mostly based on traditional field surveying. Available aerial imagery was often used as unprocessed background information for visualisation purposes as a basic background layer for field work and for vector data representation (Takács and Molnár, 2009). Land use/land cover classification of the floodplain has been primarily based on visual image interpretation (Liczkó, 2002), however, the different types of vegetation habitats, which are in focus in the botanical analysis, have not been considered there.

The monitoring of forest ecosystems in the Szigetköz has been undertaken by the Forest Research Institute (ERTI, Budapest) since 1986, also as a member of the Szigetköz Research Group (in the Hungarian Academy of Sciences) from 1995 (Illés and Szabados, 2008). Forest health status and its changes as an important indicator after tree growth rate on the dramatically changed hydrological situation has been analysed by digital image processing algorithms (pixel-based supervised image classification techniques) in the study of Illés and Somogyi (2005), where the analysis was applied to different forest types based on orthophotos from 1991 and 1999. Despite some promising results, health status could not be estimated for certain species. Another silvicultural study (ERTI, 2008) has concentrated on the detection of leaf losses based on CIR aerial image (2008, 1 m/pixel, from VITUKI Environmental Protection and Water Management Research Institute, Budapest). Though unreliability has been demonstrated by the false inclusion of shadowy areas into the leaf loss classes, it has been obvious that the region of Dunakiliti, Kisbodak and Lipót gave worse values for leaf loss in comparison to the southern part where the water-recharging system and the thicker sediment layer provide better conditions for the forests. Recently in the frame of a Hungarian-Slovakian Cross-border Cooperation Programme (2007-2013,

INMEIN, “Innovative methods for monitoring and inventory of Danube floodplain forests based on 3D technologies of remote sensing”) the analysis of airborne laser scanning data gave promising results for forest inventory (Király and Brolly, 2013).

3.2 Applied imagery

Aerial imagery was acquired for the present research over three test sites near to the villages Dunakiliti (DK), Dunaremete (DR) and Ásványráró (ASV) (Figure 3.3) in order to study an area where the data of the most recent (2004) botanical survey is accessible (Dunaremete) and other two sites, Dunakiliti, situated nearest to the Danube-diversion point and Ásványráró, where the water-recharging system has a great influence. Digital orthophotos from 2000, 2005 and 2008 are available at the Institute of Geodesy, Cartography and Remote Sensing (FÖMI, Budapest).

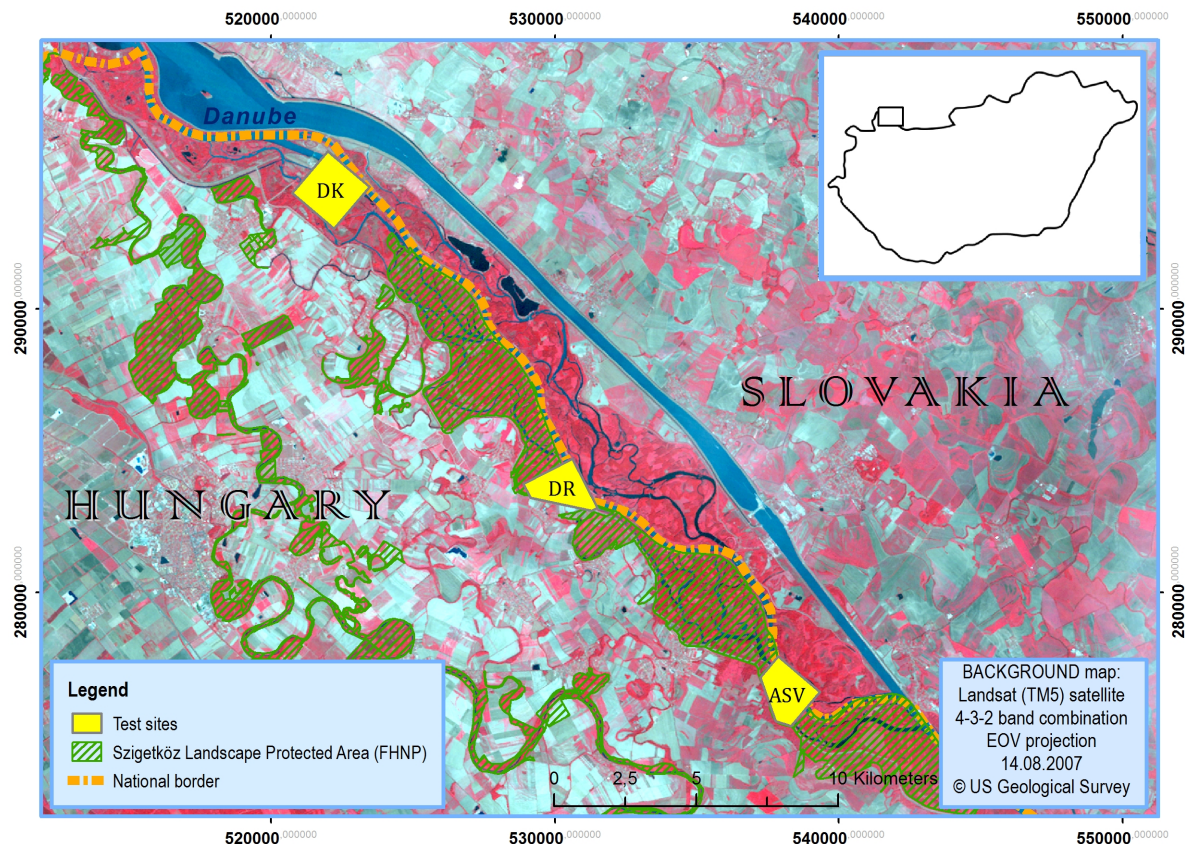


FIGURE 3.3: Test sites in the Szigetköz Danubian floodplain

In 1999 the University of West Hungary (UWH) was involved in a Phare Cross-Border-Cooperation (CBC) Project (Márkus et al., 1999), where aerial imagery was provided by

Eurosense (<http://www.eurosense.com>) and this aerial image material could be accessed and applied to the current research. Since this data set consisted of CIR images, it was selected for the analysis instead of the FÖMI orthophotos of 2000, which were RGB images. Digital (respectively digitalized) orthophotos directly used in the study with the basic parameters are summarized in Table 3.1. In Appendix A we can find the images themselves for the test site of Dunaremete in smaller format.

TABLE 3.1: Detailed information on the orthophotos used in the research. *Because of the digital camera in case of 2008, the given scale cannot be directly compared to the others.

Orthophotos	2008	2005	1999
Source	FÖMI, Budapest	FÖMI, Budapest	UWH, Phare CBC Project
Scale	1 : 74 000*	1 : 30 000	1 : 30 000
Geometric resolution	0.5 m/pixel	0.5 m/pixel	1.25 m/pixel
Applied recording type	Digital,CIR	Film,True Colour	Film,CIR
Spectral resolution	NIR, G, B	RGB	NIR, R, G
Camera type	UltraCamX	Wild RC 20	Wild RC 20
Acquisition time	06.08.2008	29.07.2005	03.08.1999
Solar azimuth angle	125.6°	209.4°	111.6°

3.3 Botanical and silvicultural maps

Classified maps based on remotely sensed data always need verification by ground reference information. After the study of the [Environmental Laboratory \(1987\)](#) field wetland identification requires the observation of three wetland parameters: hydric soils, hydrology and hydrophytic vegetation. However, in this study vegetation data (silvicultural and botanical) was used as an integrator of these wetland parameters.

In the present study thematic maps as reference data have aided the interpretation and classification of the aerial image scenes. Because of the difference between the image acquisition times and the field surveys (in the case of the vegetation habitat maps and the forest inventory data as well), their application has been done with careful considerations.

The selection of the Dunaremete test site, as principal study area, has been directly influenced by the location of detailed botanical investigations in the floodplain (see the overlapping areas in Figure 5.1). The square test site of botanical investigations (habitat map in Figure 5.1) has been stated as a good representation about its surroundings, too. The vegetation along the Danube is very similar to it regarding the hybrid poplar and willow

plantations and the near-natural woodlands between the dam and the river (Takács and Keszei, 2004), where the Á-NÉR classification system (Chapter 3.1.2) has been applied. These maps are available from 2004 and 2000 (Appendix B), covering an area of 25 km² with the scale of 1:12 500, where the accuracy of the separation between different vegetation habitats is around 10 m.

Whilst habitat maps from botanical inventory emphasize physiognomical aspects and vegetation dynamics in their classification system (Bölöni et al., 2008), silvicultural maps include forest categorisation, where the concrete species are described. Detailed information on forests at a scale of 1:10 000 (related to 2010) has been provided by the National Forest Inventory (NFI), Szombathely. Regarding the digital silvicultural database the original acquisition year was 2003, however, it has been continuously updated after field inspections. In Appendix B the delineation of the silvicultural classes (Forest Stand Type, in *hu.* FATI1: 1. Faállomány Típusa) is presented and marked on the 2008 orthophoto (Figure B.3).

Chapter 4

Methods

The detailed analysis (Chapter 5 and Chapter 6) of the data set was based on digital image analysis techniques presented in the current chapter. Chapter 4.1 is focusing on segmentation techniques as the first step in object-based image analysis (OBIA), followed by the spectral and geostatistical characterization (Chapter 4.2, Chapter 4.3). The significance of class separability analysis is described in Chapter 4.4. Chapter 4.5 is introducing the supervised classification algorithms applied. The closing section (Chapter 4.6) deals with the accuracy assessment as a crucial part of any classification approaches.

4.1 Image segmentation

The first step of the object-based image analysis is the application of segmentation, where a combined use of spectral and spatial patterns is normally built into the analysis (Lillesand et al., 2008). The three main types of segmentation are: pixel- or histogram-based (involving only spectral characteristics), edge-based (looking for edges which separate homogeneous objects) and region-based, which could have three sub-types: region growth, region merging and region splitting algorithm (Lang et al., 2006). The region-based technique also called as surface(-based) segmentation is probably the most well-known type, where the simplest application is the quadtree segmentation approach based on the splitting of the image into 4 parts firstly and with the use of a homogeneity measure for each segment further splitting and merging is applied (Barsi, 2013). Another important segmentation technique, the multi-resolution segmentation approach (defined in the eCognition software environment) belongs

to the region-based type as well, has been applied extensively in numerous geospatial studies. It is a bottom-up region merging technique, where smaller objects (firstly pixels) are merged into larger ones based on the criteria set. As it was mentioned above, a hierarchical network of image objects can be built in OBIA according to the segmentation results at different scales (using various scale parameters) and thus the representation of different spatial resolutions is simultaneous (Levick and Rogers, 2008). Average image segment (object) sizes are indirectly influenced by the *scale parameter*, which determines the maximum allowed heterogeneity of the image objects. Besides the settings of the scale parameter, weights for the image bands and for the shape and colour have to be defined. If the criterion for shape is set to 0.3, it means, that it is considered with 30% contrary to the colour with 70% (Barsi, 2013). Weighting for other shape characteristics (compactness and smoothness) has to be set as well, where 0.5-0.5 (50-50%) is often used. From the mentioned shape characteristics *compactness* equals the ratio of the border length of the image object and the square root of the number of pixels forming this object and *smoothness* is given by the ratio of the image segment's border length and the border length given by the bounding box of an image object parallel to the raster (Benz et al., 2004). The expectation during segmentation algorithm is that it will divide the image into relatively homogeneous and semantically significant groups of pixels. However, after the first segmentation procedure improvement of 'object candidates' (Burnett and Blaschke, 2003) is mostly needed to find optimum segmentation parameters according to the scale and nature of features to be detected (Mathieu et al., 2007). The segmentation based on the original VHR imagery could significantly slow down the image analysis procedure. A potential solution for a faster application applied in the study of Bucha and Slávik (2013) is primarily reducing image spatial resolution (in the concrete example from 30 cm to 2.4 m).

4.2 Spectral characterization

Besides the additional spatial information (like distances, neighbourhood characteristics, topologies) available in image segments, spectral information changes compared to pixels and thus the variation of a given feature reflectance is reduced at the object level (Blaschke et al., 2011). Spectral parameters, which have been involved in the latter analysis, are the average pixel values of the single bands applied (also included the additional first principal component layer, PC1, described in the introduction of Chapter 5.1) and vegetation indices.

Vegetation indices are dimensionless, radiometric measures indicating relative abundance and activity of green vegetation, including leaf-area index (LAI), percentage green cover, chlorophyll content, green biomass and absorbed photosynthetically active radiation (APAR) (Jensen, 2014). The Normalized Difference Vegetation Index (NDVI, Equation 4.1, a normalized ratio of the near infrared and the red bands of the image, originally developed by Rouse et al., 1973) is one of the most commonly applied vegetation index, also known as a biophysical parameter that correlates with the photosynthetic activity of vegetation, since it expresses the contrast between the high reflection in the near infrared channel and the high absorption in the visible red channel for healthy green vegetation (Xie et al., 2008) (compare to Figure 2.1). It has been often applied in order to make quantitative estimates of plant canopies (Wyatt, 2000).

$$NDVI = \frac{NIR - R}{NIR + R} \quad (4.1)$$

The index can be influenced by additive noise effects (like atmospheric path radiance) and highly sensitive to canopy background variations, where e.g., the soil is visible through the canopy (Jensen, 2014). Generally speaking about image analysis procedures vegetation indices are often treated as additional bands, nevertheless, in the object-based analysis environment they can be accessed as object features.

4.3 Geostatistical characterization

The land cover types, like vegetation can be identified from remote sensing imagery by unique spectral characteristics (Xie et al., 2008). However, aiming at vegetation classification, where a study area is covered by vegetation of complex forms or different stages (which often occurs in high spatial resolution), spectral responses could be similar among different vegetation groups or could generate spectral variations for the same vegetation class (Sha et al., 2008).

In case of HR imagery, where a group of pixels needs to be combined to characterize single trees, spectral variability for an individual tree (including sunlit crown, shaded crown, influence of factors such as branches, cones and tree morphology) is not helpful in developing unique spectral signatures for object classification as it is common in per-pixel image classifications (Wulder et al., 2004). Due to the high spectral variability vegetation patches (more specifically forest stands or an individual tree) cannot be described by the utilisation

of spectral characteristics only. Therefore, additional information is needed based on local spatial statistics that describes spatial variability.

4.3.1 Texture analysis based on GLCM

Although there are variants of texture analysis methods, further investigations are focusing on second-order statistics based on the co-occurrences of pixel values, commonly applied in numerous land-cover and vegetation mapping studies based on remotely sensed images (Berberoglu et al., 2007; Hájek, 2008; Nichol and Sarker, 2011; Wood et al., 2012; Szantoi et al., 2013).

Pixel co-occurrences are described in the so-called grey-level co-occurrence matrix (GLCM), which characterizes the probability that radiometric values of each pair of pixels from a grey-scale image co-occur in a given direction and at certain lag distance (Haralick et al., 1973).

Lévesque and King (2003) presented that the use of GLCM measures (besides semivariance range and sill, explained in Chapter 4.3.2) has been advantageous for forest structure and health modelling. Hájek (2008) has stated that GLCM textural characteristics have an essential role in the discrimination of prevailing forest types on the level of forest compartments. Forested areas as well as urban land cover classification have shown significant improvements in classification accuracies with the inclusion of GLCM in various studies (Franklin et al., 2000; Carleer and Wolff, 2006; Kim et al., 2009). Laliberte and Rango (2009) demonstrated that despite high spatial resolution (there: unmanned aerial vehicle, UAV images) the low spectral resolution significantly effects the interpretation of the imagery where texture measures can improve the classification accuracy.

Definition of GLCM

The GLCM is an $L \times L$ matrix based on a grey-scale image with a given brightness value range (mostly $L = 256$ for 8 bit data), where the value for each cell is defined by the number of occurrences of a given grey-level-combination of 2 pixels (a pixel pair with a defined h distance and θ direction which are given for a concrete matrix) divided by the total possible number of grey-level pairs (Richards and Jia, 2006). h distance and θ direction

could vary, thus numerous GLCMs exist for a selected image sample. For the GLCM itself four important variables have to be defined:

1. Moving window size,
2. Direction of the offset (θ),
3. Distance of the offset (h),
4. Image channel used.

In case of directionally unbiased target classes, the average of all directions (0° , 45° , 90° , 135°) is commonly taken (Laliberte and Rango, 2009). The distance of pixels is normally set to 1, comparing direct neighbours (Trimble, 2013). In addition the calculation of GLCM (as any other type of textures) is strictly dependent on the spatial resolution of the imagery (Jensen, 2014).

GLCM measures

For the characterization of the matrices Haralick et al. (1973) introduced 14 different metrics derived from the GLCM and those are mentioned later as texture measures or textural parameters. Besides GLCM, GLDV features (grey-level difference vector) are also used in various applications, which is defined by the sum of the diagonals in the GLCM and hereby it provides a measure of the absolute difference of neighbours (Laliberte and Rango, 2009).

From the GLCM measures 8 types have been often tested in literature (e.g., Hall-Beyer, 2007; Laliberte and Rango, 2009) and to these GLCM parameters additionally 4 GLDV features are implemented in the eCognition Developer software as object features, which have been analysed later in Chapter 5.1.4. The mentioned measures are summarized with formulas in Table 4.1.

TABLE 4.1: The most important textural parameters of GLCM and GLDV, tested later in the current study. $P_{i,j}$ is the normalized grey-level value in the cell i, j of the matrix, N is the number of rows or columns, $\mu_{i,j}$ is the mean of row i and column j , V_k is the normalized grey-level difference vector, where $k = |i - j|$. Based on Trimble (2013) where formulas are described after Haralick et al. (1973).

Textural parameter	Formula
GLCM mean	$\mu_{i,j} = \frac{\sum_{i,j=0}^{N-1} P_{i,j}}{N^2}$
GLCM standard deviation	$\sigma_{i,j}^2 = \sum_{i,j=0}^{N-1} P_{i,j}(i, j - \mu_{i,j}), \sigma = \sqrt{\sigma_{i,j}^2}$
GLCM correlation	$\sum_{i,j=0}^{N-1} P_{i,j} \frac{(i-\mu_i)(j-\mu_j)}{\sigma_i \sigma_j}$
GLCM entropy	$\sum_{i,j=0}^{N-1} P_{i,j} (-\ln P_{i,j})$
GLCM contrast	$\sum_{i,j=0}^{N-1} P_{i,j} (i - j)^2$
GLCM homogeneity	$\sum_{i,j=0}^{N-1} \frac{P_{i,j}}{1+(i-j)^2}$
GLCM dissimilarity	$\sum_{i,j=0}^{N-1} P_{i,j} i - j $
GLCM angular 2^{nd} moment	$\sum_{i,j=0}^{N-1} P_{i,j}^2$
GLDV mean	$\sum_{k=0}^{N-1} k(V_k)$
GLDV entropy	$\sum_{k=0}^{M-1} V_k (-\ln V_k)$
GLDV contrast	$\sum_{k=0}^{N-1} V_k k^2$
GLDV angular 2^{nd} moment	$\sum_{k=0}^{N-1} V_k^2$

4.3.2 The semivariogram

The optimal selection of moving window size for texture analysis is crucial. Therefore, the semivariogram has been suggested and applied in numerous studies, especially for the choice of appropriate window size for GLCM computation (Carr and Miranda, 1998; Treitz and Howarth, 2000; Tsai and Chou, 2006; Szantoi et al., 2013). The semivariogram (also called as variogram elsewhere) is a commonly used function in spatial statistics, which relates the semivariance to spatial separation and provides a concise and unbiased description of the scale and pattern of spatial variability (Curran, 1988). In case of a spatially dependent dataset, the semivariogram is used to estimate the analysed variable value in different locations considering the spatial correlation of the sample data (Balaguer-Beser et al., 2011).

The mathematical formula for the empirical semivariogram is defined in Equation 4.2 after Curran (1988):

$$\gamma(h) = \frac{1}{2m} \sum_{i=1}^m [z(x_i) - z(x_{i+h})]^2 \quad (4.2)$$

where x_i and x_{i+h} are geographical points in the image separated by \vec{h} vector called as lag distance. $z(x)$ is the attribute value (in RS image analysis the radiometric value) and m means the number of point pairs separated by \vec{h} vector. The average semivariance $\gamma(h)$ is visualised for increasing \vec{h} in the graph of the semivariogram (Figure 4.1).

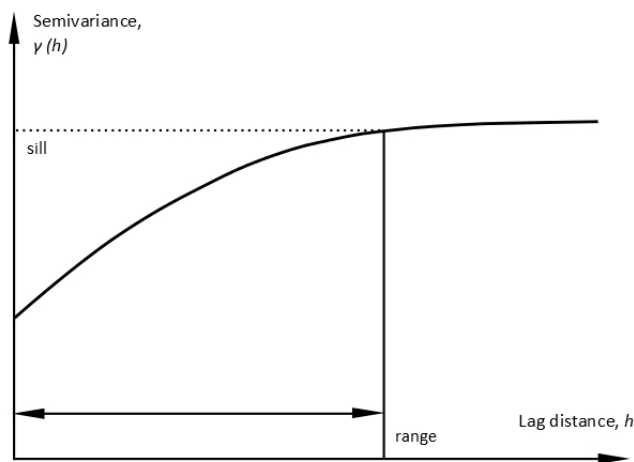


FIGURE 4.1: Schematic representation of a semivariogram.

Larger semivariances mean that the pixels divided by the lag (\vec{h}) are less similar. For the characterization of the variogram graph one of the most important parameters is the

range (Figure 4.1), which is a point on \vec{h} axis where the semivariance reaches its maximum. Regarding sample data $\gamma(h)$ reaches the range approximately at 95% of the sill (it is the maximum level of the semivariance) (Curran, 1988). Since the range defines the distance above which ground resolution elements are not related, a slightly larger lag distance could be well applicable for the optimal window size. However, the “classic” semivariogram is relatively unusual and e.g., planted woodlands can be rather described by “periodic” semivariograms (Curran, 1988), which will be presented in Chapter 5.1.3.

4.4 Class separability analysis

It has been discussed in several studies (e.g., Peng, 2005; Pereira et al., 2007; Laliberte et al., 2012; Silva et al., 2012) that a proper feature selection method has to be used in pattern recognition related applications in order to minimize the classification error. Besides aiming at higher classification accuracies, the application of feature selection methods is related to the reduction of redundant information in order to speed up the classification by an optimal number of the evaluated features (Mahmoud et al., 2011; Bindel et al., 2011).

Using any of the decision rules for classification (e.g., the maximum likelihood method, described later in the beginning of Chapter 4.5) generally cannot lead to a perfect separation of classes (see a representation for two classes in a two dimensional multispectral space related to a pair of probability distributions for a selected feature in Figure 4.2).

Beyond the mean values of classes the overlap is influenced by the standard deviations of the distributions, therefore, a combination of both the distance between means and a measure of standard deviation is required (Richards and Jia, 2006). Although the calculation of the probability error (Bayes error) (Fukunaga, 1990) should be the optimal measure for separability analysis and feature selection, its explicit and analytic expression, respectively its direct minimization is difficult to get (Guo et al., 2008). The following three major categories of separability measures: probabilistic distance, divergence and correlation-based measures are sought as alternatives, like easily evaluated criteria with a realistic performance, which generally provide bounds around the Bayes error (Guo et al., 2008).

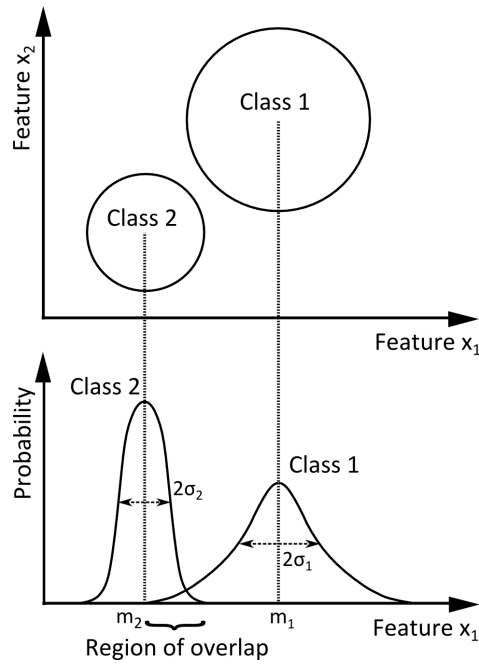


FIGURE 4.2: Representation of a two dimensional multispectral space by two features (x_1 and x_2) with two (spectral) classes and below visualizing the case of partial separability by probability distributions for the feature x_1 where some overlap is indicated.

From the group of probabilistic measures the Bhattacharyya distance (B in Equation 4.3 after Nussbaum et al., 2006; Mahmoud et al., 2011) is one of the most popular measures:

$$B = \frac{1}{8}(m_1 - m_2)^2 \frac{2}{\sigma_1^2 + \sigma_2^2} + \frac{1}{2} \ln \left[\frac{\sigma_1^2 + \sigma_2^2}{2\sigma_1\sigma_2} \right] \quad (4.3)$$

where m_1 and m_2 are the mean values and σ_1 and σ_2 are the standard deviation values of the two feature distributions. For a more detailed derivation of the Bhattacharyya distance see Kailath (1967). It has been stated as a convenient equation for normal distributions, but not rejecting the complete group of non-Gaussian cases and also discussed for a family of gamma distributions (Fukunaga, 1990). However, the infinite nature of the Bhattacharyya distance (B), having a range of a half-closed interval $[0, \infty)$, makes its interpretation difficult. Therefore, a similar measure, but with a finite dynamic range has been introduced called Jeffries-Matusita distance (JM in Equation 4.4) (Richards and Jia, 2006).

$$JM = 2 \left(1 - e^{(-B)} \right) \quad (4.4)$$

This separability measure has been applied in Section 5.1 and Section 6.3. The presence of the exponential factor in Equation 4.4 gives an exponentially decreasing weight to increasing

separations between the two analysed classes. JM distance as a function of separation between (spectral) class means is asymptotic to 2.0, thus, a JM distance of 2.0 would imply a classification of pixel (image object) data into those classes with 100% accuracy (Richards and Jia, 2006).

Thomas et al. (2002) emphasized that JM distance has advantages in case of observing normal distributions and therefore, in case of a parametric classifier (e.g., maximum likelihood) a low degree of separability would mean errors of omission/commission, however, it was indicated there that the relationship between separability and classification accuracy is non-linear. In the study of Silva et al. (2012) it has been summarized that generally JM distances above 1.8 are the indicators for good separability and the distance value below 1.8 would mean the possibility of confusion in the classification procedure between classes. However, important drawbacks of the analysed distances are the general assumption of normal distribution, the comparison of only two classes at once (Bindel et al., 2011) and in addition, they are quite computationally intensive.

4.5 Supervised classification algorithms

After selecting the most appropriate parameters for the analysis of pre-defined target classes supervised classification algorithm(s) can take place. Supervising means that the categorization of pixels, in an OBIA environment the classification of image objects (segments) is based on the training sample selection, where the numerical descriptors of the various land cover types (as target classes) present in the image are defined carefully to the computer algorithm (Lillesand et al., 2008). Finding a good representative dataset for each class involved in the analysis is crucial for a proper implementation of supervised classification (Lu and Weng, 2007). After the selection of training samples (often called as training stage) the classification of unknown segments is based on those numerical strategies (decision rules) which can be employed to compare them with the training sites (Lillesand et al., 2008). Assuming the Gaussian (normal) distribution of our data the maximum likelihood classification as a parametric classifier is often applied where a statistical distance (probability value) is calculated based on the mean values and the covariance matrix of the training sets (Tempfli et al., 2008). It is referred to as a parametric statistical supervised method, since it has been assumed that the classes can be modelled by probability distributions and, as a consequence, they are described by the parameters of those distributions (Richards and

Jia, 2006). Nevertheless, this type of classifiers often produces noisy results in complex landscapes and hinder the integration of those ancillary data into the analysis which are non-statistical in nature (Lu and Weng, 2007).

Other supervised techniques without distribution models and statistical parameters also exist, which are often referred to as non-parametric geometric methods (e.g., support vector machine, SVM or neural network, NN, a detailed description about these methods is found in Richards and Jia, 2006, nevertheless, these classifiers have not been within the scope of the current research).

In the following sub-sections (4.5.1 and 4.5.2) the class description based fuzzy algorithm (applied later in the analysis part in Chapter 5) is described firstly, which is rather a statistical classifier, however, instead of probability distributions the so-called membership functions are used. Secondly a special type of hierarchical classifier, the decision tree approach is presented considered as a non-statistical classification method (applied in Chapter 6).

4.5.1 Class description based fuzzy (CDBF) algorithm

In case of the so-called soft classifiers, uncertainties regarding image object classifications can be incorporated into the analysis. The most powerful soft classifiers are fuzzy classification systems (Benz et al., 2004) where the fuzzy logic means that instead of a traditional binary set with true or false response values a range between 0 and 1 is considered. In the fuzzy supervised classification fuzzy training class weights are defined by the known mixtures of various feature types, where a membership grade is assigned to a classified pixel or object concerning its membership in each target class (Lillesand et al., 2008). Each class of a (potentially hierarchical) classification scheme contains a class description (Figure 4.3), which consists of fuzzy membership value functions for selected features, like vegetation index and/or textural parameters (applied later in Sub-section 5.1.5). An example for membership function concerning a certain textural feature (GLDV entropy) is found in Figure 4.4.

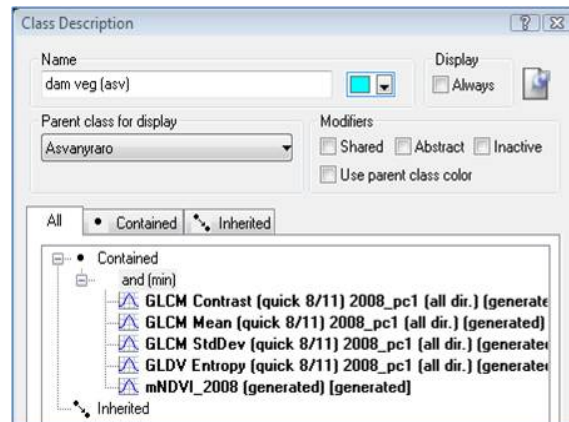


FIGURE 4.3: Class description derived from the eCognition software, for a certain class, where *dam veg(asv)* means the class of Dam vegetation from the Ásványráró test site. The listed textural features and the vegetation index are applied in the class description with separate membership functions, see an example in Figure 4.4.

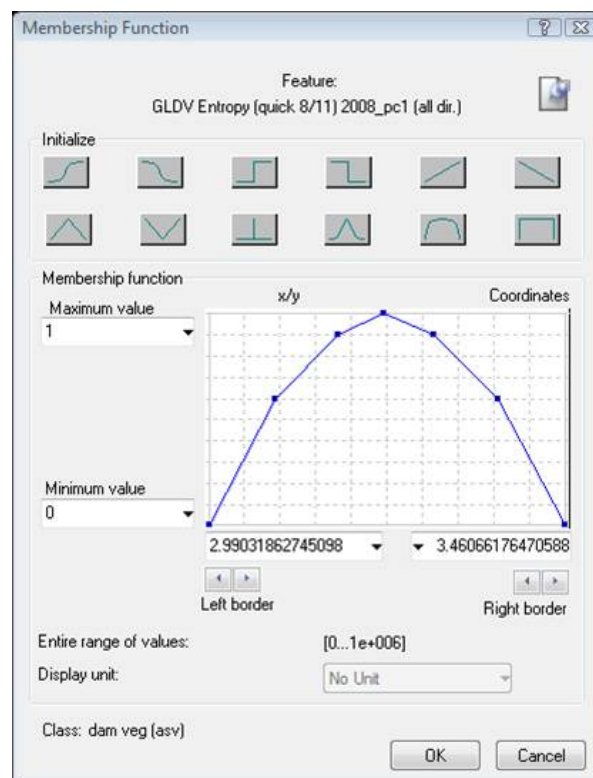


FIGURE 4.4: Membership function derived from the eCognition software for the textural feature: GLDV entropy applied to the PC1 band from the 2008 image scene (Ásványráró).

In order to get a common crisp classification for mapping purposes the fuzzy results have to be translated back to a crisp value, where the maximum membership degree of the fuzzy classification is applied as crisp class assignment (also called as defuzzification) (Benz et al.,

2004). However, if the maximum membership degree of a class is below a certain threshold, the area (image segment) remains unclassified to ensure minimum reliability.

The specific algorithm applied in the software environment eCognition is based on a membership value based fuzzy class evaluation, where the membership values concerning one specific feature are computed from the training set of image objects. In the fuzzy classification result there are actually three (default set in the software) potential classes for evaluation purposes concerning a certain image object, like the three best classes with the highest membership degrees, calculated from the membership value based class descriptions for the selected feature set (Trimble, 2013). In practice as a classification result, image objects are labelled according to the highest membership degree.

CDBF algorithm has been often applied during object-based image analysis methods (find e.g., in Johansen et al., 2007; Cleve et al., 2008; Jones et al., 2011), however, with the implementation of machine-learning functions in OBIA, like decision tree, random trees and support vector machine, various research studies (e.g., Mallinis et al., 2008; Heumann, 2011; Zhang and Liu, 2013) have been focusing on the evaluation of these latter classification methods.

4.5.2 Decision tree classification

The previously described CDBF algorithm belongs to the group of single stage classifiers, where each data sample is always tested against all classes. Contrary to that, in the case of multi-stage classification techniques, decisions are taken in various stages in order to classify each element (pixel or segment) of the image (Richards and Jia, 2006) and the sample is tested against only certain subsets of classes, thus, unnecessary computations are eliminated (Safavian and Landgrebe, 1991). The decision tree (DT) approach has a hierarchical nature, which is based on the concept of successively splitting the dataset into increasingly homogeneous subsets until terminal nodes are assigned (Laliberte and Rango, 2009). It is not based on inferential statistics and can process virtually any type of spatially distributed data (Jensen, 2014). Decision-tree classifiers are able to capture non-linear, hierarchical patterns and work as an excellent data reduction tool, capable of finding significant variables, if the dataset contains a large number of explanatory variables (Laliberte et al., 2007). A DT consists of a number of connected classifiers (decision nodes), where the root node divides firstly the image dataset to two groups of pixels/segments (i.e., a binary tree representing

Boolean functions), the internal nodes contain the further decision rules and the tree ends in the leaf nodes with class assignments (see an example in Figure 4.5).

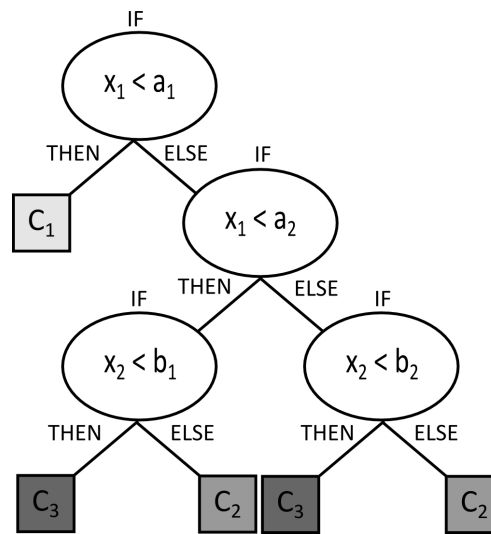


FIGURE 4.5: Example for a binary decision tree, where C_1 , C_2 and C_3 are the target classes (represented as leaf nodes). x_1 and x_2 are two features analysed and used in the internal nodes.

The leaves of the decision tree are often called as response or categorical variables (target land use/land cover classes), whilst the observed parameters from the training samples are the explanatory variables, which can be categorical or continuous (like spectral response in bands, elevation) (Laliberte et al., 2007). Explanatory variables are applied for the building of decision rules for the internal nodes, which rules can be expressed in the form of ‘IF condition THEN action ELSE action’ statements.

The three main tasks considered in the design of a decision tree are (1) finding the optimal structure for the tree, (2) choosing the optimal subset of features at each node and (3) selecting the decision rule to apply at each node (Richards and Jia, 2006). Since classification accuracy and efficiency are heavily influenced by the tree chosen, heuristic methods for decision tree design have been developed recently (Safavian and Landgrebe, 1991). These methods also called as decision tree inducers build an algorithmic framework in order to automatically construct a decision tree from a given dataset (Rokach and Maimon, 2005).

The tree growing-pruning approach of Breiman et al. (1984) is a top-down decision tree inducer, which group is clearly preferred in the literature contrary to the bottom-up approaches (Rokach and Maimon, 2005). The above mentioned method from Breiman et al.

(1984) has been implemented in eCognition 8.9 which is latter applied in Chapter 6.

Various research studies have shown promising results with the application of decision tree algorithms based on HR imagery. [Laliberte and Rango \(2009\)](#) have employed decision tree analysis for the selection of optimal texture features based on UAV (unmanned aerial vehicles) imagery for differentiating rangeland vegetation. [He et al. \(2004\)](#) discussed the integration of ancillary data (e.g., soil type, elevation) into the DT approach in order to aid the classification process of grasslands, where vegetation types have been strictly associated with other natural conditions. In the research study of [Heumann \(2011\)](#) decision tree classification has been combined with another machine-learning approach, the support vector machine classification in the OBIA environment, applied on WorldView-2 images for the mapping of mangroves. [Chubey et al. \(2006\)](#) have applied DT analysis in order to identify relationships between the derived image object metrics and individual forest inventory parameters based on Ikonos-2 satellite imagery. [Liu et al. \(2006\)](#) have emphasized the combination of decision tree classifier and OBIA to generate reusable, transferable classification rules, and hereby, to accelerate the automation process of RS information extraction. Nevertheless, a possible drawback of the DT classifier could be the increasing computation time and memory space in case of larger class numbers.

4.6 Accuracy assessment

Due to a direct need from the user community for objectively verified and communicated vegetation mapping products derived from remote sensing imagery, accuracy assessment techniques are applied to determine the quality of the resulting maps ([Xie et al., 2008](#)). It is vital to use accuracy assessment before working with these interpretations in scientific investigations and policy decisions, where the interpreted data builds up a database for latter analysis. Accuracy influences the information for land management and their validity and it is as well a basis for scientific research.

During the accuracy assessment, data comparison is done between the remote sensing result and some ground reference information, therefore a careful selection of reference data derived from field survey or other thematic datasets is required ([Morgan et al., 2010](#)). The collection of robust ground reference information is of high importance in order to represent each target category in an adequate manner ([Wyatt, 2000](#)).

Map accuracy assessment has two types, where *positional accuracy* describes the accuracy of the location of map features and *thematic accuracy* describes whether the label or attribute of a certain class in the map is the same as in the reality (Congalton and Green, 2009). Further on, it is essential to distinguish between two kinds of thematic accuracy assessments. In case of a non-site specific one, the comparison is only based on area percentages (comparing overall areas to ground estimates), which could hide the spatial misclassification, whilst a site-specific assessment compares actual places on the ground to the same place on the map resulting in a measure of correct percentage (Congalton, 2004).

The confusion matrix (also called as error matrix, Table 5.5) as a site-specific thematic accuracy assessment method gives the basis for many quantitative metrics of classification accuracy (Foody, 2002) and it has been accepted as the standard descriptive reporting tool for the accuracy assessment of remotely sensed data since the mid-1980s (Congalton, 2004). It is a square array of numbers organized in rows and columns that expresses the number of sample units assigned to a certain classified category (represented in the rows) relative to the actual category as indicated by the reference data in the columns (Congalton, 2004), nevertheless, the placement of rows and columns are transposed sometimes. The major diagonal of the error matrix represents the number of properly classified pixels (running from upper left to lower right), whilst the non-diagonal elements in the columns mean the omission errors and in the rows they stand for the commission errors (Lillesand et al., 2008). The most common measures calculated from the confusion matrix are the overall accuracy and the Kappa coefficient (sometimes called as Kappa index of agreement, KIA). However, a variety of other measures can be derived from the matrix as well, e.g., the accuracy of individual classes, if the user is interested in specific vegetation groups (Xie et al., 2008). The overall accuracy is computed by the division of the total number of correctly classified pixels by the number of the reference pixels. Accuracies for concrete classes, like producer's accuracy is calculated from the number of correctly classified pixels (in each class) by the sum of the training set pixels for the current category, whereas user's accuracy takes into account the number of pixels that were classified in that category (the sum of the rows) as denominator and hereby, it is often called as a measure for the commission error. The name of producer's accuracy refers to the interest of the producer concerning the goodness of a certain area which has been classified, whilst in case of the user's accuracy, the probability is indicated, whether a sample unit on the map actually represents that category on the ground (Congalton, 2004).

An error matrix is an appropriate beginning for many analytical statistical techniques, especially discrete multivariate techniques, which have been used for performing statistical tests on the classification accuracy of remote sensing data (Congalton, 2004). From these techniques the Kappa analysis (Cohen, 1960) is often applied, in order to statistically determine whether one error matrix is different from another (Congalton and Green, 2009). Besides that, using this technique, it is possible to test whether an individual land-cover map generated from remote sensing imagery is significantly better than a map generated by a random assignment of labels to areas (Congalton, 2004). The KHAT statistic (actually $\hat{\kappa}$, an estimate of Kappa) is based on the difference between the actual agreement in the confusion matrix (i.e., the sum of the correctly classified pixels in the major diagonal) and the chance agreement, calculated by the row and column totals in the marginals (Congalton and Green, 2009). The computation of KHAT statistic is as follows in Equation 4.5 after Lillesand et al. (2008)

$$\hat{\kappa} = \frac{N \sum_{i=1}^r x_{ii} - \sum_{i=1}^r x_{i+} x_{+i}}{N^2 - \sum_{i=1}^r x_{i+} x_{+i}} \quad (4.5)$$

where

r = number of rows in the error matrix

x_{ii} = number of observations in row i and column i on the major diagonal

x_{i+} = sum of observations in row i , generally shown as marginal total in the right side of the matrix

x_{+i} = sum of observations in column i , shown as marginal total at the bottom of the matrix

N = total number of observations included in the error matrix.

The possible ranges for the Kappa statistic have been characterized into three groups, where a strong agreement is described by a value greater than 0.80, a value between 0.40 and 0.80 stands for moderate agreement and a value below 0.40 represents poor agreement (Congalton, 2004). The Kappa analysis was introduced to the remote sensing community in 1981 and since then it has become a standard component of proper accuracy assessment procedure and nowadays it is required in most of the image analysis software packages (Congalton and Green, 2009).

Chapter 5

Spectral-textural classification

Most part of the image analysis, including texture calculations, was performed using the object-based image analysis software eCognition Developer 8.9 (www.ecognition.com). Image calculations, like image corrections (e.g., wrong line correction) and the calculation of principal component layers were worked out in Erdas Imagine 2011 (www.hexagongeospatial.com). Semivariogram computations were done in the R statistical software (<http://www.r-project.org>). Map layouts were composed in Esri ArcGIS 10.1 (www.esri.com).

5.1 Sample application to the study site of Dunaremete

As it has been described in Section 1.2, the analysis has been firstly concentrated on developing an appropriate aerial image classification method with the inclusion of texture characteristics in order to identify and map predefined vegetation habitats based on the test area (aerial images and ancillary data) in the Szigetköz Danubian floodplain. One of the three test sites, near to the village Dunaremete (Figure 5.1) with the size of approximately 2.5 km² has been selected as principal test site, adapted to the extent of the available botanical maps (2000, 2004).

The current analysis was carried out for three different dates (Table 3.1) separately, however, with the future aim of temporal connectivity. It is essential that the images have different spectral and spatial resolution.

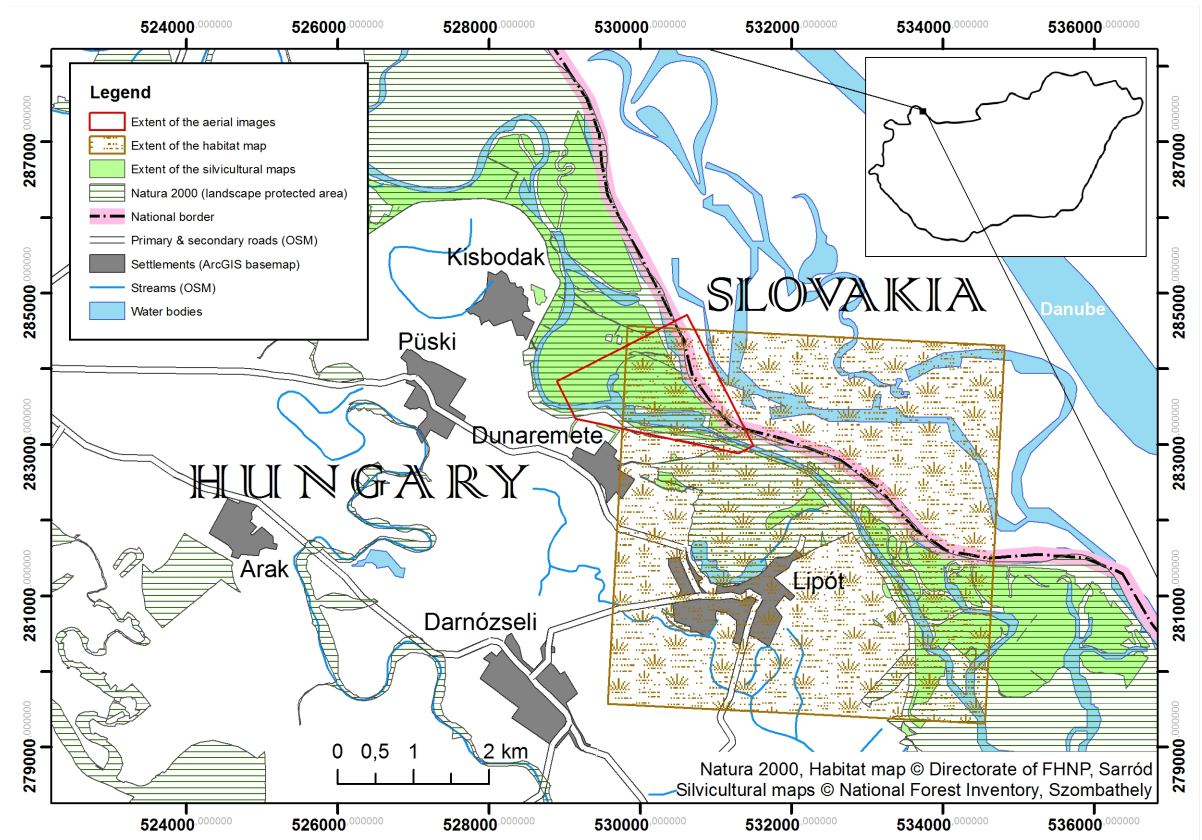


FIGURE 5.1: The study site of Dunaremete (DR). OSM in the legend means the source of Open Street Map.

Primarily, first principal component (PC1) bands as additional layers for the image analysis were calculated for each image scene (2008, 2005 and 1999) in the ERDAS Imagine software environment, in order to represent the variability of the data in one single band which can be later used for texture calculations (Tsai and Chou, 2006). In the further steps, it was important to conduct the analysis at a single geometric resolution, since further investigations are concentrating on the temporal comparability of texture measures of selected classes. Different ground spatial resolutions would lead to significantly different textures for most of the measures, as shown in Table 5.1 for the years 2008 and 2005, concerning samples from the class of Hybrid poplar.

Therefore, the 2008 and 2005 images were resampled to 1.25 m/pixel ground spatial resolution according to the original geometric resolution of the 1999 image. The main analysis steps for the principal test site of Dunaremete (including the above-mentioned ones) are summarized in Figure 5.2.

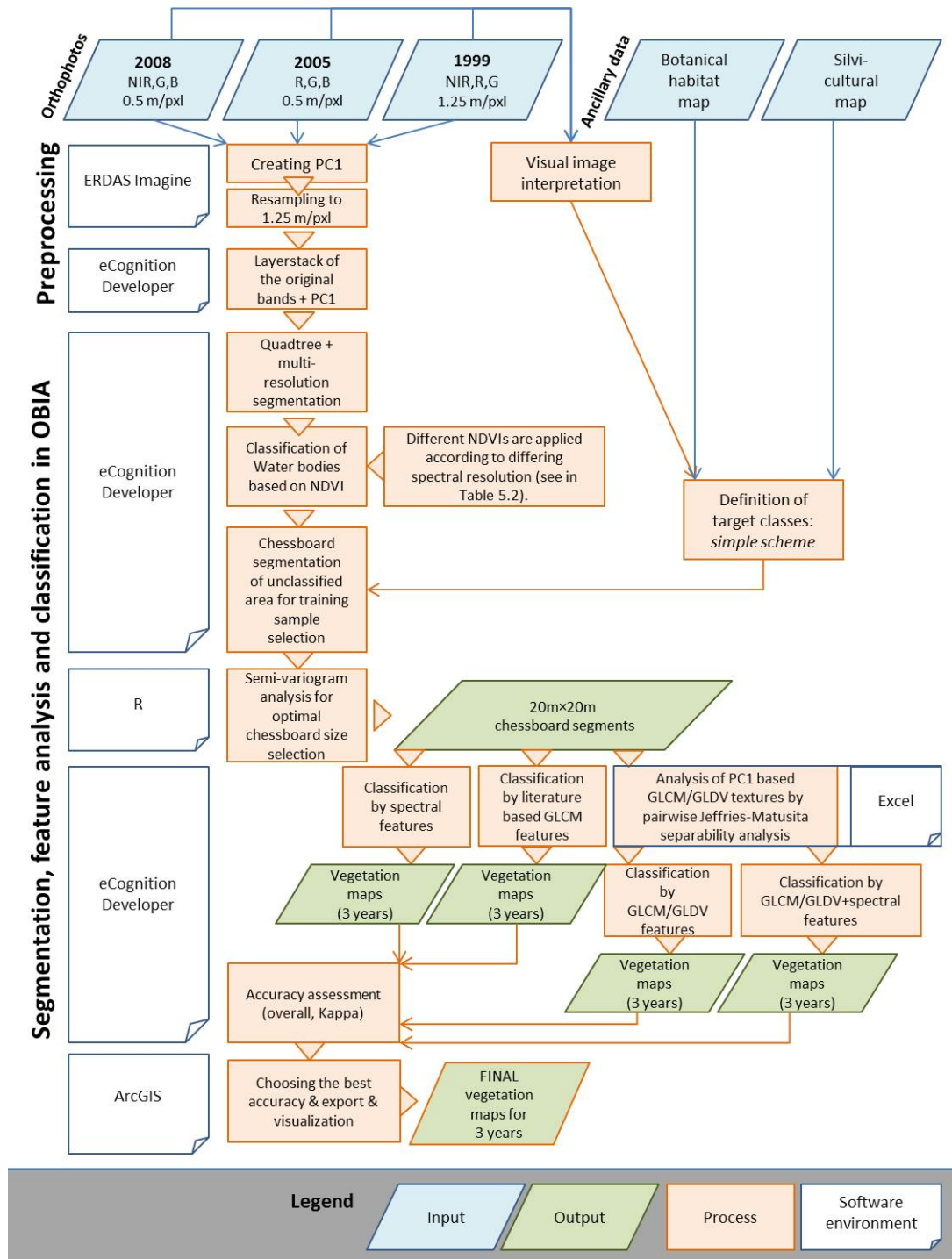


FIGURE 5.2: The main analysis steps applied to the principal test site of Dunaremete.

TABLE 5.1: Comparison of three texture measures for different ground spatial resolutions (GSR), regarding a concrete vegetation class (Hybrid poplar). Textures were calculated from the first principal component band (PC1) of the 2005 and 2008 image scenes, for the 20 m×20 m samples.

	GSR	0.5m/pxl	1.25m/pxl	0.5m/pxl	1.25m/pxl
Texture\Statistics		Mean		Standard Deviation	
GLCM Contrast (2005)		268.90	517.75	77.38	170.85
GLCM Contrast (2008)		143.05	386.52	49.77	124.08
GLCM Correlation (2005)		0.79	0.43	0.07	0.19
GLCM Correlation (2008)		0.89	0.61	0.03	0.12
GLCM Entropy (2005)		8.08	7.23	0.19	0.11
GLCM Entropy (2008)		7.69	7.17	0.23	0.10

5.1.1 Separation of water bodies

Firstly the differentiation of water bodies from the terrestrial/aquatic-terrestrial habitats was carried out on the segmented images, since their spectral characteristics are significantly different from the vegetation classes. For image segmentation a combination of quadtree and multi-resolution (MR) segmentation algorithms (described in Section 4.1) were applied in order to fasten the relatively time consuming MR segmentation. Firstly image objects are created by the quadtree based segmentation algorithm with the scale parameter of 30 and after that instead of using pixels the multi-resolution segmentation is based on the quadtree-segments applying the following parameters: scale parameter=40, shape criterion=0.3, compactness criterion=0.5. The classification of water bodies is based on the here-created image objects (Figure 5.3). Since the NDVI (1999) and the modified NDVI (BlueNDVI) (2008) values (Table 5.2) provide a good discrimination between water bodies and vegetation habitats in general, they were applied for the class description (described in Sub-section 4.5.1) of water bodies. BlueNDVI has been suggested in the study of Petersen et al. (2005) stating that it gave better results for vegetation separation in comparison to the original NDVI with the red band. The analysis of the RGB aerial image from 2005 was not straightforward due to the missing NIR band, which is always needed for an appropriate differentiation between water and any other land cover classes. Nevertheless, it was found that indices for vegetation delineation have been suggested for true colour imagery by Meyer and Camargo Neto (2008) and by Gitelson et al. (2002). Applying one of these vegetation indices: $ExG-ExR=(2\times G-R-B)-(1.4\times R-B)$ by Meyer and Camargo Neto (2008) or $(G-R)/(G+R)$ by Gitelson et al. (2002) in combination with the DN value from the Blue band gave almost the same results with the need for manual improvements. Since

the calculation for $VI=(G-R)/(G+R)$ is more straightforward, it was applied in the analysis afterwards. In Table 5.2 the applied vegetation indices are summarized.

TABLE 5.2: Vegetation indices applied to different-year images with different spectral resolutions for the test site of Dunaremete.

Orthophoto	2008	2005	1999
Spectral Resolution	NIR, G, B	RGB	NIR, R, G
Vegetation Index	modified NDVI	VI from G,R	NDVI
Formula	$(NIR-B)/(NIR+B)$	$(G-R)/(G+R)$	$(NIR-R)/(NIR+R)$

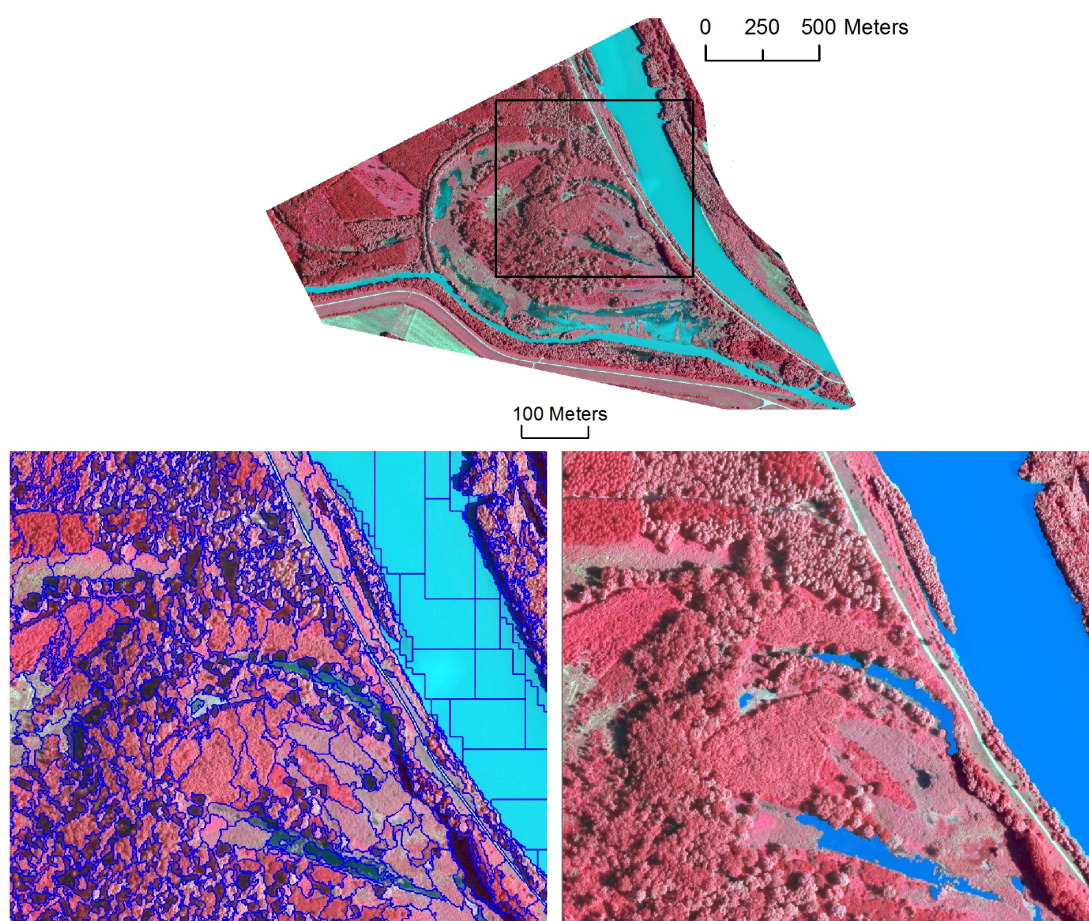


FIGURE 5.3: Segmentation example after quadtree and multi-resolution segmentation applied to the 2008 image of Dunaremete. Besides that the classification of water bodies based on the modified NDVI.

5.1.2 Classifying vegetation

Target vegetation classes were defined by a synoptic analysis of aerial imagery and ancillary data, firstly concentrating on the most occurring and characteristic vegetation patterns, where the patches could be easily identified by human eye, and they cover a significant area. The Á-NÉR botanical categorization (Sub-section 3.1.2) played an essential role in the definition of target vegetation classes. Next to the water bodies a significant area is covered by reed referred to as sedge in an earlier study, Kollár et al. (2011a), with the Á-NÉR code of B1 standing for Sedge and reed. Á-NÉR classes could not be always adapted to the aerial image based classification system, since some of the classes (e.g., Uncharacteristic, planted forest with the Á-NÉR code of R3, presented in Appendix B) don't describe species composition. Nevertheless, the species for the current case of R3 could be identified as 'mainly willow' after personal discussions with István Hahn (ELTE, Department of Plant Taxonomy and Ecology, Budapest).

For the analysis of woody vegetation, it was essential to involve detailed description from the silvicultural inventory (Appendix B, Figure B.3). The most commonly occurring forest stand types in the scene are

- hybrid poplar (FATI1: 059; Main tree species: *Populus x euramericana* 'Pannonia', FAFK: 723, an example for typical poplar stands is presented in Figure 5.4)
- mixed hybrid poplar (FATI1: 062; Main species: *Populus x euramericana* 'Pannonia', FAFK: 723, *Populus x euramericana* 'Robusta', FAFK: 713, *Populus x euramericana* 'I-273', FAFK: 727)
- domestic poplar (FATI1: 066; Species: *Populus canescens*, FAFK: 742)
- mixed willow (FATI1: 074; Species: *Salix alba*, FAFK: 811)
- willow (FATI1: 073; Species: *Salix alba*, FAFK: 811, Figure 5.5),

where FATI1 stands for Forest Stand Type (FST), FAFK for the occurring Tree Species.

As mentioned in Section 4.2, the classification of vegetation habitats based on high resolution imagery (<5 m/pixel) is not straightforward in an object-based environment because of the spectral heterogeneity of the target vegetation patches.



FIGURE 5.5: Willow species in the test site of Dunaremete. Photo from the fieldwork with István Hahn (06.11.2010)



FIGURE 5.4: Hybrid poplar stand in the Szigetköz near to the village Lipót. Photo from the fieldwork with István Hahn (06.11.2010)

Especially the forest crown reflectance represents always a complex mix of foliage spectral properties with other sources of variability including atmospheric effects, shadow pattern, background composition and instrument noise ([Hájek, 2008](#)).

Since the result of a classical multi-resolution segmentation (e.g., Figure 5.3) contains non-regularly shaped objects with spectrally homogeneous nature (homogeneity depends actually on the set of scale parameter for the segmentation approach), differences in spectral heterogeneity between image segments can be hardly studied on those image objects. Therefore, image spectral and textural properties for each vegetation habitat were assessed on a rectangular objects' basis resulting from the chessboard segmentation algorithm, where the terrestrial land was divided into unique square image objects with a predefined size.

Earlier findings (Kollár et al., 2011a) related to the present research but to a smaller test site (180 000 m²) have shown the successful use of chessboard-like image objects in vegetation classification. The size of the objects (segments) defines as well the minimum mapping unit of these classes.

The optimal size of the square segments was derived from a geostatistical analysis, described in Sub-section 5.1.3. The underlying theory is introduced in Sub-section 4.3.2.

In Figure 5.6, five square segments are presented as examples for each target vegetation class with an extent of 40 m×40 m, based on a single layer, the first principal component (PC1) from 2008.

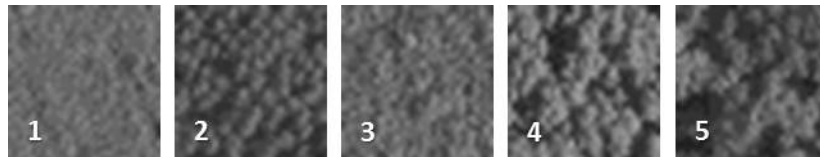


FIGURE 5.6: Target vegetation classes represented by 40 m×40 m square samples (2008, PC1, GSR: 1.25 m/pixel).
1)Reed, 2)Hybrid poplar, 3)Domestic poplar 4)Willow, 5)Willow & poplar.

The above-listed classes are present in each analysed year, except for the Domestic poplar (the 3rd sample in Figure 5.6) (“hazai nyáras” in the Hungarian designation, fitting to the silvicultural data, FATI1: 066; Species: *Populus canescens*, FAFK: 742) which appears only in 2008.

5.1.3 Application of geostatistics

As it has been described in Sub-section 4.3.1, texture characteristics based on the GLCM were analysed in detail for the target vegetation classes. The size of the square image

objects for the GLCM calculation was defined using semivariogram analysis (described in Sub-section 4.3.2, presented for the current case in Figure 5.7). Since target classes are vegetation patches with repetitive patterns, at least one period of the semivariogram has to be covered by a square-image object. The solar azimuth angle of the image acquisition time has a great influence on the arrangement of shadowy areas which is a significant factor in the calculation of textures. It means that aerial images are anisotropic and directional variograms give a more exact description about the spectral variability.

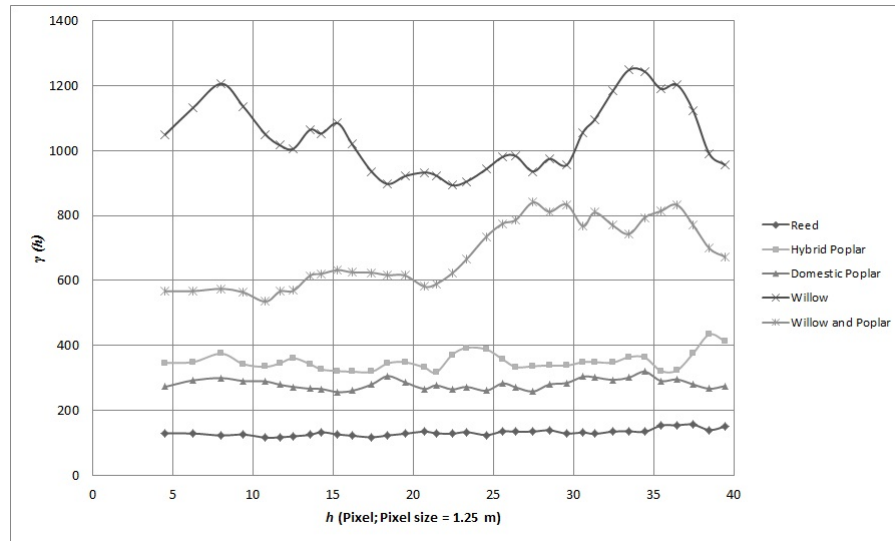


FIGURE 5.7: Directional semivariograms of the image acquired in 2008 with a solar azimuth angle of 126° for the target vegetation classes.

Directional semivariograms were computed in the R statistical software environment based on $40\text{ m} \times 40\text{ m}$ square image segments (Figure 5.6) as samples from each target vegetation class from the year 2008, based on PC1. Directional means that they have been calculated along the direction of the supposed minimum continuity (126° : the earlier mentioned solar azimuth angle) in order to describe the maximum spectral variability. After the visual interpretation of the graph (Figure 5.7) $20\text{ m} \times 20\text{ m}$ (16×16 pixels for the 1.25 m/pixel GSR) square objects were chosen concerning the optimal window size for texture analysis, which is correspondent to the findings by Tuominen and Pekkarinen (2005) applied to forest stand and bog analysis in southern Finland based on aerial photography.

GLCM needs further variables to be defined (described in Sub-section 4.3.1). For the direction of the offset the “average of all directions” and for the distance the default one (analysing direct neighbourhood) was set. Nevertheless, directional GLCMs related to the

solar azimuth angle in the different years were tested as well and analysed further in Subsection 5.1.4. Though, NIR band represents the highest reflectance values for healthy vegetation in general, it is missing in image 2005, therefore, the PC1 layer was used as basis for the calculations due to its nature of representing the maximal variability from the existing three bands in the orthophotos and hereby, providing a basis for comparable textures between the different years.

5.1.4 Feature selection

The selection of the most appropriate parameters from the numerous potential descriptors is a crucial step in any image classification approaches. Recent analysis (Kollár et al., 2011a,b) related to the current study has already proven the favourable use of GLCM texture measures for a smaller site (180 000 m²) within the same research area, where the concrete texture features were chosen after the recommendations of Hall-Beyer (2007), selecting GLCM mean, correlation and entropy (formulas are found in Table 4.1). Two other studies applied GLCM standard deviation instead of GLCM mean in the textural parameter set (Kollár et al., 2013b,c).

However, since redundant information often exists and hereby, decreases the speed of the analysis and reduces the efficiency of the classification, an objective method for parameter selection is necessary. The statistical class separability analysis (described in Section 4.4) has been found as a robust approach for selecting the most significant parameters and therefore, it was applied to the potential features (parameters/descriptors) in the current analysis, as it has been described in a recent publication (Kollár et al., 2013a). 8-8 GLCM parameters (all-directional and directional), 4-4 GLDV parameters (Table 4.1) and spectral descriptors, like vegetation indices (Table 5.2), average DN of PC1 and average DN of the Green band were analysed at the square-image objects' basis for the best separability measures. The Jeffries-Matusita (JM) separability calculation was applied to each class pair for the three different years (2008, 2005, 1999) based on a sample size of minimum 20 square image objects for each target class. Although in the literature by Congalton and Green (2009) the collection of a minimum of 50 samples for each map class is recommended as a general guideline for maps of less than 1 million acres in size and fewer than 12 classes, it could not be followed in the current study because of the relatively small test site and the 20 m × 20 m square units taken as samples.

Separabilities for class pairs in different years gave different results. Nevertheless, in order to work out a consistent analysis for the 3 years, the same textural and spectral descriptors were chosen for all the years.

From the textural parameters GLCM standard deviation, GLDV entropy, GLCM contrast and GLCM mean were chosen as the four best textural descriptors with the combination of vegetation index as the most significant spectral descriptor. In Table 5.3 JM separability values are shown for the selected (four textural and one spectral) parameters for 2008. Each texture measure represents the all-directional type. Directional GLCMs (Appendix C) did not give significantly better separabilities than the all-directional ones. Concerning the different textural parameters although GLCM mean gives a $JM \geq 1.8$ only for two class pairs, it is still significant, since it is the only one textural parameter describing separability between Hybrid poplar and Domestic poplar classes.

TABLE 5.3: Jeffries-Matusita separability analysis for the originally chosen target vegetation class pairs (Dunaremete, 2008) by the selected descriptors

	GLCM StDev	GLDV Ent	GLCM Cont	GLCM Mean	mNDVI
HP-SP	0.0	0.7	0.5	1.9	1.9
HP-W	1.9	1.6	1.6	1.4	2.0
HP-WP	1.6	0.4	0.4	0.4	1.9
HP-RD	1.8	0.9	1.0	2.0	2.0
SP-W	2.0	1.9	1.8	0.4	1.1
SP-WP	1.7	0.5	0.7	1.0	0.6
SP-RD	1.8	1.8	1.9	1.0	1.9
W-WP	0.5	1.4	1.3	0.4	0.2
W-RD	2.0	2.0	1.9	1.1	1.0
WP-RD	2.0	1.8	1.8	1.4	1.3
\sum of pairs where $JM \geq 1.8$	6	4	4	2	5

5.1.5 Classification algorithm

As it has been described in detail in Sub-section 4.5.1 the class description based fuzzy (CDBF) algorithm was applied for the classification. The selection of an appropriate number (at least 20) of vegetation samples (square image objects in that case) was a requirement to describe class characteristics by membership functions (computed from the sample statistics) concerning the earlier derived and analysed spectral and textural parameters. Classification was based on the ‘chessboard-type’ image segments. The labelling of objects depends on the highest probability derived from the membership values. Besides the here applied crisp

class assignment, probabilistic labels (classes) could be also used due to the fuzzy results for each image segment, however, this kind of analysis was not applied in the scope of this study.

5.1.6 Results

For the evaluation of classification performance appropriate accuracy assessment is inevitable (described in detail in Section 4.6). Since from the same time, as the aerial image acquisition took place, no reference map is available and it was not possible to collect reference data for the past scenes, the often used random or stratified random sampling approaches for reference sample selection could not be applied. Instead of these methods, reference samples were selected manually, based on visual image interpretation. Similarly as in the training stage of the classification, 20 m×20 m square image segments (the same number as for the training sample set and additionally 50 reference samples as background/unclassified area) were carefully chosen, not including any sample segments from the original training set. The most important accuracy measures (overall accuracy, OA and Kappa coefficient, κ) were calculated. Accuracy results are listed and compared in Table 5.4 representing the different feature sets applied to each year. Firstly the use of spectral parameters (mean of PC1 and VI) only was evaluated, then the use of 3 texture features after Kollár et al. (2013b,c), followed by the application of 4 textural parameters chosen by the Jeffries-Matusita separability analysis presented before and in the end the combination of the 4 textural parameters and the vegetation index (described in Kollár et al., 2013a). For the best classification result the complete error matrix is presented in Table 5.5. Classified maps are presented for each year (2008, 2005, 1999) separately in Figure 5.8.

TABLE 5.4: Accuracy assessment of the classification results (DR image sample for 2008, 2005 and 1999) concerning different parameter sets. OA: overall accuracy.

Aerial images	2008 (B,G,NIR)		2005 (B,G,R)		1999 (G,R,NIR)	
Features applied\Acc.measures	OA	Kappa	OA	Kappa	OA	Kappa
Mean of PC1, VI	68%	0.63	65%	0.58	64%	0.57
3 textures	72%	0.67	60%	0.53	61%	0.54
4 textures after JM	82%	0.79	77%	0.72	75%	0.71
4 textures after JM + VI	87%	0.84	83%	0.80	82%	0.78

The use of textural descriptors (defined using JM analysis) provided significant improvements (greater than 10% percent increase in overall accuracy for each year) in comparison

to the solely spectral parameter based classifications and gave better accuracies than the initially used texture measures as well. The best classification results were reached by the inclusion of both feature types, spectral and textural parameters. As spectral parameter, a vegetation index (different for each year, Table 5.2) was applied in the combined feature set. It was also tested to involve the mean (average) of PC1 as additional spectral feature as applied in the initial spectral feature set. Nevertheless, it did not improve OA in the case of the 2008 and the 1999 images, but for the 2005 RGB image the overall accuracy was enhanced with 4%. For further applications concentrating on CIR imagery the 4 textural parameters and the vegetation index is proposed.

TABLE 5.5: Error matrix for the best classification result of Dunaremete, 2008, where 4 textural parameters and vegetation index were applied.

User \ Reference class	HP	DP	W	WP	RD	Wb	Unclassified	Sum
Hybrid poplar (HP)	5072	0	0	16	0	0	768	5856
Domestic poplar (DP)	16	4864	0	0	0	0	512	5392
Willow (W)	0	0	6857	736	0	0	0	7593
Willow and poplar (WP)	16	256	752	4320	0	0	336	5680
Reed (RD)	0	0	0	0	4574	2	2032	6608
Water bodies (Wb)	0	0	43	0	41	5024	0	5108
Unclassified	16	0	28	48	505	94	9152	9843
Sum	5120	5120	7680	5120	5120	5120	12800	
Producer's acc.	99%	95%	89%	84%	89%	98%		
User's acc.	87%	90%	90%	76%	69%	98%		
Overall acc.	87%							
Kappa	0.84							

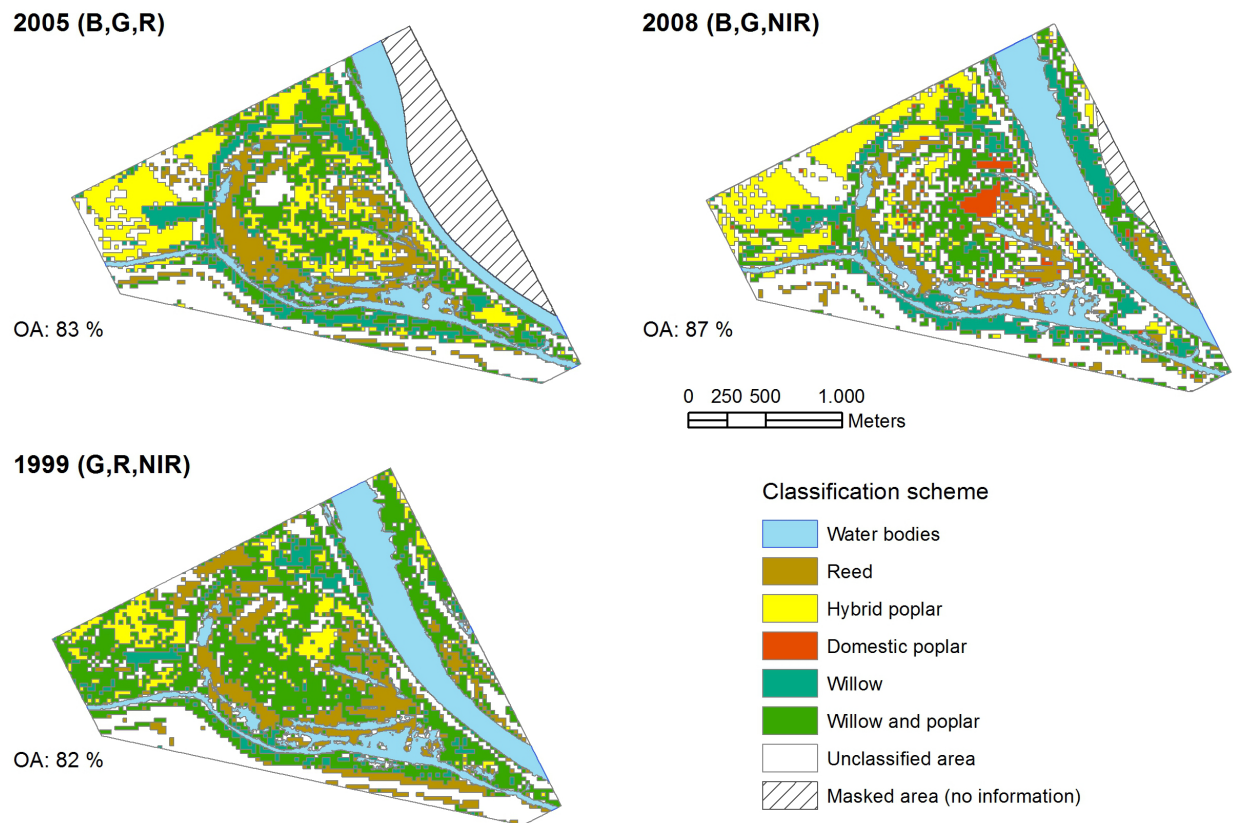


FIGURE 5.8: Classification results for DR site (2008-1999) with the application of combined (spectral & textural) feature set with a simple classification scheme based on chessboard-segments concerning vegetation classes.

5.1.7 Discussion

Vegetation classification based on chessboard-type image segments hinders the advantageous use of OBIA regarding such segmentation approaches where accurate habitat borders can be extracted from the high resolution image (e.g., the exact border of water bodies, Figure 5.3). However, multi-resolution segmentation often results in an over-segmented image, especially for those woody vegetation classes, where the shadowy areas between single tree crowns or groups of crowns (e.g., Willow and Willow & poplar habitats) have a great influence on the segments. In these cases a more compact view by the chessboard segments has been privileged and confirmed by accuracy measurements (Table 5.6). Figure 5.9 gives an example for visual comparison of different segmentation and classification results. Nevertheless, a combination between the above-mentioned segmentation types is suggested for further research.

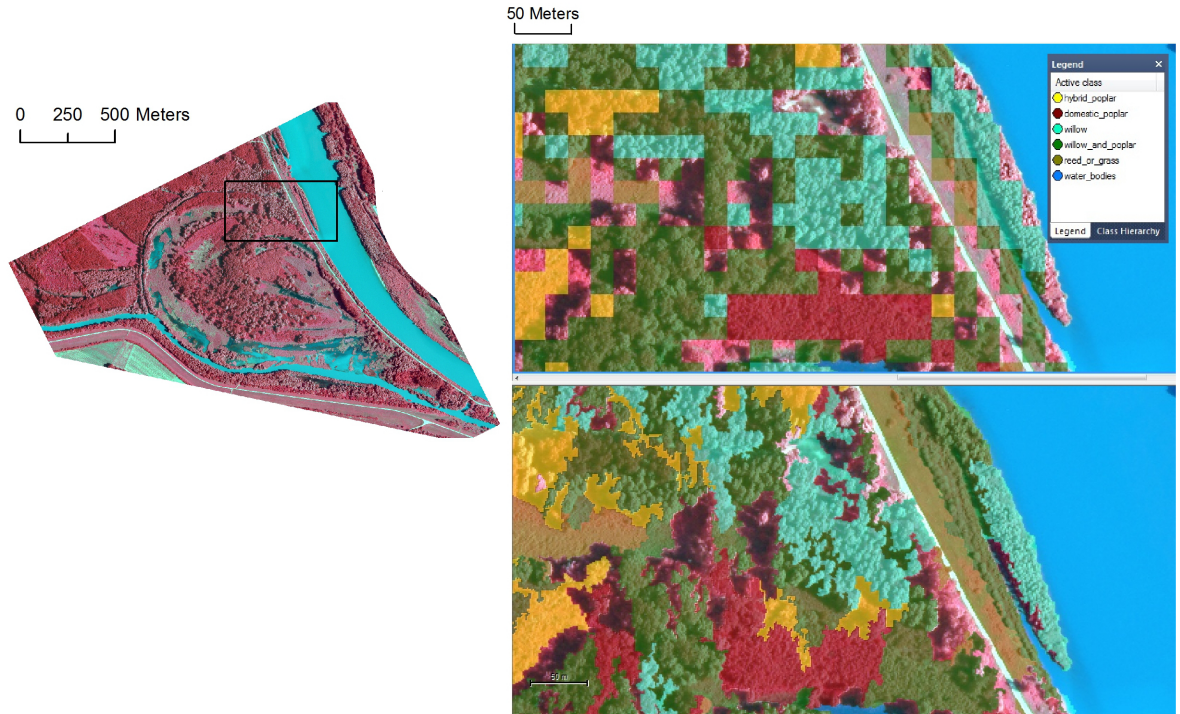


FIGURE 5.9: Comparing chessboard and multi-resolution segments from the aerial image scene of Dunaremete, 2008. Due to the transparency settings colours are brighter in the image than in the legend.

TABLE 5.6: Comparing accuracy measures for vegetation classification results based on different segmentation approaches, for the site of Dunaremete, in 3 distinct years.

Segmentation type \ Acc. measures	Aerial images 2008 (B,G,NIR)		2005 (B,G,R)		1999 (G,R,NIR)	
	OA	Kappa	OA	Kappa	OA	Kappa
Chessboard	87%	0.84	83%	0.80	82%	0.78
Multi-resolution	78%	0.74	75%	0.70	61%	0.52

Although post-classification based change detection analysis was not the focus in the current study, it would be a reasonable application to the further use of classified vegetation maps from several years. Therefore, primarily the appropriateness of the applied classification scheme and the classification accuracies had to be analysed in detail. It was seen that the overall classification accuracy decreases from 2008 to 1999 (Table 5.4), however, for each scene OA was higher than 80% in the case of applying combined feature set (including spectral and textural measures). During the development of the classification scheme, one can reconsider to merge or split classes. Looking back to the class separability analysis (Table 5.3) the unseparability of the class pair W-WP is evident, that's why the merge of these classes and its effect was experimentally investigated. The results are presented in

Table 5.7. The most significant effects of these changes are related to the class pairs HP-W and DP-W (now W means: merged WP and W), with the most significant negative changes in the JM class separability values. However, it corresponds to the expectations, since W includes now Poplar species, which is present as well in the class HP. According to that, Willow and Willow & poplar classes were handled separately in the further applications. Besides that, in each classification result (for the analysed years) more than 20% of the area remained unclassified. The question arises, whether important classes were left out at the definition of the classification scheme or the classification algorithm itself has deficiencies. A potential extension of the classification scheme is considered in the next section (Section 5.2), whereas the application of another classification algorithm is described in Sub-section 6.2.5 which is related to the transferability of the classification algorithm as well.

TABLE 5.7: Jeffries-Matusita class separability analysis in the site of Dunaremete (2008) with the merge of Willow and Willow & poplar classes (here: W), effecting the separabilities from Hybrid poplar (HP), Domestic poplar (DP) and Reed (RD) habitats. JM values are emphasized in bold for those cases where they have been decreased in comparison to the original values.

	<i>Original HP-W</i>	HP-W	<i>Orig. DP-W</i>	DP-W	<i>Orig. RD-W</i>	RD-W
GLCM STDEV	1.9	1.7	2.0	1.8	2.0	2.0
GLDV ENT	1.6	0.8	1.9	1.2	2.0	1.8
GLCM CONT	1.6	1.0	1.8	1.3	1.9	1.6
GLCM MEAN	1.4	0.8	0.4	0.7	1.1	1.2
mNDVI	2.0	1.9	1.1	0.9	1.0	1.1
Mean of PC1	1.4	0.8	0.4	0.7	1.1	1.2
Mean of G	2.0	1.7	0.3	0.4	1.5	1.4

Classification results for images acquired in different years (2008, 2005, 1999) came from independent image analyses in terms of sample selection. Due to the fact, that most of the investigated vegetation units are present in each year with slight changes (stand growth), it had to be considered whether different-year images can be analysed in a connected way. Temporal transferability analysis of image classifications is described in Section 6.3.

5.2 Classification scheme

In Sub-section 5.1.2 it has been focused only on certain vegetation habitats (based on a subjective visual recognition of characteristic vegetation patches using ancillary data), not aiming at the identification of each vegetation pattern in the test site. Therefore, a part of the area remained unclassified (in the case of DR, 2008 it was more than 30%). Defining class

labels for each vegetation pattern present in the image, and hereby, analysing the complete vegetation cover gives a better understanding about the target site and it is required for the testing of classification transferability (Chapter 6).

In the ecological community mapping study of [Rapp et al. \(2005\)](#) applied in an open and forested wetland site in the United States it has been described that the addition of new classes (i.e., using an extended classification scheme) describes the complexity of local vegetation patterns appropriately and improves the vegetation classification result.

5.2.1 Extending the classification scheme

The aerial image from 2008 for the test site of Dunaremete was applied for the investigations of classification scheme extension. Before the step of sample selection for the complementary classes, existing classes in the classification scheme had to be reconsidered. Nevertheless, due to the findings in Sub-section 5.1.7, it was reasonable to apply the originally chosen classes and complement them with additional ones.

Extending the classification scheme with classes mostly smaller in size than the earlier identified ones is not straightforward, if the time of image acquisition (2008) and the collection of ground reference information (botanical field survey, 2004) is significantly different and in this case uncertainties are expected. In order to complement the classification scheme, botanical and silvicultural maps and visual interpretation of the image were applied. A hierarchical classification scheme was built with two levels, however, the most significant one is the “detailed” level (Level II), where classes were directly distinguished based on physiological appearance and contrary to that the upper level (Level I) groups these classes by semantics only. In the study of [Johansen et al. \(2007\)](#) structural vegetation classes followed the classification scheme of Terrestrial Ecosystem Mapping derived from aerial (analogue and digital) imagery, which also helped here to find the appropriate classes for Level I.

Complementary classes to the detailed level (Level II) were partly defined using habitat maps (O10: Vegetation on edges and dams, T1: Arable land from Appendix B, Figure B.2), using silvicultural inventory (FATI1, 046: Domestic poplar-robinia; 058: Other hardwood, from Appendix B, Figure B.3) and applying visual interpretation (Road, Bare soil mixed with grass, Young stand, Shadow). Although the class of Shadow does not build a real vegetation class, its application was important, since those areas significantly vary from

other classes and have a common occurrence in the current image. The new hierarchical classification scheme is presented in Figure 5.10.

Class of water bodies was separated, as it has been described in Sub-section 5.1.1 followed by the classification of road, both based on irregularly shaped segments after the combination of quadtree and multi-resolution segmentations with the use of vegetation index (BlueNDVI) and Brightness (average DN of the bands) values in the classification.

Focusing on the classification of vegetation, class descriptions for the CDBF classification algorithm were derived based on sample objects (chessboard segments as applied in Sub-section 5.1.2) using the earlier chosen descriptors (one spectral and 4 textural parameters). In addition, a small modification was applied to the use of vegetation index. Besides the formerly chosen BlueNDVI (called as modified NDVI in Table 5.2), $\text{GreenNDVI} = (\text{NIR} - \text{G}) / (\text{NIR} + \text{G})$ was tested, since it is vital from the aspect of further analysis (temporal classification transferability) to consider transferable indices in case of images with different band combinations in different years (Table 3.1). That's why the use of GreenNDVI (with NIR and G bands) was preferable in comparison to BlueNDVI (with NIR and B bands).

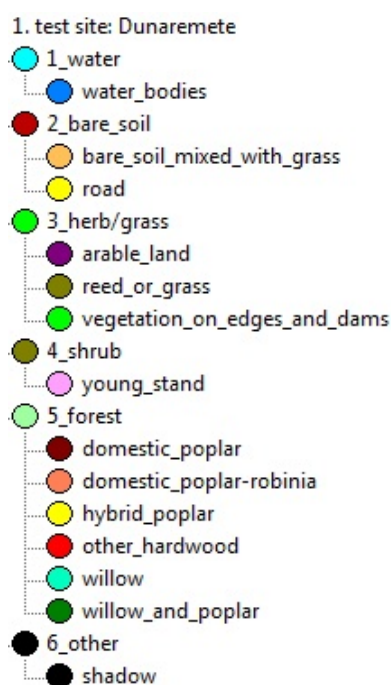


FIGURE 5.10: Hierarchical classification scheme (Level I, II) applied to the test site of Dunaremete, 2008

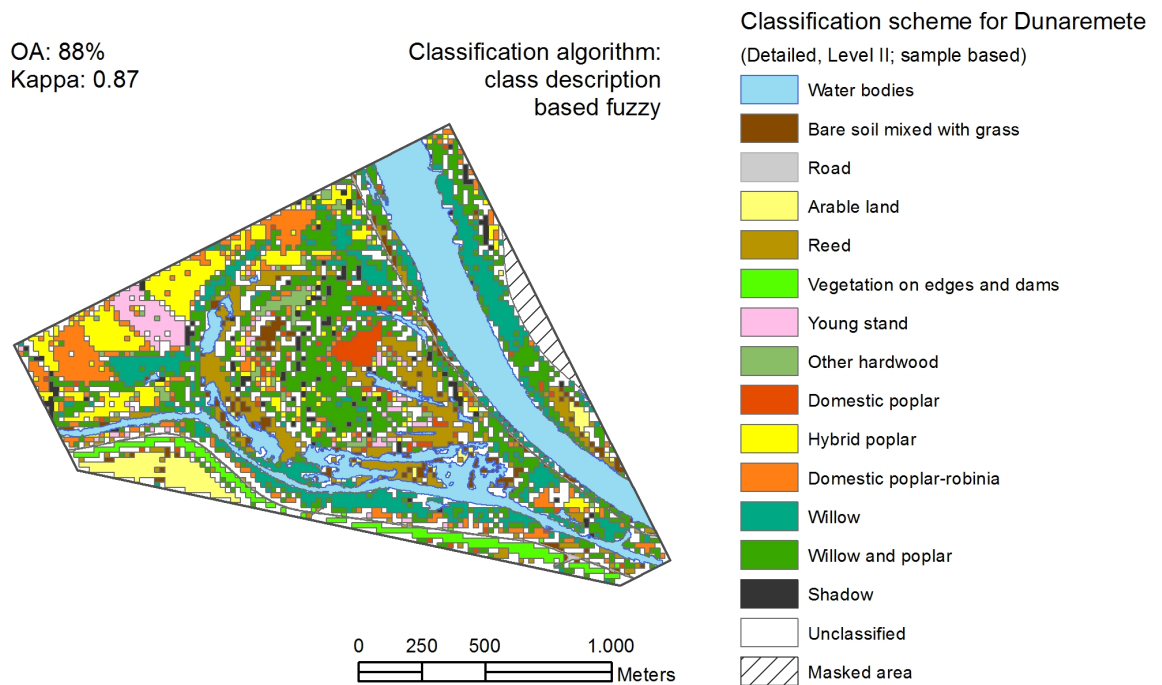


FIGURE 5.11: Classification result with the complemented classification scheme by the CDBF algorithm using GreenNDVI as vegetation index and the earlier chosen textural parameters, applied to the test site of Dunaremete, 2008

5.2.2 Result & discussion

Classification result is presented in Figure 5.11 by the class description based fuzzy algorithm with the use of GreenNDVI besides the same textural (GLCM/GLDV) features as applied previously. Around 17% of the site still remained unclassified, although this was much less than in case of the originally applied classification scheme (around 30%). The best overall accuracy was 88% and Kappa index was 0.87 (not including the class of road in the accuracy calculations because of the 20 m×20 m chessboard-based accuracy assessment method). These accuracy values are very close to the accuracy measures with the originally applied simple classification scheme (Table 5.4). The difference between the application of different vegetation indices (BlueNDVI or GreenNDVI in the combined feature set with textural measures) is summarized in Table 5.8.

An important issue regarding the classified vegetation habitats is related to classes Domestic poplar-Robinia and Hybrid poplar. Although, the mixed type of Domestic poplar-Robinia (DP-R) is only present in one compact site (Appendix B, Figure B.3), in the classification result other HP stands were labelled as DP-R. It could be established from the silvicultural

data concerning species related tree ages, that those forest stands have the same age, which is different from any other stands in the study area. Nevertheless, a statistically significant analysis for the assessment of age structure could not be carried out on that area because of the small size of the test site.

TABLE 5.8: Comparison of accuracy measures based on different vegetation indices in the combined (spectral & textural) feature set applied in the CDBF algorithm, DR, 2008.

VI in the feature set	OA	Kappa
BlueNDVI	86%	0.84
GreenNDVI	88%	0.87

Chapter 6

Classification transferability

Supervised classification algorithms as presented in Chapter 5 are always based on ‘local’ training samples directly taken from a given aerial image. However, if (1) all the test sites (different aerial images) come from the same riparian wetland area and (2) the temporal analysis is related to the recent years, where small changes are supposed, the synergic use of the derived parameters based on a principal study site, where training samples are chosen, is reasonable. The automatic application of a training image-based classification algorithm to other images can be considered as a potential image analysis method which would speed up any further investigations.

The idea of classification algorithm transfer has not been completely new in the geoinformation science. [Schöpfer et al. \(2005\)](#) have described the method of transferring classification schemes between image scenes (orthophotos) in the spatial dimension, where a classification scheme developed for a certain site was tested for another scene by importing the scheme with class descriptions without any adjustments, however, a detailed evaluation of classification quality after the transferred classification scheme and algorithm has not been the scope of that research study.

Concerning temporal transferability a recent study of [Demir et al. \(2013\)](#) demonstrated a novel approach for the detection of land cover changes based on transfer learning, where the advantage of the already available knowledge on the source image scene is taken into account for the analysis of the target image from another year.

6.1 Necessity for an objective approach

The comparability of botanical vegetation maps concerning different sites in Hungary has been an actual problem related to the vegetation database of MÉTA project (*Hu.Magyarország Élőhelyeinek Térképi Adatbázisa, Landscape Ecological Vegetation Database & Map of Hungary*, <http://www.novenyzetiterkep.hu/>), where 200 botanists have documented the vegetation heritage of the country (Takács and Molnár, 2009). According to that vegetation maps cannot be homogeneous due to those subjective factors which are considered in the mapping procedure by each of the mappers, therefore, the application of an objective analysis technique, like automated remote sensing image analysis is emerging.

On the other hand involving habitat maps of earlier monitoring into the analysis have gained significance in habitat mapping in order to better understand landscape dynamics, first of all the long-term changes and past human land use (Takács and Molnár, 2009). Nevertheless, the availability of detailed habitat maps from former times is seldom in comparison to the accessibility of archive aerial imagery, that's why their analysis offers a potential tool for the above-mentioned aims. Automated image analysis techniques help to avoid most of the subjective steps, except for the selection of representative samples needed for a supervised classification.

In the following, it was aimed at further decreasing human interaction and the related subjectivity in the image analysis procedure by avoiding sample selection in spatially and temporally more distant sites and using the known characteristics of common vegetation patterns in the classification algorithms, which were derived originally from a principal test site.

6.2 Classification transferability in the spatial dimension

For a spatial analysis of classification transferability certain requirements have to be fulfilled beforehand. The potential of classification transferability primarily depends on the representativeness of the principal site (or master scene) chosen. Furthermore, it is influenced by the remote sensing imagery applied, the location and size of the whole investigated area and related to that the variability of vegetation in the target region. Regarding the previously applied classification algorithm the use of an appropriate classification scheme is vital as

well. Related to these requirements the selected principal test site (Dunaremete) and the applied classification scheme are reviewed in the following sub-sections (6.2.1 and 6.2.2).

6.2.1 Adequacy of the principal test site

The study of Takács and Keszei (2004) has stated that the chosen square-shaped site for the botanical inventory (Appendix B, in Figure B.1) represents well the occurrence and variability of habitats in the whole Szigetköz riparian wetland. Therefore, it was assumed that the main study area selected (DR) where the first analyses were carried out based on the aerial photo (although smaller in size - related to the limited access to aerial images) is potential as ‘master scene’ for the further investigations. The three test sites, respectively the aerial images (DK, DR, ASV in Figure 3.3) don’t cover a connected area, however, all the sites belong to the same riparian wetland and have similar sizes. The images come from the same aerial image acquisition, where the studied region was overflowed on the same day (06.08.2008) within some hours under the same weather conditions. In summary, it was reasonable to test the transferability of classification algorithm developed for the principal site (DR, 2008).

6.2.2 Applied classification scheme

Before applying classification algorithm transfer to the new sites, information on the detailed vegetation cover (Level II) concerning those areas is required. Since reliable botanical maps were not available for them, image classification was carried for the aerial images of those sites by CDBF algorithm (similarly like in the case of DR, Chapter 5) using silvicultural information and visual interpretation, where OA was higher than 90%. However, having in mind that afterwards instead of independent analysis, it is going to be tested, whether similar habitats can be identified in other sites based on the master scene, the detailed classification scheme(s) (Level II) for the individual test sites were compared in Table 6.1. Besides that, in Figure 6.1 the three test sites are presented based on Level I (the generalized, unique classification scheme).

Separate classification results based on a unique classification scheme for the 3 test sites in the Szigetköz Danubian floodplain

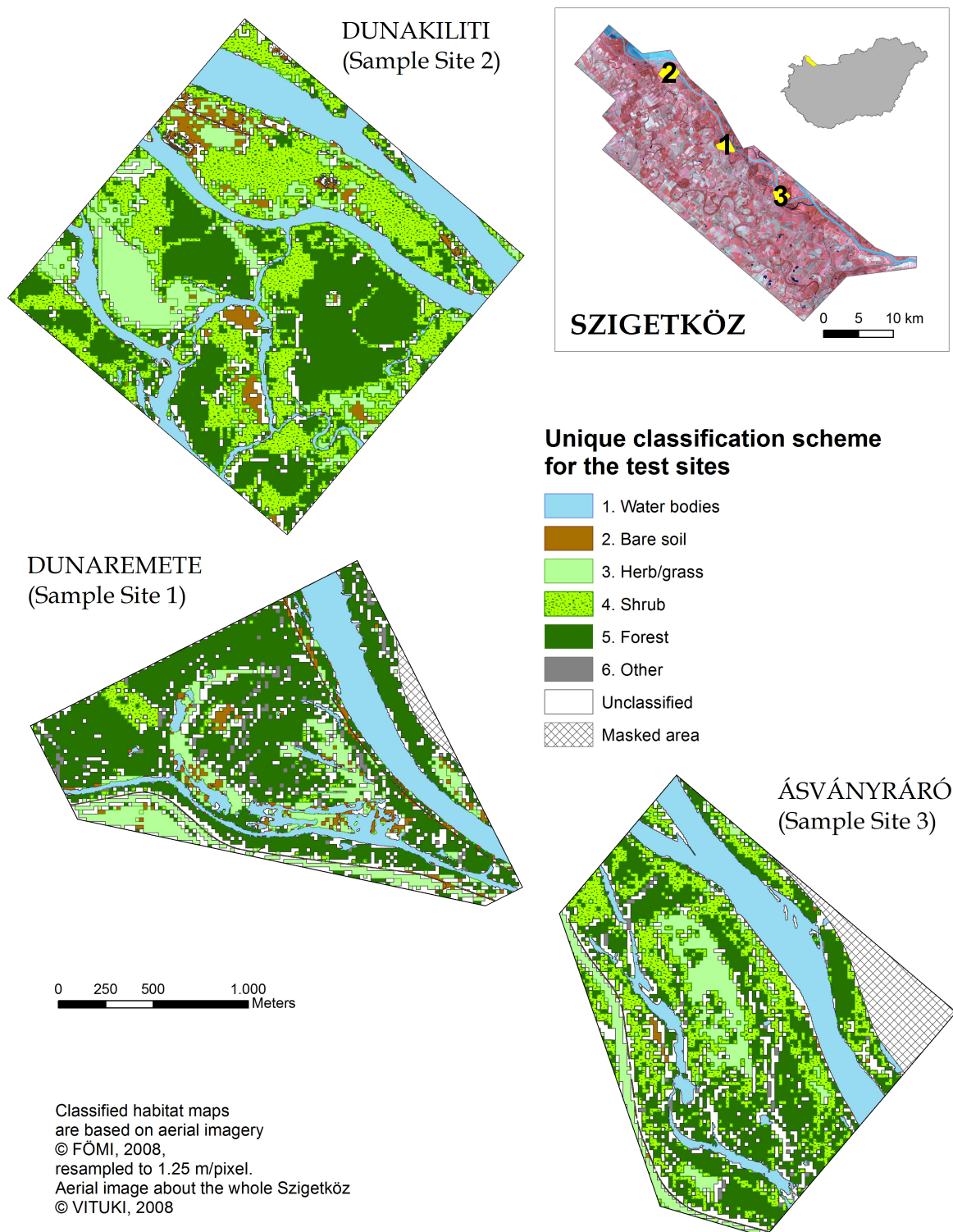


FIGURE 6.1: Application of a unique classification scheme based on separate classifications of the images from 2008, for the three sample sites (DK, DR, ASV).

TABLE 6.1: Comparison of two-level classification scheme for the 3 test sites (Dunaremete, Dunakiliti, Ásványráró, 2008). *Non-ch.: non-characteristic.

	DR (2008)	DK (2008)	ASV (2008)
Level I	Level II	Level II	Level II
1. Water	Water bodies(Wb)	Wb	Wb
2. Bare soil	Road	Road	Road
	Bare soil mixed with grass(BSG)	BSG	BSG
3. Herb/grass	Arable land		
	Reed		Reed
	Vegetation on edges and dams(VED)	VED Non-ch.* grass	VED
4. Shrub		Non-ch. shrubby(NS)	NS
	Young stand(YS)	YS	
5. Forest	Domestic poplar(DP)		DP
	Hybrid poplar(HP)	HP	HP
		Robinia	
	Other hardwood		
	Domestic poplar-robinia		
	Willow(W)	W	W
	Willow & poplar(WP)	WP	WP
6. Other	Shadow(SH)		SH

Nevertheless, since the development of the spatially unique classification scheme for the 3 test sites (Figure 6.1) was solely based on semantics and not on the analysis of image patterns (textural and spectral characteristics), transferred image classifications could not be applied.

Based on the overview about the detailed vegetation classification in the other two study areas (DK, ASV) in comparison to the principal test site (Table 6.1), the occurrence of the same or similar classes present in DK and ASV test site could be established.

6.2.3 Expected results

It was expected that for the new test sites (DK, 2008 and ASV, 2008) those classes which have been defined as ‘identical’ in Level II to those from DR, 2008 could be potentially classified by a certain classification algorithm transfer with appropriate accuracy. These vegetation classes after Table 6.1 for *Dunakiliti site* were the following 5 classes (not taking into account Water bodies): Bare soil mixed with grass (BSG), Vegetation on edges and dams (VED), Young stand (YS), Hybrid poplar (HP) and W/WP (Willow or Willow &

poplar). For *Ásványráró site* the following 6 classes were found as identical: BSG, Reed, VED, DP, HP and W/WP. It would have been difficult to identify class of Willow or Willow & poplar separately (as originally defined in Dunaremete), nevertheless, transferability could be tested by using the merge of those.

Additionally, the optimal case (with a minimum change in the classification algorithm and the primarily applied classes) would be that the new classes differing from those present in the original classification scheme (applied to DR) remain unclassified and those vegetation patches which occurred only in the master scene shall not be used as class labels for any of the segments in the new test sites. Nevertheless, misclassification was supposed due to the similarity of several vegetation classes considering the applied spectral and textural features.

6.2.4 Difficulties with the CDBF classification algorithm

Applying a certain supervised classification algorithm from the source image scene to other scenes is not straightforward.

The following example in Figure 6.2 (right-hand side) represents the first ‘transferred’ classification result for the site of Dunakiliti (DK), where the original CDBF classification algorithm (based on DR, 2008) was applied to the chessboard-segmented image scene of DK after the segmentation and classification of Water bodies. The extended classification scheme (Figure 5.10) was transferred, however, in the representation only those classes are found, which were defined as identical in Table 6.1.

On the left side of Figure 6.2 the CDBF classification based on local training samples can be seen for visual comparison. The classification result with transferred CDBF represents only those selected classes, which were appropriate for the current scene defined by Table 6.1, which means BSG, VED, HP and W/WP (not including Young stand because of its small extent). A slight modification was taken regarding W and WP habitats (identified in Dunaremete, see in Figure 5.8), since their separate recognition in the new site (DK) was difficult, hence, they have been merged.

After visual interpretation of the transferred classification result it can be stated, that although parts of the Hybrid poplar and Vegetation on edges and dams classes were detected by the current approach, it was supposed that the noticeable misclassification and omission

errors refer to the drawback of the certain classifier. Therefore, it was crucial to review the nature of the applied class description based fuzzy algorithm.

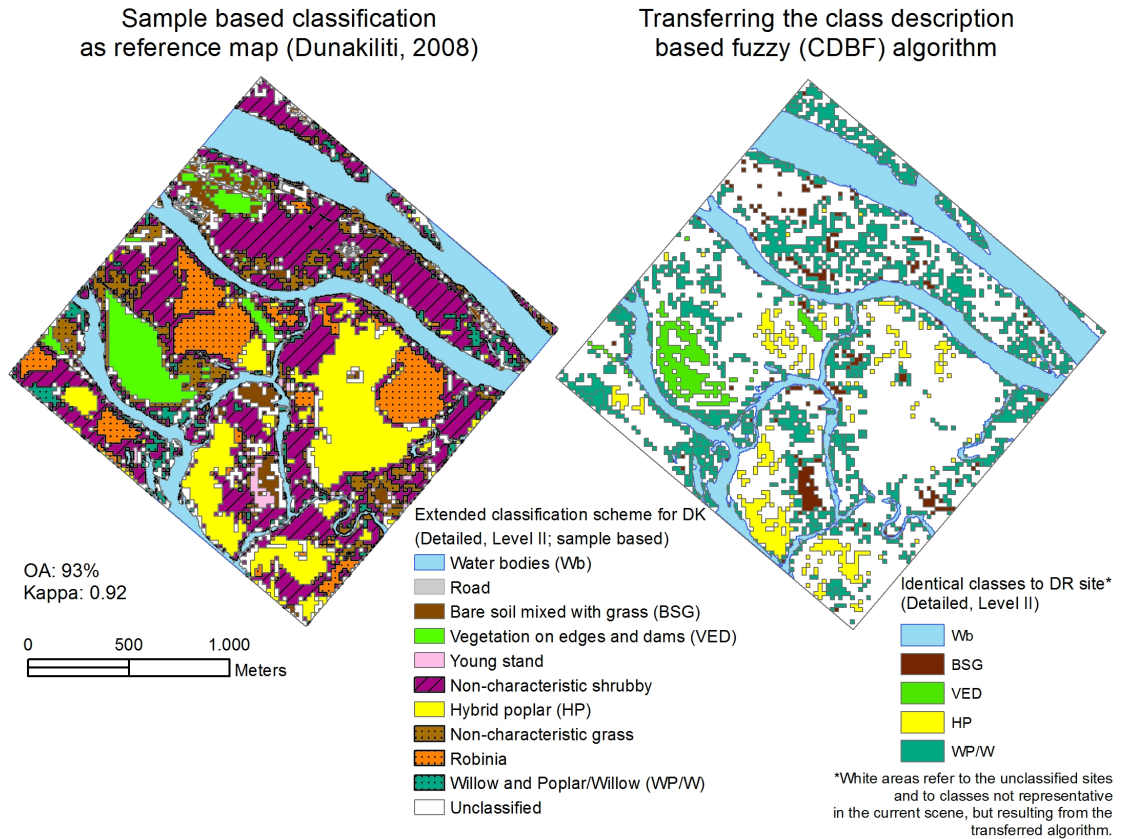


FIGURE 6.2: Transferred CDBF classification algorithm originally based on DR, 2008 applied to the test site of Dunakiliti, 2008 (right-hand side) in comparison to the training sample based classification of DK (left-hand side). The representation of the transferred CDBF classification includes only the ‘identical’ classes between the two test sites.

During a CDBF classification each target class is characterized by a class description which means a set of features (parameters) with feature value ranges (as written in Sub-section 4.5.1, see an example in Figure 4.3). Feature values for those parameters are described by membership functions (based on training sample sets), where the membership to the class is described by a statistical curve, which has its start- and endpoint in $y = 0$ which means the zero membership to the target class at those x (feature values of the discussed parameter). In other words it means that class descriptions for target classes consist of ‘closed intervals’ and slight changes in feature value ranges can already cause that certain image segments cannot be classified to a given class. This happens also due to the settings of class evaluation, i.e., whether a certain image object is classified into a given class according to the

membership functions per each feature building up a class description. The class evaluation value determines whether a certain image object can be classified to a specific class and it is between 0 and 1 (like 0% and 100%). The class evaluation value describes the most critical membership value from the chosen features in the class description for the current image segment. It is an important issue regarding the CDBF algorithm, that after default settings whenever a given feature in the class description has an evaluation value less than 0.1 (10%), the image object remains unclassified. This fact has also a great influence on the classification result.

6.2.5 Decision tree approach

6.2.5.1 Application to the main test site

Due to the above-described drawback of the applied CDBF classification algorithm another type of supervised classification algorithm was investigated, firstly based on the same principal test site of Dunaremete (2008). Furthermore, the approach was concentrating on the classification of vegetation habitats, where the classified Water bodies and Road classes were directly taken from the previous classification result (Figure 5.11).

Decision tree classifier (DT; described in detail in Sub-section 4.5.2) was applied to the scene based on the earlier chosen spectral and textural (GLCM/GLDV) features concerning the 20 m×20 m image objects from the chessboard segmentation. Accuracy measures (OA, Kappa) for the classification result were calculated and compared to the result from the CDBF algorithm, presented in Table 6.2.

TABLE 6.2: Comparing accuracy measures for the classification results based on different classification algorithms (class description based fuzzy: CDBF and decision tree: DT) regarding the test site of Dunaremete, 2008.

Classification method	OA	Kappa
CDBF	88%	0.87
Decision tree	90%	0.89

The decision tree approach showed a slightly higher accuracy, however, the difference between the originally applied CDBF algorithm and DT was not significant: not more than 2%. Classified maps after the CDBF algorithm and the DT classifier are presented in Figure 6.3.

Comparison of classification results based on the test site of Dunaremete (2008)

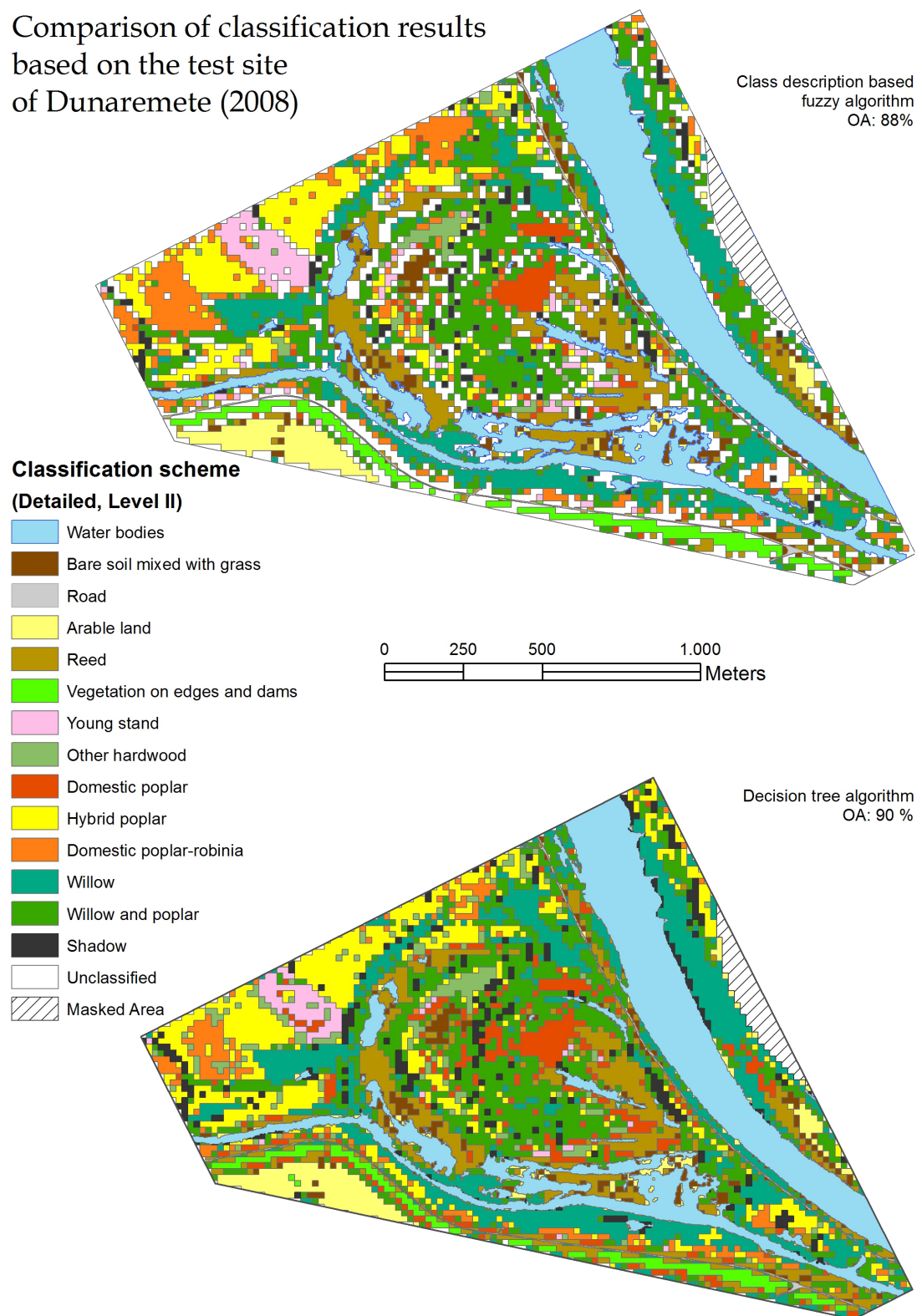


FIGURE 6.3: Comparison of classification results based on different supervised classification algorithms, applied to the test site of Dunaremete, 2008.

With the application of the DT approach no unclassified area remained, whilst in case of the CDBF classification approximately 17% of the test site was still unlabelled (Figure 6.3). Another advantage of the DT algorithm is the computation of a tree structure where the target classes appear at the end leaves and the decision rules with the applied parameters and their ‘separating’ values in the internal nodes (explained in detail in Sub-section 4.5.2), which can be directly tested for other study sites.

The current decision tree computed from the training sample set and applied to the site of Dunaremete (2008) is presented in Figure 6.4.

Since the decision tree classification algorithm gave promising results for the principal test site regarding classification accuracy and the presence of no unclassified objects, its application for spatial transferability was tested in the following Sub-section 6.2.5.2.

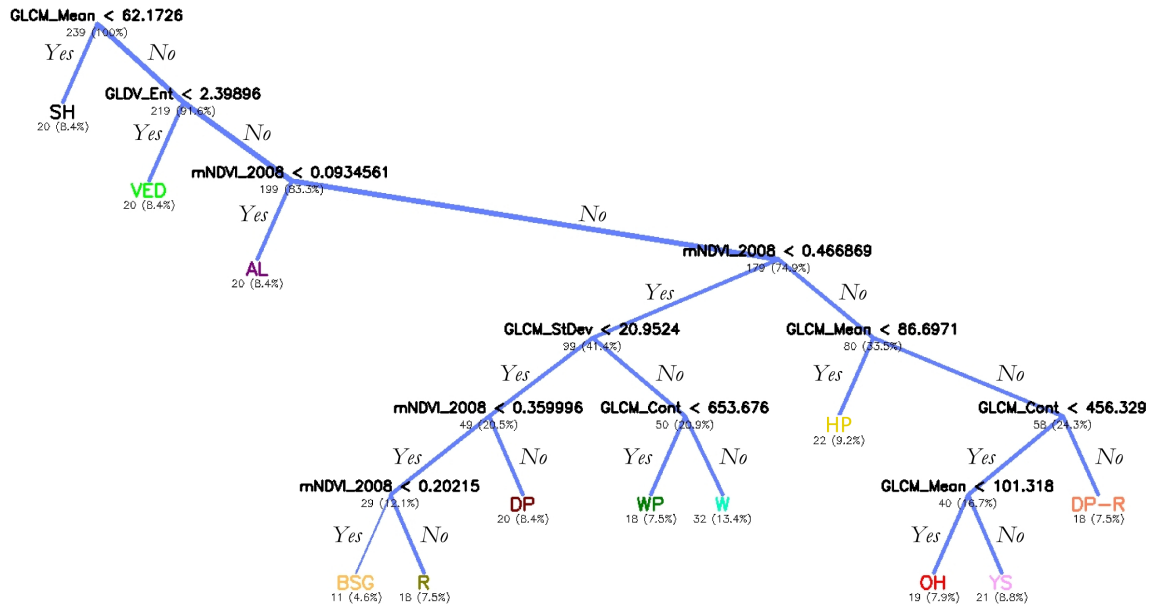


FIGURE 6.4: Structure of the decision tree computed in eCognition Developer based on the test site of Dunaremete (aerial image scene from 2008) with the extended classification scheme. Class abbreviations at the end leaves: SH:Shadow, VED:Vegetation on edges and dams, AL:Arable land, BSG:Bare soil mixed with grass, R:Reed, DP:Domestic poplar, WP:Willow & poplar, W:Willow, HP:Hybrid poplar, OH:Other hardwood, YS:Young stand, DP-R:Domestic poplar-robinia.

6.2.5.2 Analysis of classification algorithm transfer

For the testing of vegetation classification transferability decision tree algorithm defined for DR site was applied to the chessboard-segmented images (site of DK, ASV) after the

separation of Water bodies and the classification result was compared with a reference sample set defined by visual interpretation and silvicultural information for accuracy assessment. A general flowchart regarding the here applied methods is presented in Figure 6.5.

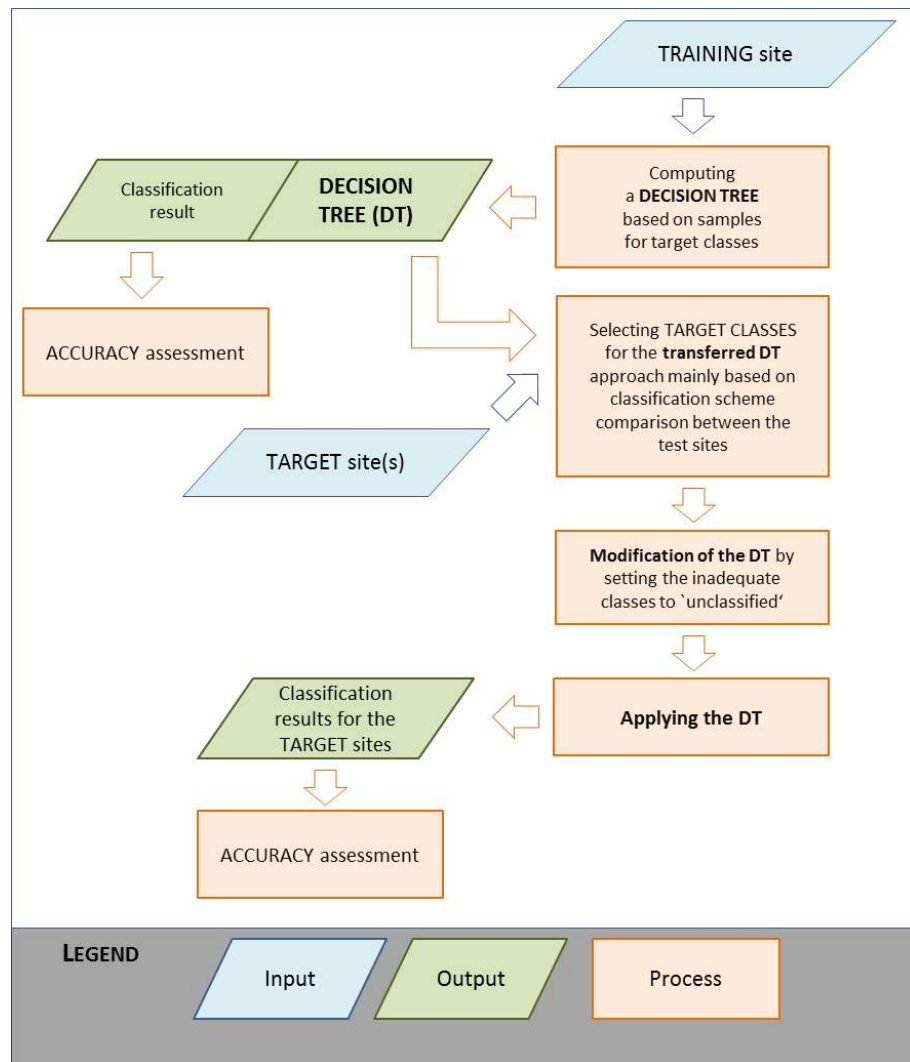


FIGURE 6.5: Methods applied for the analysis of decision tree transfer from the training site to the target sites

Application to the site of Dunakiliti Due to the difficulty of visual interpretation and the poor overall accuracy of the classified results based on the original classification scheme (originated from the site of Dunaremete), the above-presented decision tree (Figure 6.4) was slightly changed setting the non-representative classes (in DK) at the end leaves to ‘Unclassified’. From the representative classes (summarized in Sub-section 6.2.3) further three

classes (BSG, W/WP and YS) were excluded from the current analysis due to misclassification issues and besides, that they are smaller than 150 000 m² (calculated from the sample based classification).

The result of the adapted decision tree algorithm is found in Figure 6.6 (right-hand side), where the overall accuracy is 91%. Into the accuracy assessment besides reference samples for the target vegetation classes, samples for Water bodies and Unclassified area (as background) were included as well. Confusion matrix with the selected classes is represented in Table 6.3. In the case of HP class both accuracies (producer's and user's) were higher than 85%, which showed its potential for further investigations. Nevertheless, since the producer's accuracy for VED was under 60% its automatic classification could not be considered as acceptable for further analysis.

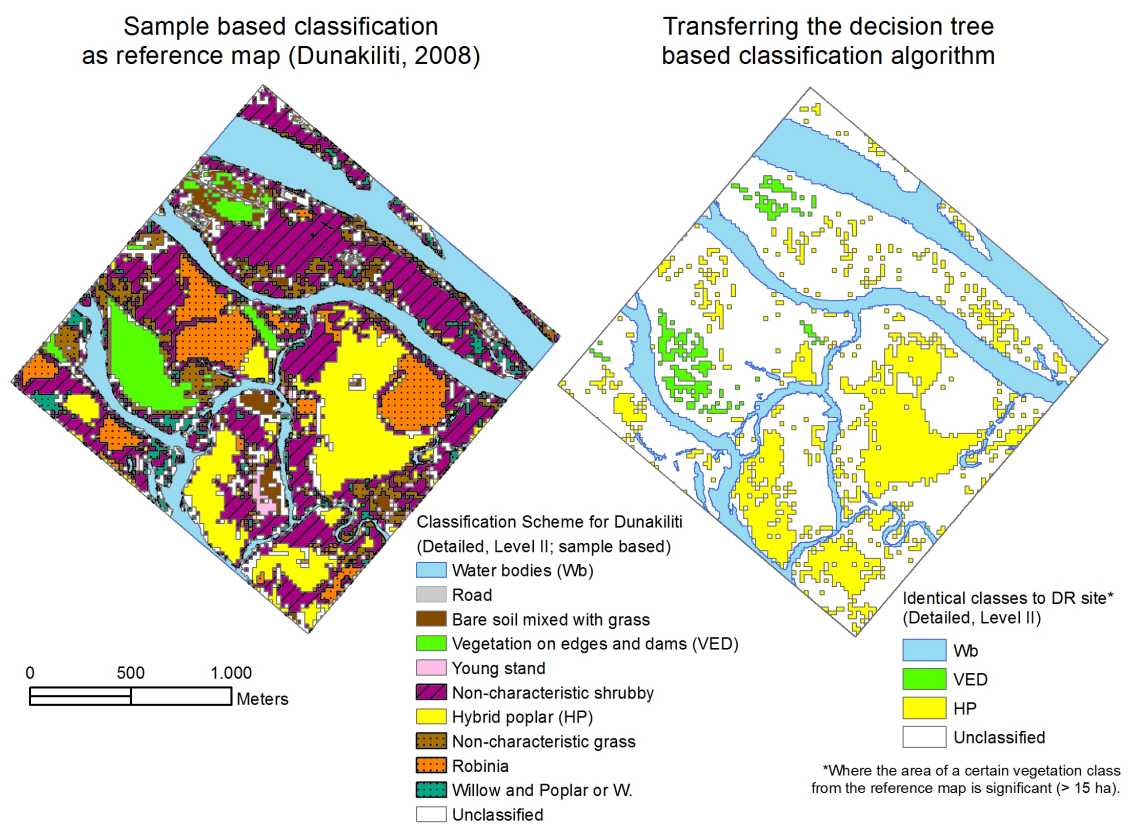


FIGURE 6.6: Classification result after transferring DT algorithm to the scene of Dunakiliti (2008), representing only the identical classes with a significant occurrence (size).

TABLE 6.3: Error matrix for the classification of selected classes in the site of Dunakiliti (aerial image scene from 2008) based on the application of transferred decision tree.

User \ Reference class	Wb	Uncl.	VED	HP	Sum
Water bodies (Wb)	5120	2	0	0	5122
Unclassified (Uncl.)	0	23806	2304	1024	27134
Vegetation on edges and dams (VED)	0	0	2816	0	2816
Hybrid poplar (HP)	0	256	0	6656	6912
Sum	5120	24064	5120	7680	
Producer's acc.	100%		55%	87%	
User's acc.	100%		100%	96%	
Overall acc.	91%				
Kappa	0.85				

Application to the site of Ásványráró In case of the ASV site, the following three vegetation classes: Reed, Hybrid poplar (HP) and Willow/Willow & poplar (W/WP, considered as a merged class) were analysed with the transferred decision tree, since they appeared similar to those classes present in the master scene of DR site (after Table 6.1) and besides, they have a significant size ($>150\,000\text{ m}^2$, calculated based on silvicultural information and sample based classification result).

Using the analogy of the application to the site of Dunakiliti, end nodes in the decision tree (Figure 6.4) were only taken into account for the recently defined three target classes (class of Water bodies was segmented and classified beforehand). For the excluded classes end leaves were set to 'Unclassified'.

After accuracy calculations with the selected reference samples OA value (61%) showed a poor agreement for the classification results, mainly caused by the omission error of Reed class and the low user's accuracy for W/WP. In the case of Hybrid poplar habitat although both accuracy values (producer's: 71%, user's accuracy: 75%) were higher than the OA, they were much lower than the same values in case of Dunakiliti. These results concerning low accuracies are discussed in the following Sub-section 6.2.6.

6.2.6 Results and discussion

The above-described findings showed that transferring DR-site-based decision tree algorithm gave promising results for the detection and classification of Hybrid poplar class in the study

site of Dunakiliti. However, in the test area of Ásványráró the same approach was less reliable based on lower accuracy results.

Regarding the user-defined Hybrid poplar class in the different test areas, pattern differences could be detected by visual comparison. However, for an objective judgement the review of the originally applied silvicultural reference data with Forest Stand Type (FST) information (*Hu.FATI1*, Appendix B, Figure B.3) was crucial.

In the ASV site the user-defined Hybrid poplar class is described by four FSTs: Hybrid poplar (FATI1:059), Domestic poplar-Hybrid poplar (DP-HP, FATI1:060), Other wood-Hybrid poplar (OW-HP, FATI1:062) and Hybrid poplar-Domestic poplar (HP-DP, FATI1:067), where from the listed stands around 40% belongs to the Hybrid poplar FST. Besides, pattern variation seems to be high for the Hybrid poplar FST, which could be explained by the age structure. But since tree age information from the National Forest Inventory does not refer to those stands represented in Figure B.3, its detailed analysis was not involved in the current study. For the principle test site (DR) around 50% of the occurring FSTs belongs to the Hybrid poplar FST, which was also taken into account for the earlier training sample selection regarding the user-defined HP class. It means that for the decision tree computation only 50% of the HP-class-related training samples were chosen from the HP FST, whilst the other samples were HP stands mixed with other types. In contrast, for the test site of Dunakiliti Hybrid poplar FST is represented by approximately 80%.

According to that the application of complementary analysis with the change of training and target sites (mentioned-above in Figure 6.5) was essential. Therefore, new decision trees had to be computed for DK and ASV sites, as training sites and in the transfer analysis to the other study areas the focus was put on the classification of Hybrid poplar class (based on the findings in Sub-section 6.2.5.2), applied as an ‘active’ end leaf in the DTs. Small modification was done concerning the feature set applied in the decision tree computations, where BlueNDVI or GreenNDVI was tested as vegetation index, besides the unchanged textural parameters. For accuracy assessment a reference set of Water bodies, Hybrid poplar and ‘Background’ classes were used for each study site separately, regarding those cases where the transferred DTs have been applied. Producer’s and user’s accuracies concentrating on the Hybrid poplar class are summarized in Table 6.4. Concerning the training site as source for the DT computation, OA values were also calculated for those test

areas and are presented in Table 6.4. Best results came from the transfer of the DK-training-site-based decision tree with the application of BlueNDVI as vegetation index (Figure 6.7).

Based on the above-described complementary analysis it is concluded that the detection and classification of the user-defined Hybrid poplar class with transferred algorithm(s) is the most reliable (PA and UA measures are $\geq 90\%$), when the training samples only include the Hybrid poplar Forest Stand Type. In the current study it means the application of DK-training-site-based decision tree to the target sites (DR, ASV), presented in Figure 6.8. From the aspect of further analysis the use of BlueNDVI in the feature set for DT computation is decisive for the detection of Hybrid poplar stands.

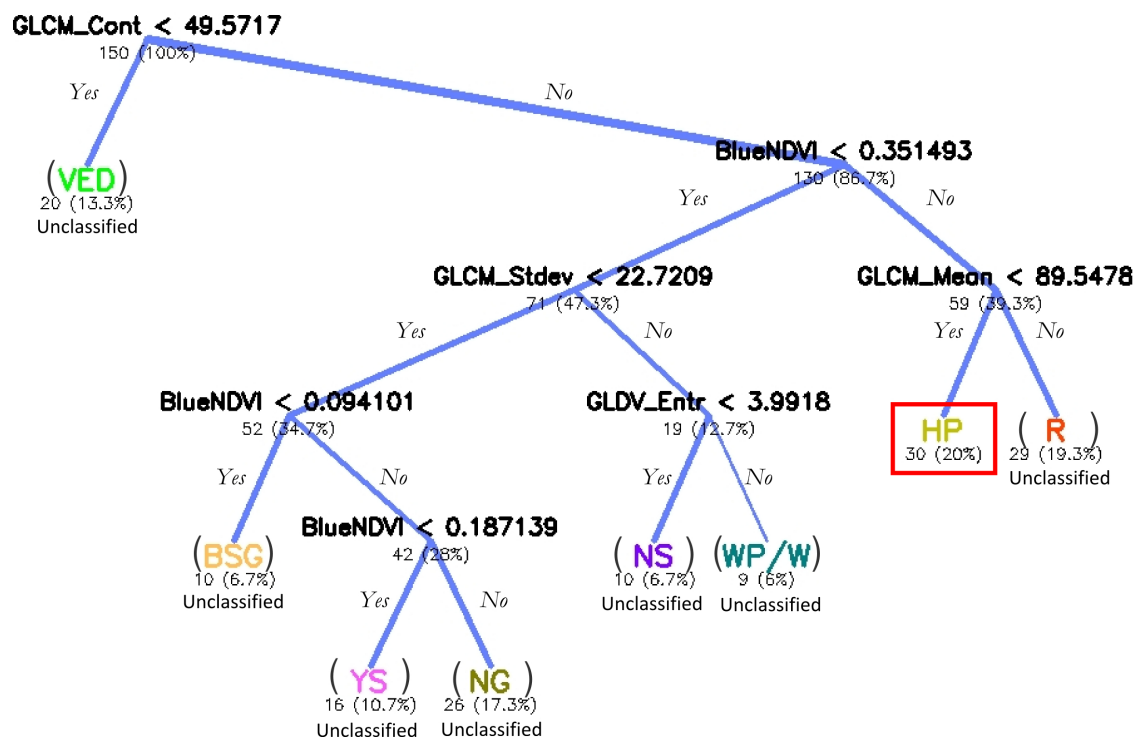


FIGURE 6.7: DK-training-site-based decision tree. New vegetation classes (not used in the site of DR) are NG: Non-characteristic grass, NS: Non-characteristic shrubby, R: Robinia. However, except for Hybrid poplar class all the others are set to Unclassified in the DT-transfer approach.

Furthermore, focusing on the detection of a single vegetation habitat (Hybrid poplar stands in the current study), it was reasonable to complement the analysis of the original DT computed for DK, 2008 (Figure 6.7) with the computation of a new decision tree, where target classes were Hybrid poplar and Background (training samples from every other type of vegetation classes were merged into the class of Background). It means that Hybrid poplar

was exclusively separated by the computed decision tree without further modifications in the end leaves regarding the settings of irrelevant classes. The new decision tree (Figure 6.9) included only the BlueNDVI feature, although each of the 4 textural parameters were chosen in the initial parameter set for decision tree computation. Accuracy measures (Table 6.5) showed that PA and UA were $\geq 87\%$ in each case concerning the training site (DK) and the target sites (DR and ASV). Although the application of the original decision tree algorithm generally gave a better classification performance for the detection of Hybrid poplar stands, the recent application is considerable for further use, since it provides a faster analysis method.

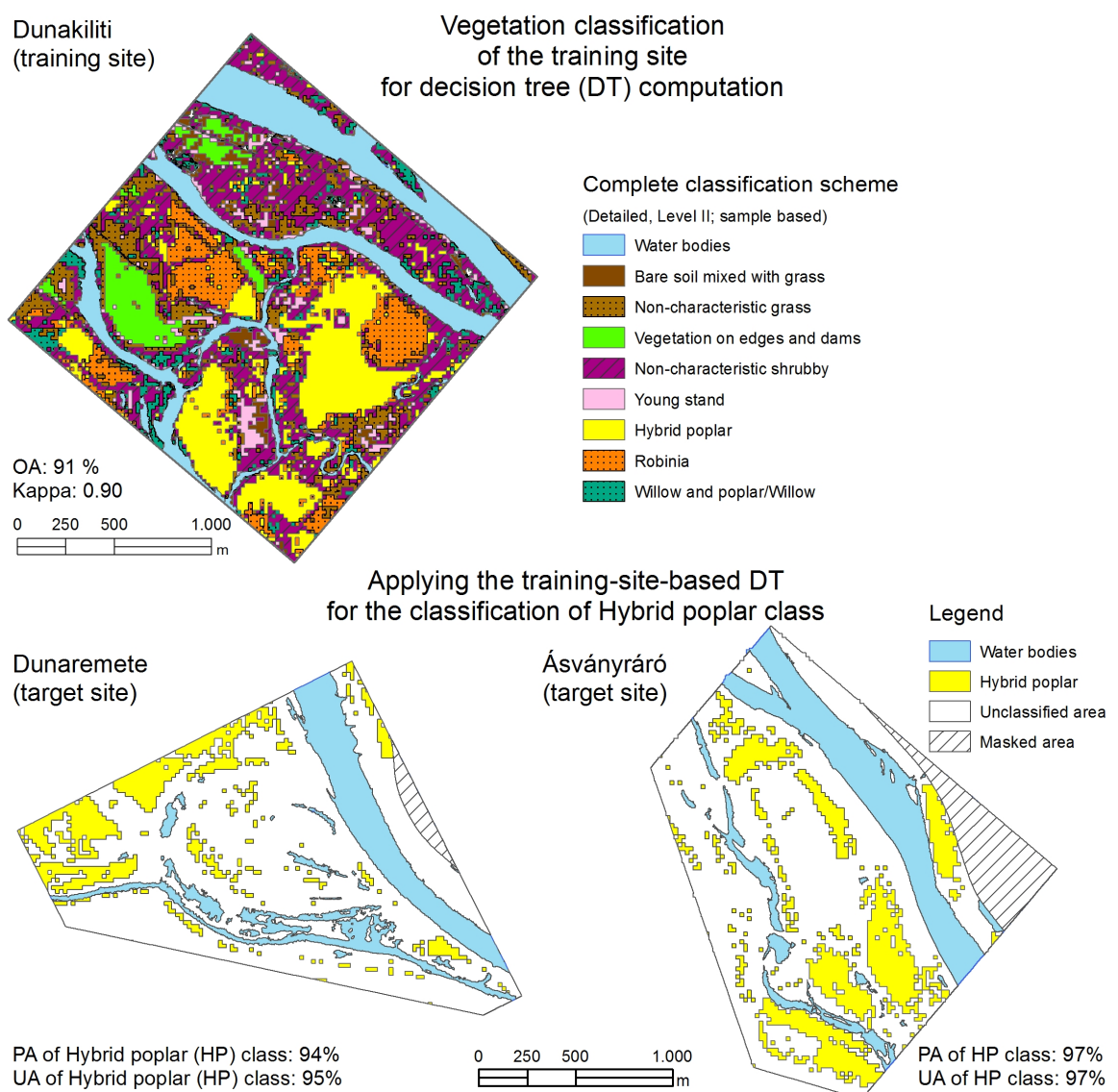


FIGURE 6.8: Transferring the DK-training-site-based decision tree to the other test sites (Dunaremete and Ásványráró), where the DT shown in Figure 6.7 is applied.

TABLE 6.4: Accuracy measures for the classification of user-defined Hybrid poplar class, based on different decision tree transfers. The column VI applied means the certain vegetation index (VI) which was used in the feature set for DT computation. PA stands for producer's, UA for user's accuracy. Ts: training site, Ns: new site.

Training site	VI applied	New site	PA(Ns)	UA(Ns)	PA(Ts)	UA(Ts)	OA(Ts)
Dunaremete	G NDVI	DK site	87%	96%	73%	96%	90%
	B NDVI		80%	100%	73%	92%	84%
	G NDVI	ASV site	71%	75%			
	B NDVI		71%	61%			
Dunakiliti	G NDVI	DR site	15%	76%	87%	100%	88%
	B NDVI		94%	95%	90%	100%	91%
	G NDVI	ASV site	97%	95%			
	B NDVI		97%	97%			
Ásványráró	G NDVI	DK site	83%	93%	97%	92%	89%
	B NDVI		83%	96%	97%	97%	90%
	G NDVI	DR site	5%	100%			
	B NDVI		14%	98%			

TABLE 6.5: Comparison of accuracies for the application of modified decision tree based on the site of Dunakiliti, applied to the 3 different test sites. Modification means the change of the classification scheme, focusing on the separation of Hybrid poplar stands only.

Training site for DT	PA	UA
Dunakiliti	93%	88%
Target sites for DT		
Dunaremete	94%	87%
Ásványráró	89%	94%

In summary, if training samples are taken only from those forest stands where the FST is Hybrid poplar, not mixed by other type of wood, the training-site-based decision tree classifier is applicable for the classification of the generally meant (user-defined) Hybrid poplar stands (also including the mixed FST, e.g., Domestic poplar-Hybrid poplar). Besides, the application of BlueNDVI (with NIR and B bands) instead of GreenNDVI (with NIR and G bands) applied to the NIR-G-B imagery (2008) in the decision tree approach is essential for the appropriate detection of Hybrid poplar stands in other images by the transferred method.

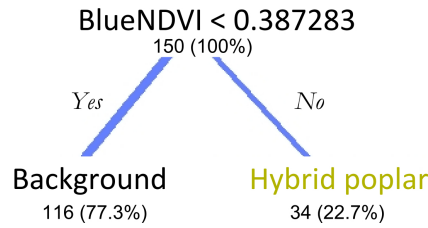


FIGURE 6.9: Modified decision tree focusing on the separation of Hybrid poplar based on the site of Dunakiliti, 2008.

6.3 Classification transferability in the temporal dimension

In Section 5.1 aerial image-based vegetation classifications with the ‘simple’ classification scheme have been presented for a concrete site for three different dates independently, where during this time period (1999-2008) vegetation cover did not change rapidly in general. It means that most of the classes analysed for the different dates separately are detectable in each year. This fact provided the basis for the following attempt, where it was aimed at transferring the classification algorithm defined for the most recent year (2008) to the former time(s), concentrating on the test site of Dunaremete. Applying such a method a further step can be taken towards an objective automated analysis in time, where the advantage of avoiding the time consuming and possibly inconsistent training sample selection is vital.

Since it was proved in Section 5.1 that the combined use of textural and spectral parameters give the best classification results, it was important that the analysed images have similar spectral resolution for the appropriate transfer of vegetation index. Therefore, it was supposed that the application on the 2005 (RGB) image without vegetation index would be difficult. It was assumed that for those aerial image scenes, where the spectral and geometric resolutions are the same or very similar and the image acquisition time interval is not longer than 10 years certain vegetation patches can be detected and mapped with appropriate accuracies. It was supposed that the direct application of spectral characteristics (e.g., vegetation index) plays an essential role in the separation of water and vegetation (Sub-section 6.3.1). Nevertheless, it was described in detail after that, whether the use of vegetation index is needed for the transferred vegetation classification algorithms.

6.3.1 Separation of water bodies

The classification of water bodies by vegetation indices after segmentation was applied independently to the images (2008, 2005 and 1999) in Sub-section 5.1.1. In each case a different index was used due to the fact of altering band combinations by different image acquisitions. Nevertheless, by changing the index applied to 2008 to $(\text{NIR}-\text{G})/(\text{NIR}+\text{G})$ (GreenNDVI, also mentioned before in Sub-section 5.2.1) the same index can be applied to the image of 1999 in an automated way. Thus, a combination of GreenNDVI and Brightness (average DN of the three bands) was applied in the class description (Figure 6.10) for the unique classification of segments into the class of water bodies.

Besides class of water bodies, class of road was classified beforehand applied to segments from the multi-resolution segmentation, since its separation was simply based on the GreenNDVI and Brightness values similarly as applied in Sub-section 5.2.1. It helps to avoid the potentially misclassified image objects later, along the road. Nevertheless, class of road is not represented in some of the figures because of its small extent.

Afterwards in the main part of the analysis class of water bodies and road were handled as already known (masked) and they were not included in the investigations.

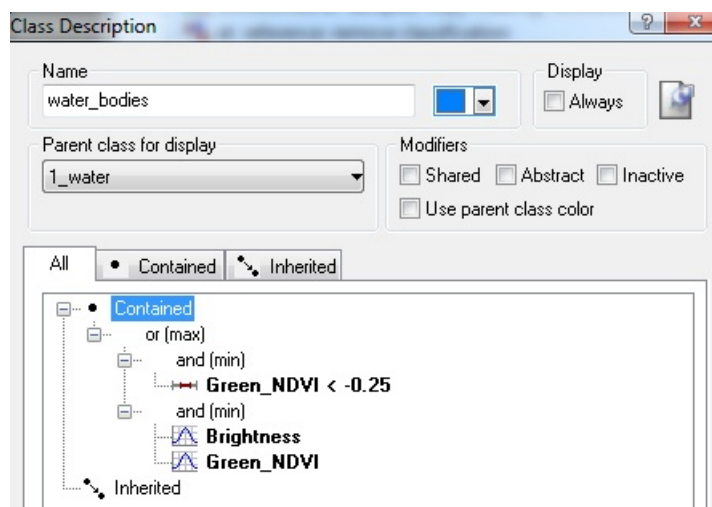


FIGURE 6.10: Class description of water bodies applied to the 2008 and 1999 image scene in the site of Dunaremete. Feature value range in the second *and(min)* expression (which means both have to be fulfilled in the same time) are $20 \geq \text{Brightness} \leq 90$ and $-0.25 \geq \text{GreenNDVI} \leq 0.1$.

6.3.2 Transfer of classification algorithms

Transferring the class description based fuzzy algorithm lead to non-appropriate classification results (Figure 6.11, b), where for an adequate comparison with the occurring vegetation classes Figure 6.11, (a) represents the original CDBF-based classification result for the scene of 1999 (Dunaremete) with the simple classification scheme. Although the same or similar vegetation classes were supposed to be found in 1999, around the half of the site (52%) remained unclassified and the class of Hybrid poplar is completely missing in the classified scene.

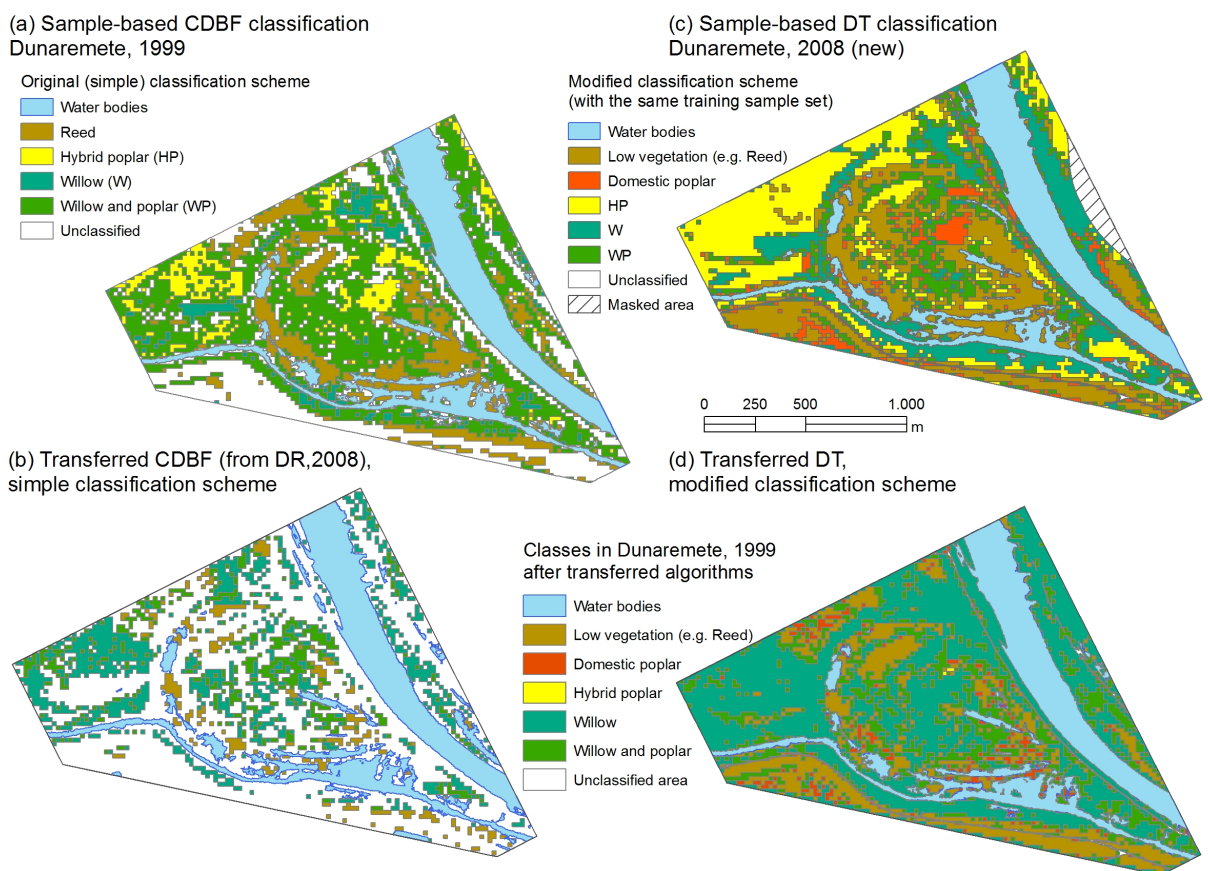


FIGURE 6.11: Classification results after transferring unchanged CDBF and DT algorithms with simple and slightly modified classification schemes to the former (1999) scene of Dunaremete.

Dealing with the transferability in the spatial dimension, it has been discussed in Subsection 6.2.5 that the decision tree approach is privileged to apply, therefore, it was also adopted to the analysis of temporal classification transferability. Firstly the concrete decision tree (Figure 6.12) had to be computed based on the training scene (DR, 2008), where

the simple classification scheme was modified by the extension of Reed class to Low vegetation (Figure 6.11, c). The 2008 scene-based decision tree was applied to the image object level of unclassified chessboard segments and gave the following classification result in Figure 6.11, (d). Hybrid poplar stands are also missing in the DT-based classification, and the most occurring woody vegetation class is willow (around 40% of the site), including those stands as well, which were supposed to be Hybrid poplar. In contrast, the classification of Low vegetation class visually seems to be promising, therefore, producer's and user's accuracies were calculated and are summarized in Table 6.6, also including PA and UA for the DT-classification of the 2008 image.

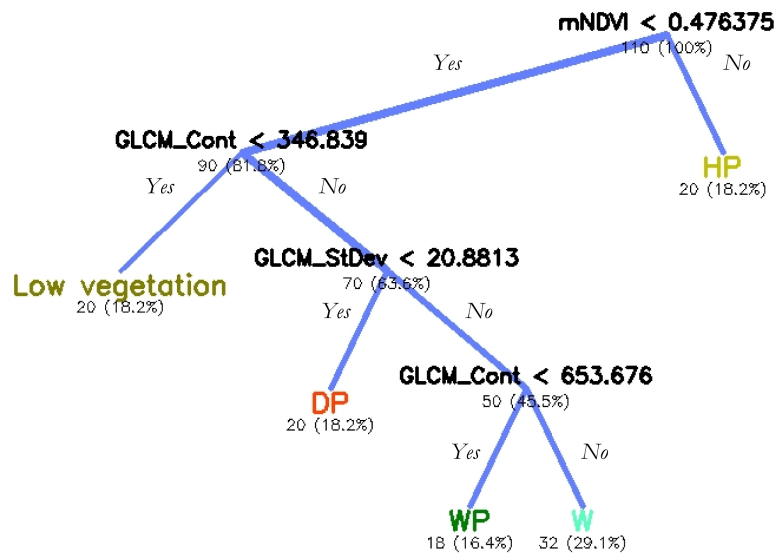


FIGURE 6.12: Structure of the decision tree with the simple classification scheme (slightly modified) based on the scene of DR, 2008 and latter applied to the scene of 1999.

TABLE 6.6: Producer's and user's accuracy for the class of Low vegetation in the decision tree-transfer for the original image scene (2008) as training image and for 1999 as target image scene.

Image	Role in the DT computation	PA	UA
Dunaremete (2008)	Training scene	93%	86%
Dunaremete (1999)	Target scene	72%	86%

Findings from Section 6.2 were confirmed by the above-described examples for temporal classification transferability, stating that transferring decision tree-based algorithms can be feasible for the classification of certain vegetation class(es) (here: Low vegetation). Nevertheless, further improvements had to be applied in order to get appropriate accuracies (PA was under 75% for Low vegetation in DR, 1999, presented in Table 6.6). With the

reclassification of Willow and Willow & poplar classes into ‘general forest areas’ (woody vegetation) the analysis would be applicable for the separation of grass (low) and woody (high) vegetation, described in Section 6.4.

Considering the original class labels, one can observe that class of Hybrid poplar could not be detected with the transferred decision tree in the 1999 image, which could mean the presence of vegetation structural (pattern) differences in the stands for the two years (1999 and 2008) and besides, a higher level of similarity is supposed between the class of HP (1999) and the class of Willow (1999) based on the classification result from DT-transfer. The lower level of textural difference for HP-W class pair in 1999 was also confirmed by the Jeffries-Matusita class separability values (Appendix C). Nevertheless, separability was provided there by vegetation index between those classes for the concrete scenes (DR 1999, 2008).

For a further analysis of training image-based classification, it was essential to compare vegetation patches (classes) in the source (training) and target image scene and evaluate the appropriateness of the applied spectral and textural parameters used in the classification. It is described in Sub-section 6.3.3.

6.3.3 Class separability analysis

This sub-section concentrates on the analysis of the applied spectral and textural parameters defined for different aerial image scenes (2008 and 1999) applying Jeffries-Matusita class separability analysis with training sample sets. It was supposed that despite different spectral band compositions (2008: B,G,NIR; 1999: G,R,NIR) but with the same geometric resolution (both with 1.25 m/pixel) certain parameters applied before can be compared between those scenes. Firstly (Sub-section 6.3.3.1) the applied parameters are analysed for the class of Low vegetation, which was expected as a vegetation class with similar characteristics, detectable by the transferred decision tree (classification is found in Figure 6.11, d). Secondly (Sub-section 6.3.3.2) vegetation structural differences are going to be demonstrated by the same analysis method.

6.3.3.1 Detecting a stable parameter for temporal vegetation analysis

Initially, it was assumed that vegetation pattern similarities and differences in distinct years are not significantly influenced by the different characteristics of the applied CIR imagery (2008, 1999). Therefore, it was supposed that certain parameters exist, which characterize similar vegetation classes in different years and are not independent descriptors for the single years. If this hypothesis is true, it means that temporally stable parameters do exist, which can be used to detect similar vegetation patches. Beyond that, it was supposed that textural parameters could show a more stable character in comparison to spectral parameters, e.g., the here applied vegetation index. In order to prove that, a detailed objective comparison was worked out for the target classes occurring in each image scene, where the application of the JM separability analysis based on training samples from each scene provided an appropriate method.

Furthermore, a *stable parameter* (descriptor) for a concrete class means, that it describes a certain class similarly in the compared scenes by utilising similar feature value ranges (low separability by JM analysis) and besides, it can be proved that the analysed feature value range is significantly different from the other (vegetation) classes (high separabilities by JM analysis for single years and for different years). Fulfilling these conditions, the analysed parameter is proved as a stable descriptor for temporal vegetation analysis. Generally, a stable parameter is supposed to be well applicable for the automated detection of similar vegetation patterns in different years and can detect significant vegetation pattern differences as well. The analysis steps required for the determination of stable parameter(s) are summarized in Figure 6.13.

From the simple classification scheme (applied originally for the separate classification of image scenes, Figure 5.8) the class of Reed (respectively its training sample set for each scene) was chosen for the JM separability analysis, where it was supposed to be similar in the different years. Initially it was essential to review, whether the applied parameters were significant for class separation regarding vegetation class pairs with Reed in each scene separately. Therefore, the JM separability values were calculated and are presented in Table 6.7. It can be observed that textural parameters provide clear separabilities in the cases of W-R and WP-R class pairs (both years) contrary to the vegetation index (GreenNDVI).

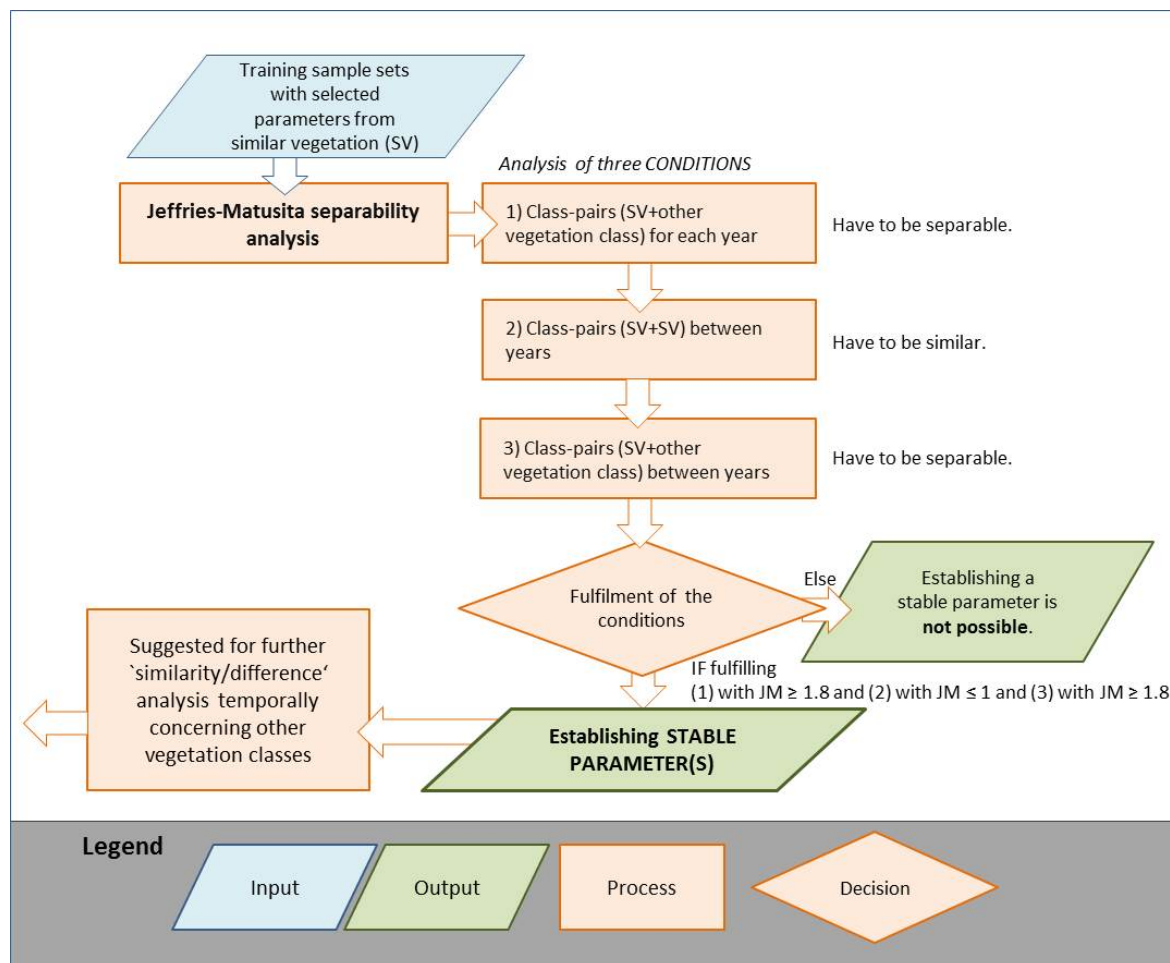


FIGURE 6.13: Analysis steps required for stable parameter assessment. Examples for the analysis of condition 1) in Table 6.7, for condition 2) in Table 6.8, for condition 3) in Table 6.9 can be found.

TABLE 6.7: Jeffries-Matusita separability values for class-pairs with Reed concerning the site of Dunaremete for 1999 and for 2008. The selected textural and spectral parameters are related to the former results in Chapter 5.1.4.

	HP-R		W-R		WP-R	
	1999	2008	1999	2008	1999	2008
GLDV ENT	1.8	1.0	2.0	2.0	1.6	1.8
GLCM STDEV	1.9	1.8	2.0	2.0	1.8	2.0
GLCM CONT	1.9	1.0	2.0	1.9	1.7	1.8
GLCM MEAN	1.7	2.0	0.3	1.1	0.9	1.4
GreenNDVI	2.0	2.0	0.3	1.0	1.2	1.4

Another important remark is the extreme change (decrease in JM separabilities from 1999 to 2008) regarding two textural parameters for the class pair of HP-R. Nevertheless, by

GLCM STDEV texture feature and by GreenNDVI the mentioned class pair is separable with $JM \geq 1.8$.

Testing of similarities and separabilities was done in two steps, firstly it had to be analysed, whether the samples taken for Reed (in the scene of 2008 and 1999) were identical (Table 6.8), secondly whether samples taken for Reed in 2008 were clearly separable from other target vegetation classes defined in the scene of 1999 (Table 6.9).

TABLE 6.8: Analysing similarity for the class of Reed defined in different image scenes (DR 1999, 2008) by the earlier chosen features applying the Jeffries-Matusita class separability analysis, where G NDVI means GreenNDVI.

		Reed from 2008			
From 1999	G NDVI	GLCM MEAN	GLDV ENT	GLCM STDEV	GLCM CONT
Reed	1.21	0.09	0.85	1.17	0.91

In Table 6.8 all the JM values are under 1.3, which means the similarity of classes as it was required. Nevertheless, in Table 6.9 the required separabilities only exist for the class of Reed (2008) and the forest sites (1999) with GLDV ENT, GLCM STDEV and GLCM CONT textural parameters. Since the expected separabilities could not be detected for GreenNDVI and GLCM mean features in the cases of Reed-HP, Reed-W and Reed-WP, JM values for these parameters were not calculated for other class pairs of Reed and non-forest sites. According to that vegetation index (GreenNDVI) and GLCM mean were found as inappropriate descriptors for a temporal comparison. Although, GLCM mean has been listed as one of the textural parameters, which was applied before, it was correlated with the mean of PC1, that's why it is considered here as a spectral and not a 'real' textural feature.

From the three appropriate textural parameters derived from Table 6.8 and from Table 6.9 GLDV entropy showed the smallest JM value (best value for similarity) for Reed classes (1999-2008), but considering class separations for the different years (Table 6.7) it had a low separability value (1.0) for HP-R in 2008. Taking into account all the three tables presented above the best descriptor is GLCM STDEV, called as stable parameter later.

Since other non-forest sites (Arable land, Vegetation on edges and dams, Smooth and Rough fallow land, Shadow) defined in the scene of 1999 were generally not separable from Reed (2008) by the mentioned textural parameters, instead of Reed the extended class of Low vegetation (defined in Sub-section 6.3.2) was suggested for further analysis.

TABLE 6.9: Analysing separability between the class of Reed (2008) and other vegetation classes from the former scene (1999) by the earlier chosen features applying the Jeffries-Matusita class separability analysis for the site of Dunaremete. HP: Hybrid poplar; W: Willow; WP: Willow & poplar; ArLa: Arable Land; VED: Vegetation on edges and dams; Smooth FL: Smooth fallow land; Rough FL: Rough fallow land.

From 1999	Reed from 2008					
	G NDVI	GLCM MEAN	GLDV ENT	GLCM STDEV	GLCM CONT	
HP	0.44	1.87	2.00	2.00	2.00	
W	0.96	0.53	2.00	2.00	2.00	
WP	0.01	1.18	2.00	1.99	1.94	
ArLa			1.00	1.32	1.06	
VED			1.84	0.33	1.42	
Smooth FL			0.15	0.11	0.21	
Rough FL			1.59	1.83	1.55	
Shadow			1.00	1.03	0.61	

6.3.3.2 Detecting vegetation with structural differences

The above-established stable descriptor (GLCM standard deviation) was further applied to the analysis of other vegetation classes, firstly to the class of Hybrid poplar. Analysis steps presented in Figure 6.13 were followed, since those conditions are applicable for the detection of similar vegetation patterns.

Firstly class pair separabilities regarding 1999 and 2008 separately are presented in Table 6.10, where the lower JM values for the class pair HP-WP was reasonable (since Hybrid poplar species are present in both classes), but changes concerning the poor separability for HP-W in 1999 in comparison to the high value (1.9) in 2008 was considerable.

TABLE 6.10: Jeffries-Matusita separability values for class pairs with Hybrid poplar concerning the site of Dunaremete for 1999 and for 2008.

	HP-R		HP-W		HP-WP	
	1999	2008	1999	2008	1999	2008
GLCM STDEV	1.9	1.8	1.1	1.9	0.7	1.6

Analysing the second condition where Hybrid poplar stands from different years were compared by GLCM standard deviation the JM separability value equals 2.00, which means a concrete separability between the analysed sample sets. Without further investigations it proved that the analysed vegetation classes (defined and expected as Hybrid poplar) are not similar and significant vegetation pattern changes occurred. These changes are reasonable,

since vegetation structure could significantly change due to the growth of the stands (or the settlement of new stands after harvesting).

Regarding the classes of Willow and Willow & poplar in the temporal comparability analysis (second condition in Figure 6.13) JM value is 1.39 for both cases, which means the similarity of those vegetation patterns for the different years, however, their detection could not be straightforward (similarities have been discussed between HP-W and HP-WP classes in Table 6.10), also showed by the analysis of the third condition, where clear separability values would have been expected (Table 6.11 and in Table 6.12).

TABLE 6.11: Analysing the separability between class of Willow (DR, 2008) and other vegetation classes from the former scene (1999) by GLCM STDEV applying the Jeffries-Matusita class separability analysis.

Willow from 2008	
From 1999	GLCM STDEV
Reed	1.56
Hybrid poplar	0.27
Willow & poplar	0.86

TABLE 6.12: Analysing the separability between class of Willow & poplar (DR, 2008) and other vegetation classes from the former scene (1999) by GLCM STDEV applying the Jeffries-Matusita class separability analysis.

Willow & poplar from 2008	
From 1999	GLCM STDEV
Reed	0.94
Hybrid poplar	1.29
Willow	1.85

6.3.4 Transferring a generalized classification scheme

After the findings in Sub-section 6.3.2 and Sub-section 6.3.3 a generalized classification of grass (low vegetation) and forest cover (high vegetation) was suggested for an appropriate classification algorithm transfer in the temporal dimension.

After an earlier presented decision tree with the modified classification scheme (computed for the 2008 image, Figure 6.12), where low vegetation was already defined, GreenNDVI (called mNDVI there) was a significant parameter for the separation of vegetation classes. Referring to the separation of Hybrid poplar and Reed GreenNDVI was the only descriptor among the analysed features which provided 100% separability by the JM value (2.0) for the image

scenes separately (Table 6.7). However, in the temporal comparison it could not be defined as a stable parameter in contrast to GLCM STDEV. For these reasons, decision trees based on the 2008 image (Dunaremete) were computed on the basis of reclassified training sample sets for HL (high vegetation) and LV (low vegetation) classes with the GLCM standard deviation feature in addition with and without GreenNDVI. The structures of the computed decision trees are found in Figure 6.14 and in Figure 6.15 with the indication of the main nodes, since in some of the end leaves in the originally computed trees only a few number of image segments were found.

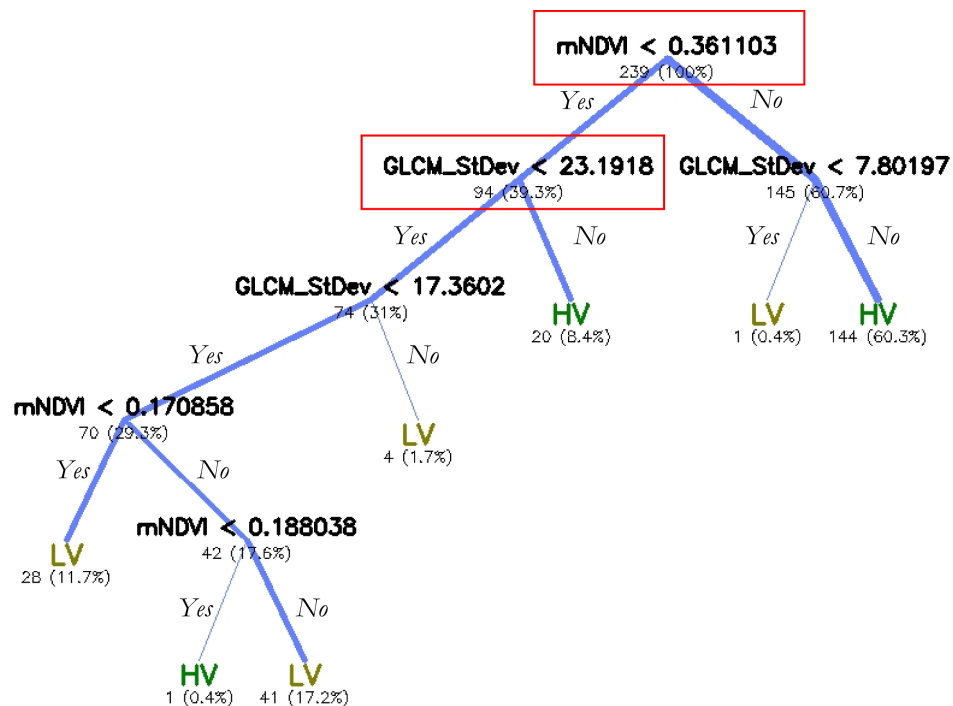


FIGURE 6.14: Structure of the decision tree (DT1 later) for the separation of high and low vegetation based on the scene of DR, 2008, applying GLCM STDEV and GreenNDVI (mNDVI) in the feature set. LV: Low vegetation, HV: High vegetation class.

Classification results with the generalized classification scheme are presented parallel in Figure 6.16. For appropriate accuracy assessment reference square image objects were chosen carefully, not overlaid with the originally chosen training segments (70 square samples for LV and 170 samples for HV, not including water bodies and road). With the use of GLCM STDEV and GreenNDVI in the feature set for decision tree computation classification results reached a high agreement to the reference sample set (OA: 98%, Kappa: 0.95 for 2008; OA: 99%, Kappa: 0.98 for 1999). Excluding vegetation index resulted in slightly worse results with 97% for OA and 0.91 for the Kappa value concerning the training image (2008), however, regarding the DT-transfer to the target scene of 1999 accuracy values decreased

significantly (OA: 79%, Kappa: 0.57). Therefore, the application of both features, GLCM STDEV and GreenNDVI in the feature set for DT computation (applied to the 2008, NIR-G-B image) was selected for further analysis.

Since GreenNDVI was found as a non-significant descriptor and GLCM STDEV as a significant one in the temporal analysis, it was assumed and verified that ignoring the decision node of mNDVI in Figure 6.14 (DT1) and applying only the marked GLCM STDEV (with the value of 23.19) to the 1999 image gave the same classification result as applying the original tree (Figure 6.14).

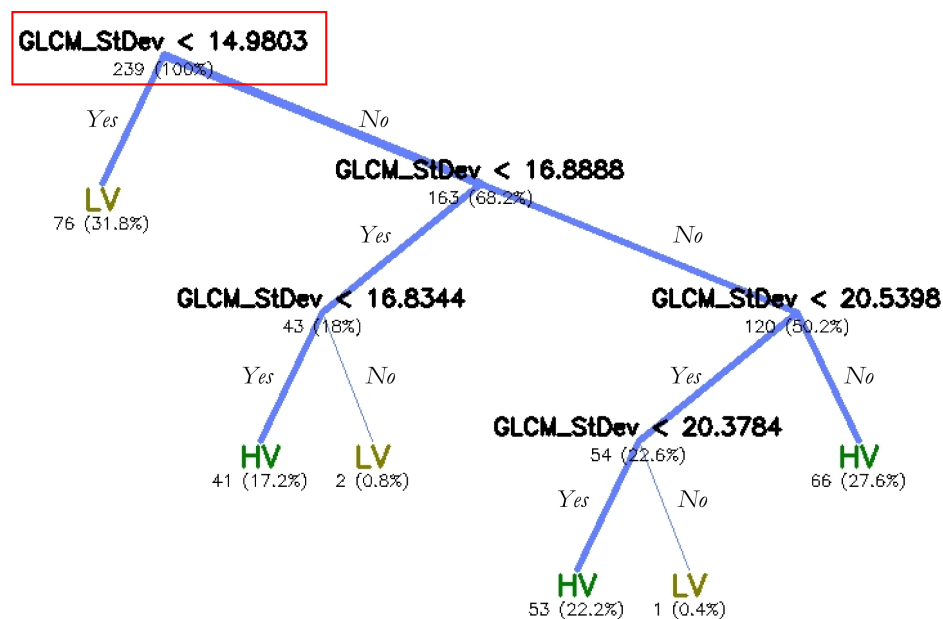


FIGURE 6.15: Structure of the decision tree (DT2 later) for the separation of high and low vegetation based on the scene of DR, 2008, applying exclusively GLCM STDEV in the feature set. LV: Low vegetation, HV: High vegetation class.

Furthermore, a backward analysis of classification transferability was tested based on the 1999 image. Therefore, the sample based classification (decision tree) with the generalized classification scheme was computed for that image. New decision tree calculations were based on the GLCM STDEV textural parameter with and without GreenNDVI, where the computed trees gave the same structure, not including vegetation index as a decision node. The new DT describes that if $GLCM\ STDEV < 25.04$ then the image segments are classified as low vegetation, else they get the class label of high vegetation. Applying this decision tree classification results provided a 100% agreement and it means that using GLCM STDEV only was sufficient for the appropriate separation of high and low vegetation classes in that aerial image (1999, NIR-R-G). Nevertheless, since VI was necessary for appropriate class

separabilities in the scene of 2008, decision tree computed for the former (1999) scene (not including VI), could not perform well applied to 2008, giving an OA of 65%.

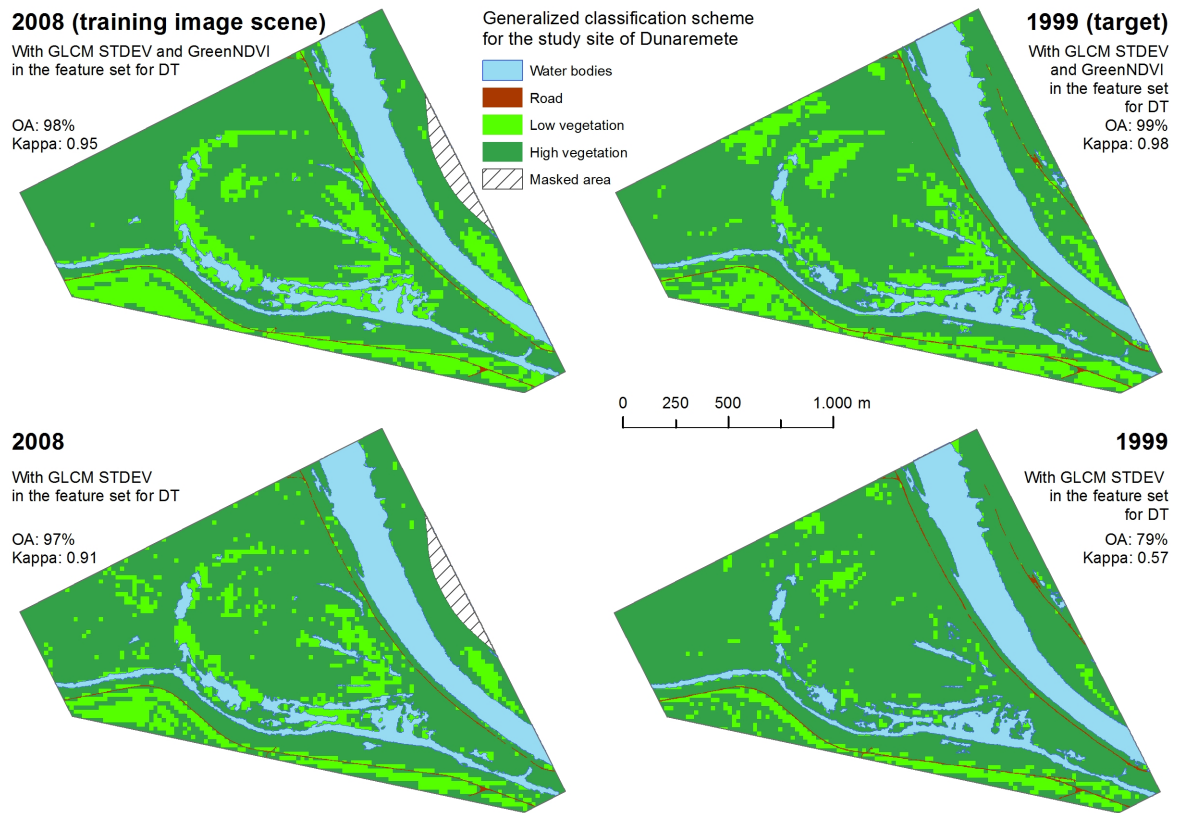


FIGURE 6.16: Comparison of decision tree-based classification results with a generalized classification scheme using different initial feature sets for DT computation, applied for 2008 and 1999 in the site of Dunaremete.

6.3.5 Results

In summary, it was proved that a certain textural parameter (GLCM standard deviation) in contrast to spectral descriptors (e.g., vegetation index) is a significant descriptor for temporal vegetation analysis. GLCM standard deviation as a stable (reliable) parameter in the temporal investigations is suggested for further use in similarity/difference analysis of vegetation patterns in the different year images based on training sample sets. The classification algorithm of decision tree computed for the scene of 2008 with GLCM STDEV and GreenNDVI gave promising results for high and low vegetation separation and it was also applicable for the earlier image of 1999 by DT-transfer. A slight change in the decision tree by ignoring the initial node with GreenNDVI in DT1 (Figure 6.14) and the use of

GLCM STDEV only was sufficient for the classification of the 1999 aerial image. Decision tree computed separately (based on training samples) for the 1999 image proved also the appropriateness of GLCM STDEV as a single descriptor in the classification tree. Beyond that, based on the example of the 1999 image, GLCM STDEV can be proposed as a unique feature for high and low vegetation separation for images with NIR-R-G spectral band combination. Nevertheless, the decision tree computed from 1999 could not be transferred to 2008, respectively the transfer of decision tree backwards (from 1999 to 2008) could not work in the analysed images due to the need for GreenNDVI concerning the class separability of HP-RD in 2008.

6.4 Spatio-temporal classification transferability

We have seen that transferring a concrete classification algorithm from one test site to another (Section 6.2) or from one time to an earlier image (Section 6.3) is not straightforward, however, under certain conditions (e.g., with the application of appropriate classification algorithm, classification scheme, training site) the classification gave promising results.

In the following as a further step towards an automated aerial image analysis, it was considered, whether the spatial or temporal transferability results were applicable for a spatio-temporal extension. Since it was not feasible based on transferable classification algorithms to conduct detailed vegetation/forest mapping for aerial images with 9-years difference due to forest structural differences (Section 6.3), the detection of Hybrid poplar stands (analysed in Sub-section 6.2.6) could not be temporally extended by transferred algorithms. Instead of that, based on the decision tree classification and the generalized classification scheme applied to the temporal classification transferability in Sub-section 6.3.4, the applicability of the same algorithm was considered for spatial transferability.

Firstly it was assumed that after the separation of water bodies the ‘multi-resolution-segmented’ image (Figure 5.3) could be analysed for classification parallel to the chessboard segment-based method. This consideration was based on the ‘simplified’ land cover analysis, where grass cover (low vegetation) has significantly smoother texture in contrast to forest cover with higher textural variation for the MR-segments, which was not going to be split into further complex habitats.

Since from the previous section the firstly applied decision tree algorithm (DT1, Figure 6.14) gave the best classification result for the temporal transferability, firstly it was tested based on MR-segments for the study site of Dunaremete in 2008 and 1999, where the accuracies were slightly lower than by the chessboard-based application (summarized in Table 6.13). For the spatial extension classification algorithm (DT1) was transferred to the other test site (Dunakiliti, 2008) based on the two segmentation types, where the classification performance (Figure 6.17) showed lower accuracies (Table 6.13), however, still acceptable for further investigations.

TABLE 6.13: Accuracy assessment of the classification results based on the same decision-tree approach (DT1 from Figure 6.14), applied to three different image scenes. Besides, the performance of different segmentation methods for classification were analysed.

DT1	Dunaremete - 2008		Dunaremete - 1999		Dunakiliti - 2008	
	MR	Chessboard	MR	Chessboard	MR	Chessboard
OA	95%	98%	94%	99%	87%	92%
Kappa	0.87	0.95	0.88	0.98	0.74	0.83

Considering the results from the accuracy assessment method it is essential to emphasize that the chessboard-based reference objects (reference samples) could not measure the accuracy of vegetation class borders, which was clearly improved by the multi-resolution-segmentation-based analysis. Therefore, it is foreseen in the future research to apply additional accuracy calculations for the assessment of objective accuracy measures.


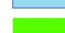

It was achieved to separate forested and non-forested wetlands, however, the earlier proposed generalized classification scheme from the two-level scheme (Sub-section 6.2.2, Figure 6.1) could not be applied, mainly caused by the rare representation of bare soil and the often mixed herb/grass and shrub categories. It is supposed that a larger principal test site could enhance the training site-based decision tree for a better classification performance in other areas. However, for an automated image analysis a spatially and temporally transferable decision tree has and will have its limitations due to the differences in the applied imagery.

Application of transferred decision tree approach

Study site of Dunakiliti
(2008)

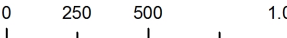
Based on
chessboard segmentation

Generalized classification scheme

-  Water bodies
-  Low vegetation (LV)
-  High vegetation (HV)

Overall accuracy: 92%
Kappa: 0.83

0 250 500 1,000 m



Based on
multi-resolution segmentation

Overall accuracy: 87%
Kappa: 0.74

FIGURE 6.17: Transferred decision tree-based (DT1 from Figure 6.14) classification results with a generalized classification scheme based on different segmentations, applied to the site of Dunakiliti (2008).

Chapter 7

Summary

Automated image analysis techniques in general went through a rapid development in the recent years due to the necessity for evaluating an increasing amount of remotely sensed data in a feasible manner. With those methods the interpretation of available high resolution (HR) aerial imagery can be automated and the analysis results enhance the assessment of vulnerable riparian wetland environments, where botanical and silvicultural inventories couldn't take place regularly and are subjective due to the surveyor's experience.

In the current research supervised vegetation habitat classification was worked out for selected test sites in the Szigetköz Danubian floodplain (Hungary) based on HR aerial imagery. Firstly different parameter sets (spectral and/or textural) were analysed for classification performance on chessboard-segmented images (with 20×20 m segments) from three different years focusing on the same test site, based on a user-defined classification scheme after botanical and silvicultural inventories. Best classification accuracies were reached with the application of a combined set of vegetation index and four textural parameters, calculated from the Grey Level Co-occurrence Matrix, as input for the class description based fuzzy algorithm. The most reliable classification results (87% and 88% overall accuracies) with a simple and an extended classification scheme were reached for the last image (2008), having originally higher ground spatial resolution (0.5 m/pixel) and better image quality according to the digital image acquisition type.

Since the above described classification methods were conducted on image scenes based on locally selected training samples, it was foreseen to analyse training-image based automated applications for a spatially and temporally extended analysis of the same wetland area.

The mapping of different vegetation habitats defined and classified on the training image was not feasible based on transferred classification algorithms applied previously. Nevertheless, concerning spatial transferability, another classification method, the decision tree (DT, firstly tested on the training site) with the same spectral-textural feature set was found to be transferable for the detection of Hybrid poplar stands under those conditions, that the selected samples in the training image are characterized by the Forest Stand Type of Hybrid poplar (based on silvicultural reference data), although the user-defined Hybrid poplar class includes mixed stands, e.g., Domestic-poplar-Hybrid poplar FST as well.

Regarding the temporal transferability, it was assessed by Jeffries-Matusita statistical distance calculations based on training samples from different aerial images (2008: NIR-G-B, 1999: NIR-R-G) that similarities (Low vegetation) and differences (e.g., Hybrid poplar class) in vegetation patterns from distinct years are detectable by a stable textural parameter, GLCM standard deviation (STDEV), which is also suggested for latter analysis in decision tree transfer. Transferring the training-image (2008) based decision tree with the feature set of GLCM STDEV and vegetation index (GreenNDVI), computed for a generalized classification scheme (high and low vegetation), gave 99% overall accuracy for the target scene (1999). By ignoring the vegetation-index-related decision node in the originally computed DT for 2008, the transferred decision tree classifier resulted in the same classification performance for the scene of 1999 with the single use of GLCM STDEV. Hereby, it was verified that GLCM STDEV is a stable and significant parameter in temporal image classification. Beyond that, based on the decision tree structure computed based on the 1999 NIR-R-G image, GLCM STDEV is proposed as a single descriptor for the separation of low and high vegetation classes (like density slicing method for a single-band image) without the use of the earlier applied image classification algorithms, applied to aerial imagery with the same spectral band combination.

Training image-based decision tree classification was applicable for the separation of forested (high vegetation) and non-forested (low vegetation) areas in the spatial dimension as well. Thus, the spatial and temporal extension of a concrete classification approach was found to be feasible and is suggested for spatio-temporal monitoring studies where a rapid assessment of a generalized vegetation cover is necessary.

Chapter 8

Conclusions & future research

8.1 Conclusions

High resolution aerial imagery based automated image analysis provides an objective method for the understanding of vegetation patches and processes, spatial and temporal differences compared to the field investigation based vegetation monitoring. The above-described analysis results can serve as a supportive tool for the work of botanical and silvicultural surveyors producing and updating vegetation and forest habitat maps.

Based on the applied imagery (with the spatial resolution of 1.25 m/pixel) and the available botanical and silvicultural data significant vegetation classes were identified for the training stage and for the selection of reference samples during the supervised classification. However, the applied aerial images and the ancillary (botanical and silvicultural) data were temporally different, where the reliability of the applied vegetation classification scheme could be problematic. Beyond that, additional forest stand based information (e.g., age) would have enhanced the investigations with the application of age structure analysis.

Generally the use of colour-infrared aerial images is essential, since the vegetation indices (e.g., NDVI, BlueNDVI, GreenNDVI) provide a concrete separability from water bodies, enhance the separation of complex vegetation habitats and are also important for the automated detection of Hybrid poplar stands and for the separation of high and low vegetation in NIR-G-B images (2008).

It is concluded that decision tree transfer methods can be effective for the rapid assessment of Hybrid poplar vegetation cover applied to CIR aerial images from the same aerial image acquisition, covering the same riparian wetland with similar forest cover. Furthermore, by decision tree transfer the separation of forested (high vegetation) and non-forested (low vegetation) areas can be speeded up for a spatio-temporal monitoring, based on CIR aerial imagery.

The application of Jeffries-Matusita statistical separability calculations is vital for feature space reduction and considerable for latter investigations where the significant textural parameters are to be found in a one-year and in a multi-temporal image analysis.

The applied accuracy assessment method proved that vegetation classification accuracies for the 20 m×20 m image segments were higher compared to the classification of irregular image objects from the multi-resolution segmentation. However, accuracy measures were calculated from the 20 m×20 m square samples as reference samples, not analysing vegetation habitat borders. Therefore, a more specific accuracy assessment would be needed.

8.2 Future research

By analysing most recent imagery and detailed reference information collected in the same time would ensure the definition of a more accurate classification scheme and a more reliable accuracy assessment applied to the vegetation classification. Furthermore, if the detailed silvicultural reference information provides reliable stand age information, automated aerial image analysis has the potential for building an optimal vegetation/forest mapping method concentrating on the combination of species composition and age structure.

Applying a generalized classification scheme with forested and non-forested (possibly divided into the classes of bare soil, herb/grass and shrub) sites to HR aerial images with MR-segments can potentially provide accurate habitat delineation for a rapid assessment of riparian wetlands. An appropriate comparison to the analysis of medium resolution satellite images, e.g., Landsat (Kollár, 2010), would emerge the significance of HR imagery based applications and its applicability for more accurate biomass estimation.

Based on an analogue NIR-R-G aerial image (1999) textural parameter was found as a more significant descriptor for the separation of high and low vegetation, in contrast to the

recent (2008) digital imagery with the NIR-G-B spectral band combination. Nevertheless, the analysis of further imagery is needed for the verification of this assumption.

Automated image analysis techniques developed in the current research could complement a recent research activity, related to the INMEIN (“Innovative methods for monitoring and inventory of Danube floodplain forests based on 3D technologies of remote sensing”) project as a Hungarian-Slovakian Cross-border Cooperation project, where actual aerial photography (2013) is to be analysed and potentially combined with the analysis of airborne laser scanning data presented in [Király and Brolly \(2013\)](#).

Moreover, testing the presented aerial image classification methods to other Danubian floodplains (e.g., Gemenc in Hungary, Csallóköz in Slovakia, Danube Floodplain National Park in Austria) or other areas with similar vegetation (forest) cover could prove their universal applicability for vegetation mapping purposes.

Chapter 9

Theses

1. The class description based fuzzy algorithm as a supervised image classifier, applied to segmented aerial images from different years, provides the best vegetation classification result, if the input parameter set includes spectral and textural parameters, not only spectral or only textural features. Based on the accuracy analysis in the present research, the following parameters provide the best results: GLCM (Grey Level Co-occurrence Matrix) standard deviation, GLCM contrast, GLCM mean, GLDV (Grey Level Difference Vector) entropy, vegetation index.
2. It was proved, that a decision tree classifier with a spectral-textural parameter set, developed on a segmented CIR aerial image for the detection of the Hybrid poplar class, can be transferred spatially to other areas.

The transfer can be successful only, if the training samples belong entirely to the Hybrid poplar Forest Stand Type (FST, FATI1 code in the *Hu.* silvicultural classification scheme, FATI1:NNY). Using other mixed FSTs as training samples, e.g., Domestic poplar-Hybrid poplar (FATI1:NNY-HNY), although being predominantly populated with Hybrid poplar species (*Populus x euramericana 'Pannonia'*), leads to classification errors. The developed method can be used for rapid forest inventories using CIR aerial imagery, focusing on the assessment of Hybrid poplar stands.

3. Based on a systematic Jeffries-Matusita class separability analysis, the GLCM standard deviation was found to be a stable textural parameter, applicable for the 20m × 20m (16 × 16 pixel) square sample-based evaluation of vegetation pattern similarities

and differences in CIR aerial images acquired in different years with different techniques but having the same geometric resolution (1.25 m/pixel).

4. Accuracy analysis of image processing results proved that a decision tree classifier with its spectral-textural parameter set, developed on a most recent CIR aerial image, can be transferred for the analysis of an older image of the same area for the separation of high and low vegetation. The images need to have the same spatial resolution and include the near-infrared band.
5. It was proved that the use of GLCM standard deviation as a textural parameter is sufficient for the separation of high and low vegetation classes based on aerial imagery with the NIR-R-G spectral band combination.
6. On segmented CIR aerial imagery with common spatial resolution, but from different years and sites of the same wetland it was proved that vegetation can be automatically classified into forested and non-forested areas with a most recent training image-based decision tree classifier. This method provides a rapid assessment technique based on object-based aerial image analysis, which is spatially and temporally transferable, in order to map the cover of high and low vegetation areas often required in environmental modelling and monitoring studies.

Appendix A

Aerial Images (1999-2008)

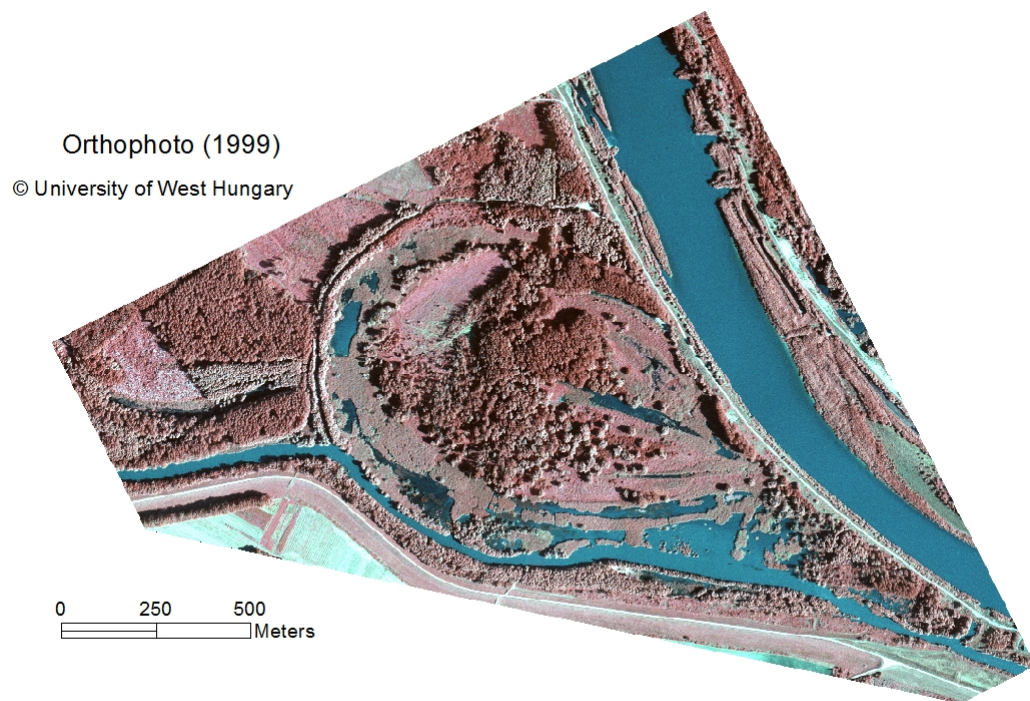


FIGURE A.1: CIR (NIR-R-G) orthophoto about the test site of Dunaremete from 1999.

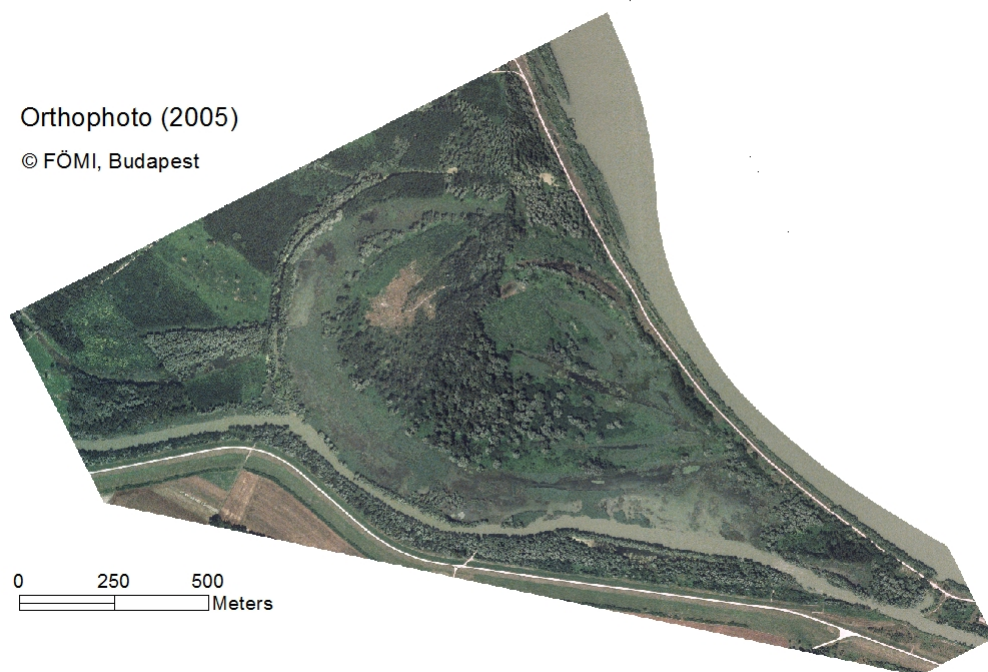


FIGURE A.2: RGB orthophoto about the test site of Dunaremete from 2005.

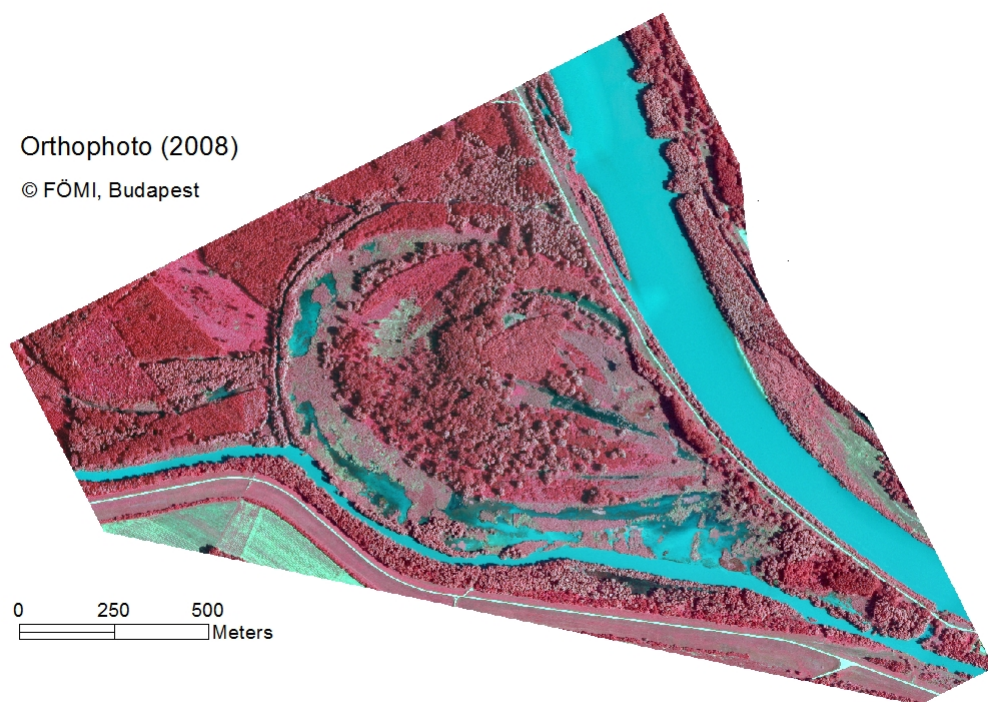


FIGURE A.3: CIR (NIR-G-B) orthophoto about the test site of Dunaremete from 2008.

Appendix B

Ancillary Data

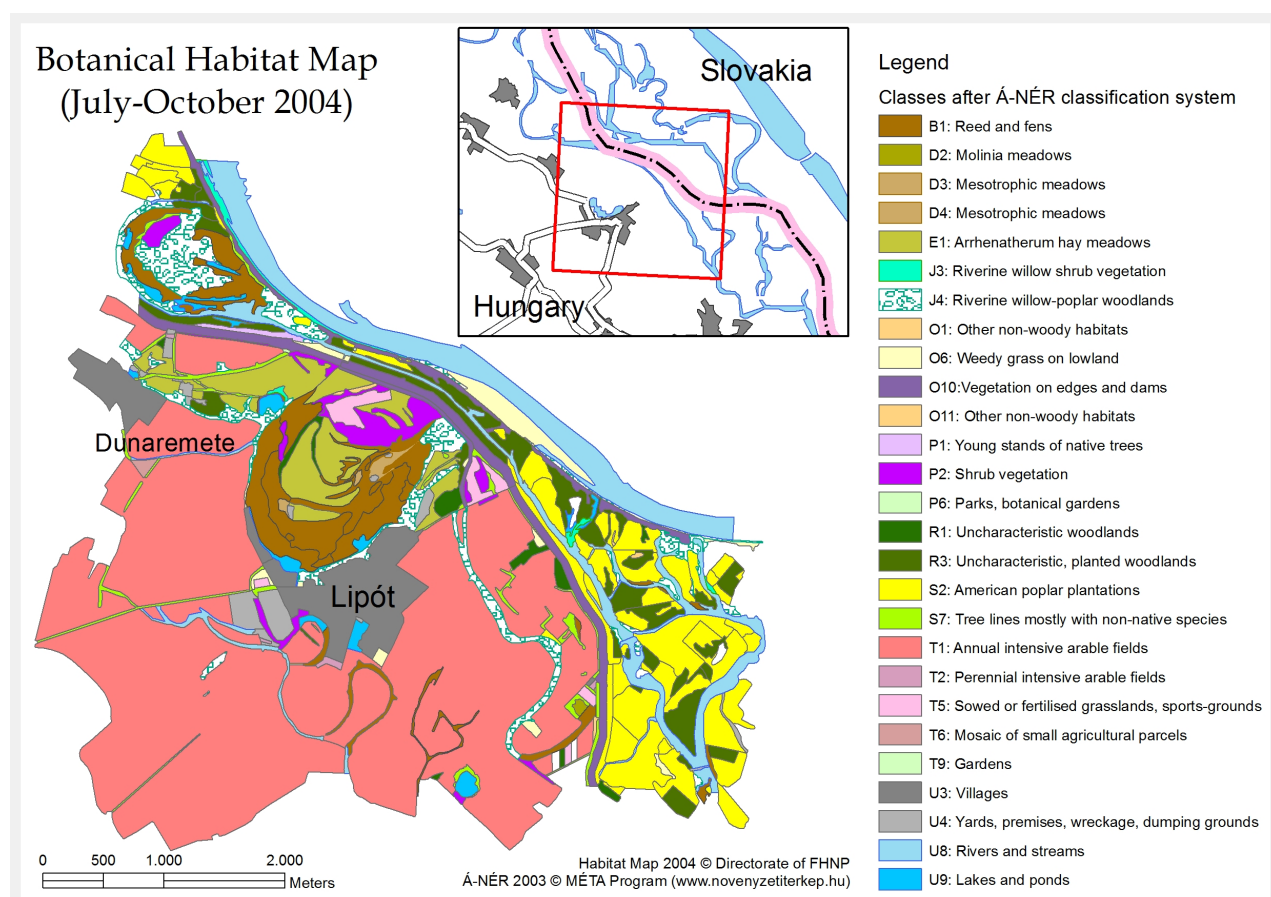


FIGURE B.1: Complete habitat map from 2004 based on the survey of the Fertő-Hanság National Park, as part of the National Biodiversity Monitoring System

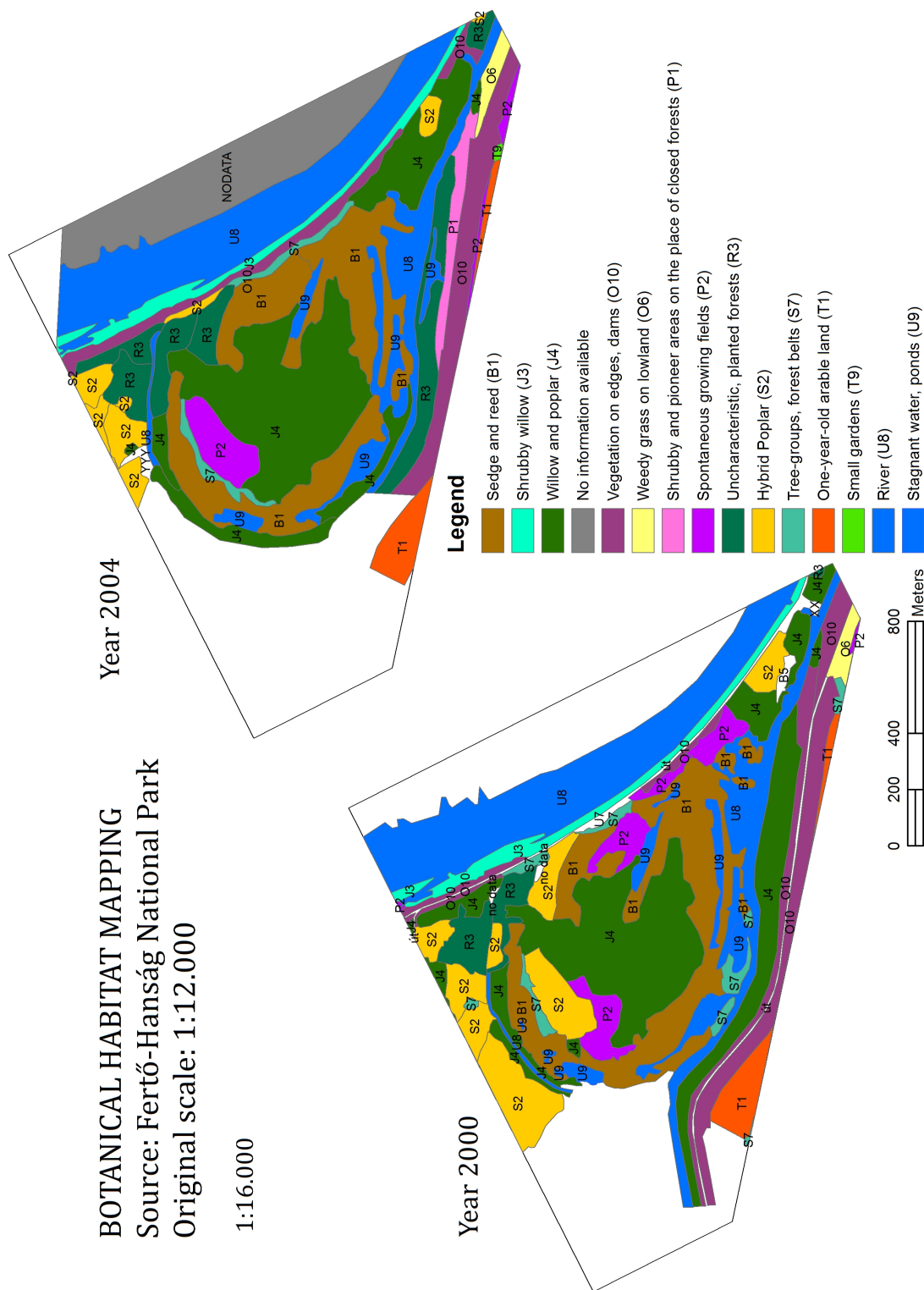
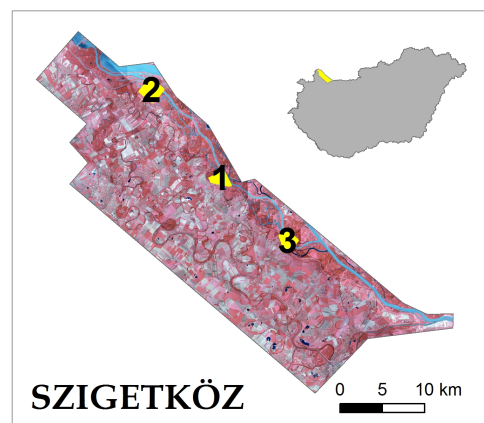
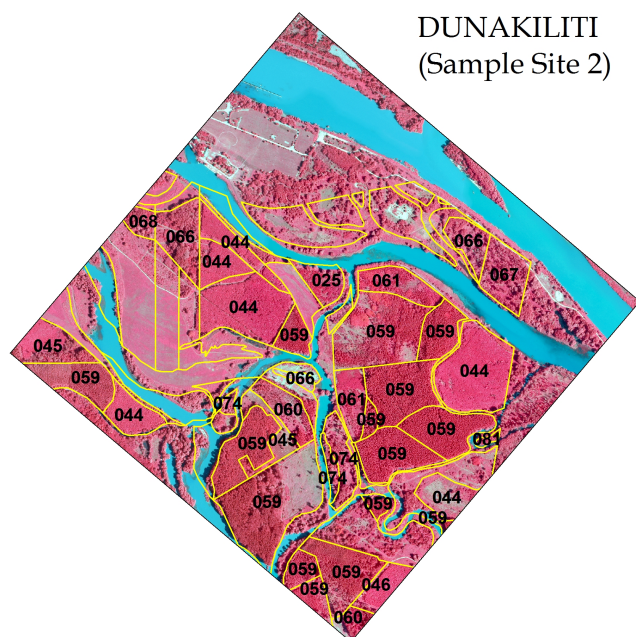
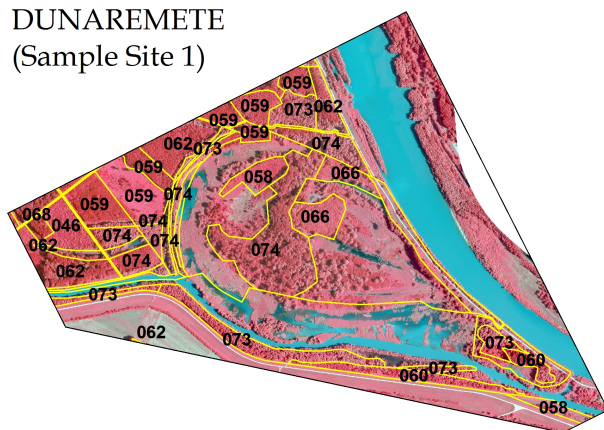


FIGURE B.2: Subsets from the habitat maps (2000, 2004) overlapped by the applied aerial image



DUNAREMETE
(Sample Site 1)



0 250 500 1.000
Meters

Silvicultural data © Forestry Directorate, Szombathely, 2010,
Aerial imagery 2008 © FÖMI, Budapest,
resampled to 1.25 m/pixel.
Aerial image about the whole Szigetköz 2008 © VITUKI.

Forest Stand Types (FATI1, Hu. 1. faállomány típusa)
occurring in the sample sites

Code*	Hungarian name	English name
025	KST: Kocsányos tölgyes	English oak
044	A: Akácós	Robinia
045	A-NNY: Nemes nyáras-akácós	Hybrid poplar- Robinia
046	A-HNY: Hazai nyáras-akácós	Domestic poplar- Robinia
058	EKL: Egyéb kemény lombos	Other hardwood
059	NNY: Nemes nyáras	Hybrid poplar
060	NNY-HNY: Hazai nyáras-nemes nyáras	Domestic poplar- Hybrid poplar
061	NNY-A: Akácós-nemes nyáras	Robinia- Hybrid poplar
062	NNY-EL: Egyéb lomb elegyes-nemes nyáras	Other wood- Hybrid poplar
064	NFÜ: Nemes fűzes	Hybrid willow
066	HNY: Hazai nyáras	Domestic poplar
067	HNY-NNY: Nemes nyáras-hazai nyáras	Hybrid poplar- Domestic poplar
068	HNY-A: Akácós-hazai nyáras	Robinia- Domestic poplar
073	FÜ: Fűzes	Willow
074	FÜ-E: Elegyes fűzes	Other wood- Willow
081	ELL: Egyéb lágy lombos	Other softwood

*Codes are given by the National Forest Inventory (Szombathely).
Bold-type words in stand-type-combinations mean
that those forest stand types build 50-70% of the stand.

ÁSVÁNYRÁRÓ
(Sample Site 3)

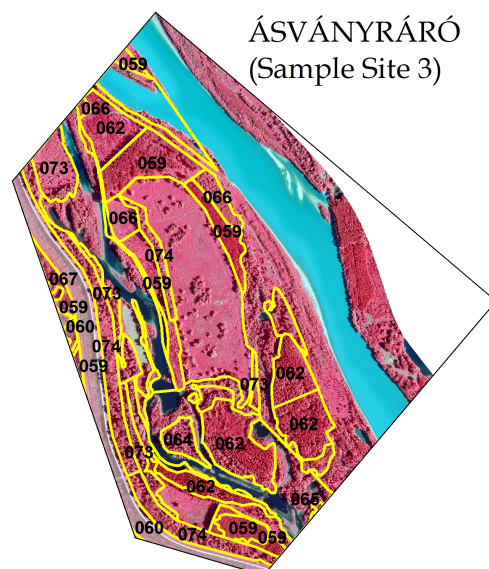


FIGURE B.3: Silvicultural data (Forest Stand Type) about the three test sites.

Appendix C

Feature separability analysis

TABLE C.1: Jeffries-Matusita separability values for texture features and vegetation indices concerning the image scene of DR, 1999. HP: Hybrid poplar, W: Willow, WP: Willow & poplar, RD: Reed.

	HP-W	HP-WP	HP-RD	W-WP	W-RD	WP-RD
GLCMContAllD	1.53	0.14	1.93	1.21	1.98	1.66
GLDVConAllD	1.53	0.14	1.93	1.21	1.98	1.66
GLDVEntAllD	1.55	0.17	1.84	1.18	1.99	1.56
GLCMDissAllD	1.52	0.15	1.89	1.26	2.00	1.51
GLDVMeanAllD	1.52	0.15	1.89	1.26	2.00	1.51
GLCMStdDevD	1.11	0.65	1.86	0.11	1.97	1.78
GLCMStdDevAllD	1.11	0.65	1.85	0.11	1.97	1.78
GLCMContD	1.42	0.24	1.98	1.15	1.99	1.56
GLDVConD	1.42	0.24	1.98	1.15	1.99	1.56
GLCMDissD	1.30	0.28	1.95	1.18	1.99	1.42
GLDVMeanD	1.30	0.28	1.95	1.18	1.99	1.42
GLDVEntD	1.37	0.30	1.90	1.24	1.99	1.49
GLDVAngD	1.06	0.40	1.75	1.14	1.96	1.05
GLDVAngAllD	1.24	0.27	1.66	1.12	1.95	1.12
GLCMEntAllD	0.66	0.29	1.50	0.84	1.82	0.90
GLCMHomAllD	0.44	0.35	1.12	0.83	1.79	0.35
GLCMMeanAllD	1.08	0.27	1.66	0.53	0.28	0.92
GLCMMeanD	1.08	0.27	1.66	0.53	0.28	0.92
GLCMHomD	0.13	0.41	1.24	0.73	1.65	0.31
GLCMAngAllD	0.48	0.37	1.26	0.88	1.64	0.54
GLCMEntD	0.44	0.18	0.99	0.69	1.53	0.51
GLCMAngD	0.42	0.22	0.95	0.72	1.47	0.44
GLCMCorrAllD	0.11	0.55	0.75	0.82	0.51	1.09
GLCMCorrD	0.04	0.77	0.70	0.67	0.52	1.09
GreenNDVI	1.78	0.37	1.95	0.80	0.26	1.21
NDVI	1.91	0.54	1.95	0.81	0.10	0.95

TABLE C.2: Jeffries-Matusita separability values for texture features and vegetation index concerning the image scene of DR, 2005

	HP-W	(HP-WP	HP-RD	W-WP	W-RD	WP-RD
GLCMStdevAllD	1.98	1.11	0.69	0.68	2.00	1.71
GLCMStdevD	1.97	1.10	0.69	0.69	2.00	1.71
GLCMEntAllD	1.80	1.04	0.74	1.00	1.99	1.84
GLDVEntAllD	1.98	0.95	0.58	1.21	2.00	1.59
GLDVAngAllD	1.96	0.79	0.76	1.28	1.98	1.53
GLCMMeanD	1.80	0.42	2.00	1.02	0.37	1.67
GLCMMeanAllD	1.80	0.43	2.00	1.02	0.37	1.67
GLDVEntD	1.83	0.72	0.59	0.71	1.99	1.52
GLCMAngAllD	1.67	0.98	0.68	0.87	1.93	1.72
GLDVAngD	1.75	0.59	0.68	0.81	1.97	1.52
GLDVMeanAllD	1.98	0.83	0.58	1.27	2.00	1.46
GLCMDissAllD	1.98	0.83	0.58	1.27	2.00	1.46
GLDVConAllD	1.96	0.91	0.49	1.18	1.99	1.42
GLCMContAllD	1.96	0.91	0.49	1.18	1.99	1.42
GLDVMeanD	1.82	0.74	0.61	0.70	1.97	1.36
GLCMDissD	1.82	0.74	0.61	0.70	1.97	1.36
GLDVConD	1.75	0.87	0.58	0.64	1.90	1.38
GLCMContD	1.75	0.87	0.58	0.64	1.90	1.38
GLCMEntD	1.45	0.78	0.73	0.59	1.89	1.67
GLCMHomAllD	1.60	0.37	0.85	0.76	1.91	1.37
GLCMAngD	1.41	0.73	0.69	0.59	1.83	1.58
GLCMCorrAllD	1.09	0.90	0.14	0.17	1.64	1.52
GLCMHomD	1.22	0.27	0.60	0.45	1.76	1.07
GLCMCorrD	0.71	0.89	0.06	0.03	1.12	1.30
VI=(G-R)/(G+R)	0.75	1.08	0.33	0.34	0.59	0.83

TABLE C.3: Jeffries-Matusita separability values for texture features and vegetation indices concerning the image scene of DR, 2008

	HP-DP	HP-W	HP-WP	HP-RD	DP-W	DP-WP	DP-RD	W-WP	W-RD	WP-RD
GLCMStdvAllid	0.02	1.94	1.60	1.76	1.96	1.69	1.81	0.52	2.00	1.99
GLCMStdvD	0.02	1.94	1.60	1.76	1.96	1.70	1.80	0.53	2.00	1.99
GLDVEntAllid	0.66	1.55	0.44	0.95	1.90	0.50	1.85	1.38	1.99	1.82
GLDVEntD	0.39	1.60	0.41	1.14	1.89	0.40	1.78	1.38	1.99	1.83
GLDVConAllid	0.45	1.61	0.42	1.04	1.77	0.72	1.92	1.30	1.94	1.80
GLCMContAllid	0.45	1.61	0.42	1.04	1.77	0.72	1.92	1.30	1.94	1.80
GLCMContD	0.30	1.67	0.46	1.10	1.78	0.72	1.86	1.26	1.95	1.74
GLDVConD	0.30	1.67	0.46	1.10	1.78	0.72	1.86	1.26	1.95	1.74
GLCMDissD	0.37	1.65	0.29	1.05	1.80	0.43	1.86	1.28	1.99	1.70
GLDVMeanD	0.37	1.65	0.29	1.05	1.80	0.43	1.86	1.28	1.99	1.70
GLCMDissAllid	0.57	1.53	0.27	0.93	1.75	0.41	1.91	1.29	1.98	1.70
GLDVMeanAllid	0.57	1.53	0.27	0.93	1.75	0.41	1.91	1.29	1.98	1.70
GLDVAngD	0.54	1.35	0.30	0.96	1.84	0.18	1.71	1.31	1.97	1.62
GLCMEntAllid	0.32	1.37	0.46	1.44	1.52	0.38	1.79	0.60	1.96	1.82
GLDVAngAllid	0.93	1.16	0.35	0.67	1.78	0.41	1.80	1.19	1.96	1.55
GLCMAngAllid	0.46	0.98	0.32	1.31	1.23	0.31	1.73	0.42	1.86	1.69
GLCMCorrAllid	0.21	0.37	0.89	0.65	0.96	1.65	0.35	0.58	1.57	1.90
GLCMEntD	0.04	1.17	0.46	1.38	1.08	0.35	1.50	0.26	1.83	1.67
GLCMMeanAllid	1.94	1.38	0.44	1.98	0.40	1.01	0.99	0.35	1.14	1.42
GLCMMeanD	1.93	1.37	0.43	1.98	0.40	1.02	0.98	0.36	1.14	1.43
GLCmHomAllid	0.68	0.70	0.05	0.48	0.45	0.51	1.75	0.68	1.80	0.69
GLCMAngD	0.05	1.11	0.46	1.34	1.04	0.35	1.48	0.24	1.79	1.63
GLCMCorrD	0.19	0.33	0.83	0.21	0.66	1.54	0.02	0.70	0.78	1.57
GLCMHomD	0.22	0.71	0.04	0.49	0.27	0.09	1.25	0.57	1.78	0.77
GreenNDVI	1.92	1.97	1.88	1.99	1.21	0.61	1.87	0.19	1.03	1.35
BlueNDVI	1.93	1.97	1.85	2.00	1.05	0.41	1.98	0.25	1.33	1.62

Bibliography

- Addink, E. A., de Jong, S. M., and Pebesma, E. J. (2007). The importance of scale in object-based mapping of vegetation parameters with hyperspectral imagery. *Photogrammetric Engineering & Remote Sensing*, 73(8):905–912.
- Andersen, H. (2004). *Hydrology, nutrient processes and vegetation in floodplain wetlands*. PhD thesis, The Royal Veterinary and Agricultural University, Department of Agricultural Science, Denmark.
- Balaguer-Beser, A., Hermosilla, T., Recio, J., and Ruiz, L. (2011). Semivariogram calculation optimization for object-oriented image classification. *Modelling in Science Education and Learning*, 4(7):91–104.
- Barsi, Á. (2013). Képszegmentálási eljárások alkalmazása a távérzékelésben. In Papp, G. and Bischof, A., editors, *Geomatikai Közlemények (Publications in Geomatics)*, volume XVI, pages 83–88, Sopron. MTA CSFK Geodéziai és Geofizikai Intézete.
- Benz, U. C., Hofmann, P., Willhauck, G., Lingenfelder, I., and Heynen, M. (2004). Multi-resolution, object-oriented fuzzy analysis of remote sensing data for GIS-ready information. *ISPRS Journal of Photogrammetry and Remote Sensing*, 58(3-4):239–258.
- Berberoglu, S., Curran, P., Lloyd, C., and Atkinson, P. (2007). Texture classification of Mediterranean land cover. *International Journal of Applied Earth Observation and Geoinformation*, 9(3):322–334.
- Bindel, M., Hese, S., Berger, C., and Schmallius, C. (2011). Feature selection from high resolution remote sensing data for biotope mapping. In Heipke, C., Jacobsen, K., Rotensteiner, F., Müller, S., and Sörgel, U., editors, *High-Resolution Earth Imaging for Geospatial Information*, ISPRS Archives.

- Blaschke, T. (2010). Object based image analysis for remote sensing. *ISPRS Journal of Photogrammetry and Remote Sensing*, 65(1):2–16.
- Blaschke, T., Johansen, K., and Tiede, D. (2011). Object-based image analysis for vegetation mapping and monitoring. In Weng, Q., editor, *Advances in Environmental Remote Sensing: Sensors, Algorithms and Applications*, pages 241–271. CRC Press Taylor & Francis Group, United States.
- Bock, M., Panteleimon Xofis, Jonathan Mitchley, Rossner, G., and Wissen, M. (2005). Object-oriented methods for habitat mapping at multiple scales – case studies from Northern Germany and Wye Downs, UK. *Journal for Nature Conservation*, 13(2–3):75–89.
- Böloni, J., Molnár, Z., Illyés, E., and Kun, A. (2008). Térképezési célú, növényzeti alapú élőhelyosztályozás magyarországon (az Á-NÉR 2003 és 2007 rendszer). *Tájökológiai Lapok*, 6(3).
- Breiman, L. F. J., Olshen, R., and Stone, C. (1984). *Classification and Regression Trees*. Wadsworth Int., Belmont and CA.
- Bucha, T. and Slávik, M. (2013). Improved methods of classification of multispectral aerial photographs: evaluation of floodplain forests in the inundation area of the Danube. *Folia Forestalia Polonica, Seria A - Forestry*, 55(2).
- Burnett, C. and Blaschke, T. (2003). A multi-scale segmentation/object relationship modelling methodology for landscape analysis. *Ecological Modelling*, 168(3):233–249.
- Carleer, A. P. and Wolff, E. (2006). Urban land cover multi-level region-based classification of VHR data by selecting relevant features. *International Journal of Remote Sensing*, 27(6):1035–1051.
- Carr, J. R. and Miranda, F. P. d. (1998). The semivariogram in comparison to the co-occurrence matrix for classification of image texture. *Geoscience and Remote Sensing, IEEE Transactions on*, 36(6):1945–1952.
- Chubey, M. S., Franklin, S. E., and Wulder, M. A. (2006). Object-based analysis of Ikonos-2 imagery for extraction of forest inventory parameters. *Photogrammetric Engineering & Remote Sensing*, 72(4):383–394.

- Cleve, C., Kelly, M., Kearns, F. R., and Moritz, M. (2008). Classification of the wildland–urban interface: A comparison of pixel- and object-based classifications using high-resolution aerial photography. *Computers, Environment and Urban Systems*, 32(4):317–326.
- Cohen, J. (1960). A coefficient for agreement for nominal scales. *Educ. Psychol. Meas.*, 20:37–46.
- Congalton, R. G. (2004). Putting the map back in map accuracy assessment. In Lunetta, R. and Lyon, J., editors, *Remote sensing and GIS accuracy assessment*, pages 1–11. CRC Press.
- Congalton, R. G. and Green, K. (2009). *Assessing the Accuracy of Remotely Sensed Data: Principles and Practices*. CRC Press Taylor & Francis Group, USA and Broken Sound Parkway NW, second edition.
- Curran, P. J. (1988). The semivariogram in remote sensing: An introduction. *Remote Sensing of Environment*, 24(3):493–507.
- Davidson, N. and Finlayson, C. (2007). Earth observation for wetland inventory, assessment and monitoring. *Aquatic Conservation: Marine and Freshwater Ecosystems*, 17(3):219–228.
- Davis, P., Staid, M., Plesca, J., and Johnson, J. (2002). Evaluation of airborne image data for mapping riparian vegetation within the Grand Canyon: Report-02-470.
- Demir, B., Bovolo, F., and Bruzzone, L. (2013). Updating land-cover maps by classification of image time series: A novel change-detection-driven transfer learning approach. *IEEE Transactions on Geoscience and Remote Sensing*, 51(1):300–312.
- Dezső, B., Fekete, I., Gera, D., Giachetta, R., and László, I. (2012). Object-based image analysis in remote sensing applications using various segmentation techniques. *Annales Univ. Sci. Budapest., Sect. Comp.*, 37:103–120.
- Environmental Laboratory (1987). Corps of engineers wetlands delineation manual: Wetlands research program technical report.
- ERTI (2008). Összefoglaló a 2008-as monitoring év eredményeiről: Készült a magyar-szlovák közös jelentés anyagához.

- European Commission (2011). Our life insurance, our natural capital: an EU biodiversity strategy to 2020: (244 final).
- Fekete, G., Molnár, Z., and Horváth, F., editors (1997). *A magyarországi élőhelyek leírása, határozója és a nemzeti Élőhely-osztályozási Rendszer*. Magyar Természettudományi Múzeum, Budapest.
- Foody, G. M. (2002). Status of land cover classification accuracy assessment. *Remote Sensing of Environment*, 80:185–201.
- Förster, M. and Kleinschmit, B. (2008). Object-based classification of Quickbird data using ancillary information for the detection of forest types and NATURA 2000 habitats. In Blaschke, T., Lang, S., and Hay, G. J., editors, *Object-Based Image Analysis - Spatial Concepts for Knowledge-Driven Remote Sensing Applications*, Lecture Notes in Geoinformation and Cartography, pages 275–290. Springer-Verlag, Berlin Heidelberg.
- Franklin, S. E., Hall, R. J., Moskal, L. M., Maudie, A. J., and Lavigne, M. B. (2000). Incorporating texture into classification of forest species composition from airborne multispectral images. *International Journal of Remote Sensing*, 21(1):61–79.
- Fukunaga, K. (1990). *Introduction to Statistical Pattern Recognition*. Morgan Kaufmann Academic Press, San Francisco San Diego, second edition.
- Fuller, R. M., Groom, G. B., Mugisha, S., Ipulet, P., Pomeroy, D., Katende, A., Bailey, R., and Ogutu-Ohwayo, R. (1998). The integration of field survey and remote sensing for biodiversity assessment: a case study in the tropical forests and wetlands of Sango Bay, Uganda. *Biological Conservation*, 86(3):379–391.
- Gergel, S. E., Stange, Y., Coops, N. C., Johansen, K., and Kirby, K. R. (2007). What is the value of a good map? An example using high spatial resolution imagery to aid riparian restoration. *Ecosystems*, 10(5):688–702.
- Gitelson, A. A., Kaufman, Y. J., Stark, R., and Rundquist, D. (2002). Novel algorithms for remote estimation of vegetation fraction. *Remote Sensing of Environment*, 80:76–87.
- Green, D. and Hartley, S. (2000). Integrating photointerpretation and GIS for vegetation mapping: Some issues of error. In Millington, A. and Alexander, R., editors, *Vegetation Mapping: from Patch to Planet*, pages 103–134. John Wiley & Sons, Inc., Chichester.

- Guo, B., Damper, R., Gunn, S. R., and Nelson, J. (2008). A fast separability-based feature-selection method for high-dimensional remotely sensed image classification. *Pattern Recognition*, 41(5):1653–1662.
- Hahn, I., Gergely, A., and Barabás, S. (2011). Changes in the active floodplain vegetation of the Szigetköz. *Annali di Botanica*, (1):1–8.
- Hájek, F. (2008). Process-based approach to automated classification of forest structures using medium format digital aerial photos and ancillary GIS information. *European Journal of Forest Research*, 127(2):115–124.
- Hall, R. J. (2003). The roles of aerial photographs in forestry remote sensing image analysis. In Wulder, M. A. and Franklin, S., editors, *Remote Sensing of Forest Environments*, pages 47–75. Springer US.
- Hall-Beyer, M. (2007). The GLCM tutorial home page. <http://fp.ucalgary.ca/mhallbey/tutorial.htm>[Last updated 21 February 2007].
- Haralick, R. M., Shanmugam, K., and Dinstein, I. (1973). Textural features for image classification. *Man and Cybernetics Systems*, 3(6):610–621.
- He, C., Li, Y., Li, X., Shi, P., Pan, Y., and Chen, J. (2004). Zoning grassland protection area by using remote sensing and cellular automata model with a case study in Xilingol typical steppe grassland in northern China. In *Geoscience and Remote Sensing Symposium, 2004. IGARSS '04. Proceedings. 2004 IEEE International*, volume 6, pages 3629–3632 vol.6.
- Heumann, B. W. (2011). An object-based classification of mangroves using a hybrid decision tree—support vector machine approach. *Remote Sensing*, 3(11):2440–2460.
- Ihse, M. (2007). Colour infrared aerial photography as a tool for vegetation mapping and change detection in environmental studies of Nordic ecosystems: A review. *Norsk Geografisk Tidsskrift - Norwegian Journal of Geography*, 61(4):170–191.
- Ijjas, I., Kern, K., and Kovács, G., editors (2010). *Feasibility Study. The Rehabilitation of the Szigetköz Reach of the Danube*.
- Illés, G. and Somogyi, Z. (2005). A szigetközi ártéri erdők egészségi állapotának ortofotókon alapuló elemzése és értékelése. *Tájökológiai Lapok*, 3(2):335–360.

- Illés, G. and Szabados, I. (2008). 20 éves az erdészeti monitoring a Szigetközben. *Erdészeti Kutatások 2007-2008*, 92:95–120.
- Jensen, J., editor (2014). *Remote Sensing of the Environment: An Earth Resource Perspective*. Pearson, second edition.
- Johansen, K., Arroyo, L. A., Phinn, S., and Witte, C. (2010a). Comparison of geo-object based and pixel-based change detection of riparian environments using high spatial resolution multi-spectral imagery. *Photogrammetric Engineering & Remote Sensing*, 76(2):123–136.
- Johansen, K., Bartolo, R., and Phinn, S. (2010b). Special feature – Geographic object-based image analysis. *Journal of Spatial Science*, 55(1):3–7.
- Johansen, K., Coops, N. C., Gergel, S. E., and Stange, Y. (2007). Application of high spatial resolution satellite imagery for riparian and forest ecosystem classification. *Remote Sensing of Environment*, 110(1):29–44.
- Jones, D., Pike, S., Thomas, M., and Murphy, D. (2011). Object-based image analysis for detection of Japanese knotweed s.l. taxa (polygonaceae) in Wales (UK). *Remote Sensing*, 3(12):319–342.
- Kailath, T. (1967). The divergence and Bhattacharyya distance measures in signal selection. *IEEE Transactions on Communication Technology*, 15(1).
- Kamagata, N., Hara, K., Mori, M., Akamatsu, Y., Li, Y., and Hoshino, Y. (2008). Object-based classification of Ikonos data for vegetation mapping in Central Japan. In Blaschke, T., Lang, S., and Hay, G. J., editors, *Object-Based Image Analysis - Spatial Concepts for Knowledge-Driven Remote Sensing Applications*, Lecture Notes in Geoinformation and Cartography, pages 459–475. Springer-Verlag, Berlin Heidelberg.
- Kayitakire, F., Hamel, C., and Defourny, P. (2006). Retrieving forest structure variables based on image texture analysis and Ikonos-2 imagery. *Remote Sensing of Environment*, 102(3-4):390–401.
- Kim, M., Madden, M., and Warner, T. (2009). Forest type mapping using object-specific texture measures from multispectral Ikonos imagery: Segmentation quality and image classification issues. *Photogrammetric Engineering & Remote Sensing*, 75(7):819–829.

- Király, G. and Brolly, G. (2006). Estimating forest stand parameters applying airborne laser scanning and Quickbird images. In Koukal, T. and Schneider, W., editors, *Proceedings of International Workshop on 3D Remote Sensing in Forestry*, pages 79–90, Vienna.
- Király, G. and Brolly, G. (2013). Inventory and monitoring of Danube floodplain forests by innovative remote sensing technology - first results from INMEIN project. In *Catchment processes in regional hydrology: experiments, modeling and predictions in Carpathian drainage basins*.
- Kollár, S. (2010). Az objektum alapú képosztályozás és a vizes élőhelyek kutatása. (The object based image analysis and the research of wetlands.). *Geodesy & Cartography, Hungarian Special Journal*, 62(8):32–37.
- Kollár, S., Vekerdy, Z., and Márkus, B. (2011a). Forest habitat change dynamics in a riparian wetland. *Procedia Environmental Sciences*, 7(0):371–376.
- Kollár, S., Vekerdy, Z., and Márkus, B. (2011b). Hullámtéri élőhelylehatárolás távérzékelési alapon. In Lakatos, F., Polgár, A., and Kerényi-Nagy, V., editors, *Tudományos Doktorandusz Konferencia*, pages 119–123. Nyugat-magyarországi Egyetem, Erdőmérnöki Kar, Sopron.
- Kollár, S., Vekerdy, Z., and Márkus, B. (2013a). Aerial image classification for the mapping of riparian vegetation habitats. *Acta Silv. Lign. Hung.*, 9:119–133.
- Kollár, S., Vekerdy, Z., and Márkus, B. (2013b). Geostatistical characterization of wetland habitats. In Neményi, M., Varga, L., Facskó, F., and Lőrincz, I., editors, *Science for Sustainability*, pages 106–111, Sopron. University of West Hungary Press.
- Kollár, S., Vekerdy, Z., and Márkus, B. (2013c). The role of geostatistical measures in the classification of riparian vegetation - case study about a Hungarian floodplain. In Thinh, N. X., editor, *Modellierung und Simulation von Ökosystemen*, pages 227–236., Aachen. Shaker Verlag.
- Kristóf, D. (2005). *Távérzékelési módszerek a környezetgazdálkodásban*. PhD thesis, University of Szent István, Gödöllő.
- Laliberte, A., Browning, D., and Rango, A. (2012). A comparison of three feature selection methods for object-based classification of sub-decimeter resolution UltraCam-L imagery. *International Journal of Applied Earth Observation and Geoinformation*, 15:70–78.

- Laliberte, A., Fredrickson, E. L., and Rango, A. (2007). Combining decision trees with hierarchical object-oriented image analysis for mapping arid rangelands. *Photogrammetric Engineering & Remote Sensing*, 73(2):197–207.
- Laliberte, A. and Rango, A. (2009). Texture and scale in object-based analysis of subdecimeter resolution unmanned aerial vehicle (UAV) imagery. *IEEE Transactions on Geoscience and Remote Sensing*, 47(3):761–770.
- Landres, P. B., Morgan, P., and Swanson, F. J. (1999). Overview of the use of natural variability concepts in managing ecological systems. *Ecological Applications*, 9(4):1179–1188.
- Lang, S., Albrecht, F., and Blaschke, T. (2006). *Introduction to Object-based Image Analysis: OBIA-Tutorial V 1.0: 1-96*. Salzburg.
- Lang, S., Corbane, C., and Pernkopf, L. (2013). Earth observation for habitat and biodiversity monitoring. In Jekel, T., Car, A., Strobl, J., and Griesebner, G., editors, *GI Forum 2013. Creating the GISociety*, pages 478–486, Berlin/Offenbach. Herbert Wichmann Verlag.
- Langanke, T., Burnett, C., and Lang, S. (2007). Assessing the mire conservation status of a raised bog site in Salzburg using object-based monitoring and structural analysis. *Landscape and Urban Planning*, 79(2):160–169.
- Lefsky, M. and Cohen, W. (2003). Selection of remotely sensed data. In Wulder, M. A. and Franklin, S., editors, *Remote Sensing of Forest Environments*, pages 13–46. Springer US.
- Lévesque, J. and King, D. J. (2003). Spatial analysis of radiometric fractions from high-resolution multispectral imagery for modelling individual tree crown and forest canopy structure and health. *Remote Sensing of Environment*, 84(4):589–602.
- Levick, S. R. and Rogers, K. H. (2008). Structural biodiversity monitoring in savanna ecosystems: Integrating lidar and high resolution imagery through object-based image analysis. In Blaschke, T., Lang, S., and Hay, G. J., editors, *Object-Based Image Analysis - Spatial Concepts for Knowledge-Driven Remote Sensing Applications*, Lecture Notes in Geoinformation and Cartography, pages 477–491. Springer-Verlag, Berlin Heidelberg.
- Licskó, B. (2002). A Szigetköz digitális felszínborítás térképeinek elkészítése légi felvételek kiértékelésével. *Térinformatika*, (3):13–15.

- Lillesand, T., Kiefer, R., and Chipman, J. (2008). *Remote Sensing and Image Interpretation*. John Wiley & Sons, Inc., United States, 6th edition.
- Liu, Y., Li, M., Mao, L., Xu, F., and Huang, S. (2006). Review of remotely sensed imagery classification patterns based on object-oriented image analysis. *Chinese Geographical Science*, 16(3):282–288.
- Lu, D. and Weng, Q. (2007). A survey of image classification methods and techniques for improving classification performance. *International Journal of Remote Sensing*, 28(5):823–870.
- Lymburner, L. (2005). *Mapping Riparian Vegetation Functions Using Remote Sensing and Terrain Analysis*. PhD thesis, University of Melbourne.
- Mahmoud, A., Elbially, S., Pradhan, B., and Buchroithner, M. (2011). Field-based landcover classification using TerraSAR-X texture analysis. *Advances in Space Research*, 48(5):799–805.
- Mallinis, G., Koutsias, N., Tsakiri-Strati, M., and Karteris, M. (2008). Object-based classification using Quickbird imagery for delineating forest vegetation polygons in a Mediterranean test site. *ISPRS Journal of Photogrammetry and Remote Sensing*, 63(2):237–250.
- Maltby, E. and Barker, T., editors (2009). *The Wetlands Handbook: Section I: Wetlands in the Global Environment*. Blackwell Publishing Ltd.
- Márkus, I., Bácsatyai, L., Bartha, D., Konkolyiné Gyuró, É., Király, G., and Czimmer, K. (1999). *Development of GIS of Fertő-Hanság National Park and Szigetköz Land Protection District. Final Report. Trilaterális Phare CBC Ausztria-Magyarország Szlovákia 1995 Program*.
- Mathieu, R., Aryal, J., and Chong, A. (2007). Object-based classification of ikonos imagery for mapping large-scale vegetation communities in urban areas. *Sensors*, 7:2860–2880.
- MEA, editor (2005). *Ecosystems and Human Well-being: Wetlands and Water: Synthesis: Millennium Ecosystem Assessment*. World Resources Institute, Washington and DC.
- Mendenhall, C. D., Daily, G. C., and Ehrlich, P. R. (2012). Improving estimates of biodiversity loss. *Biological Conservation*, 151(1):32–34.

- Meyer, G. E. and Camargo Neto, J. (2008). Verification of color vegetation indices for automated crop imaging applications. *Computers and Electronics in Agriculture*, 63(2):282–293.
- Millington, A. and Alexander, R. (2000). Vegetation mapping in the last decades of the twentieth century. In Millington, A. and Alexander, R., editors, *Vegetation Mapping: from Patch to Planet*, pages 321–331. John Wiley & Sons, Inc., Chichester.
- Morgan, J. L., Gergel, S. E., and Coops, N. C. (2010). Aerial photography: A rapidly evolving tool for ecological management. *BioScience*, 60(1):47–59.
- Nichol, J. E. and Sarker, M. L. (2011). Improved biomass estimation using the texture parameters of two high-resolution optical sensors. *IEEE Transactions on Geoscience and Remote Sensing*, 49(3):930–948.
- Nussbaum, S., Niemeyer, I., and Canty, M. J. (2006). SEATH—a new tool for automated feature extraction in the context of object-based image analysis. In Lang, S., Blaschke, T., and Schöpfer, E., editors, *Bridging Remote Sensing and GIS 1st International Conference on Object-based Image Analysis*.
- Ozdemir, I. and Karnieli, A. (2011). Predicting forest structural parameters using the image texture derived from WorldView-2 multispectral imagery in a dryland forest, Israel. *International Journal of Applied Earth Observation and Geoinformation*, 13(5):701–710.
- Ozesmi, S. L. and Bauer, M. E. (2002). Satellite remote sensing of wetlands. *Wetlands Ecology and Management*, 10:381–402.
- Peng, H. (2005). Feature selection based on mutual information: Criteria of max-dependency, max-relevance, and min-redundancy. *IEEE Transactions on Pattern Analysis and Machine Intelligence*, 27(8):1226–1238.
- Pereira, R. R., Azevedo Marques, P. M., Honda, M. O., Kinoshita, S. K., Engelmann, R., Muramatsu, C., and Doi, K. (2007). Usefulness of texture analysis for computerized classification of breast lesions on mammograms. *Journal of Digital Imaging*, 20(3):248–255.
- Petersen, S., Stringham, T., and Laliberte, A. (2005). Classification of willow species using large-scale aerial photography. *Rangeland Ecology & Management*, 58((6)):582–587.

- Rapp, J., Wang, D., Capen, D., Thompson, E., and Lautzenheiser, T. (2005). Evaluating error in using the national vegetation classification system for ecological community mapping in Northern New England, USA. *Natural Areas Journal*, 25(1).
- Richards, J. A. and Jia, X., editors (2006). *Remote Sensing Digital Image Analysis: An Introduction*. Springer-Verlag, Heidelberg, 4th edition.
- Rokach, L. and Maimon, O. (2005). Decision trees. In Maimon, O. and Rokach, L., editors, *Data Mining and Knowledge Discovery Handbook*, pages 165–192. Springer US.
- Rouse, J., Haas, R., Schell, J., and Deering, D. (1973). Monitoring vegetation systems in the great plains with ERTS. In Fraden, S., Marcanti, E., and Becker, M., editors, *Third ERTS-1 Symposium*, pages 309–317, Washington D.C.
- Running, S., Loveland, T., Pierce, L., Nemani, R., and Hunt, E. (1995). A remote sensing based vegetation classification logic for global land cover analysis. *Remote Sensing of Environment*, 51:39–48.
- Safavian, S. and Landgrebe, D. (1991). A survey of decision tree classifier methodology. *IEEE Transactions on Systems, Man and Cybernetics*, 21(3):660–674.
- Schöpfer, E., Lang, S., and Blaschke, T. (2005). A green index incorporating remote sensing and citizens perception of green space. In Moeller, M. and Wentz, E., editors, *ISPRS Archives 2005*, volume XXXVI-8/W27.
- Sha, Z., Bai, Y., Xie, Y., Yu, M., and Zhang, L. (2008). Using a hybrid fuzzy classifier (HFC) to map typical grassland vegetation in Xilin River Basin, Inner Mongolia, China. *International Journal of Remote Sensing*, 29(8):2317–2337.
- Silva, C., Marcal, A., Pereira, M., and Mendonça, T. (2012). Separability analysis of color classes on dermoscopic images. In Campilho, A. and Kamel, M., editors, *ICIAR 2012: LNCS 7325*, pages 268–277. Springer-Verlag, Berlin and Heidelberg.
- Simon, T., Szabó, M., Draskovits, R., Hahn, I., and Gergely, A. (1993). Ecological and phytosociological changes in the willow woods of Szigetköz, NW Hungary, in the past 60 years. *Abstracta Botanica*, 17(1-2):179–186.
- Smith, S., Büttner, G., Szilagyi, F., Horvath, L., and Aufmuth, J. (2000). Environmental impacts of river diversion: Gabčíkovo barrage system. *Journal of Water Resources Planning and Management*, 126(3):138–145.

- Szabó, M. (2005). *Vizes élőhelyek tájökológiai jellemvonásai a Szigetköz példáján*. PhD thesis, ELTE, Budapest.
- Szantoi, Z., Escobedo, F., Abd-Elrahman, A., Smith, S., and Pearlstine, L. (2013). Analyzing fine-scale wetland composition using high resolution imagery and texture features. *International Journal of Applied Earth Observation and Geoinformation*, 23(0):204–212.
- Takács, G. and Keszei, B. (2004). *Felső-Szigetköz élőhely-térképezése: T5x5_065*. Sarród, Hungary.
- Takács, G. and Molnár, Z., editors (2009). *National Biodiversity Monitoring System XI. Habitat mapping*. Hungarian Academy of Sciences, Institute of Ecology and Botany and Ministry of Environment and Water, Vácrátót and Budapest, 2nd modified edition.
- Tempfli, K., Kerle, N., Janssen, L. L. F., and Huurneman, G. C., editors (2008). *Principles of Remote Sensing: An introductory textbook*, volume 2 of *ITC Educational Textbook Series*. ITC, Enschede, The Netherlands, fourth edition.
- Thomas, V., Treitz, P., Jelinski, D., Miller, J., Laffleur, P., and McCaughey, J. (2002). Image classification of a northern peatland complex using spectral and plant community data. *Remote Sensing of Environment*, 84:83–99.
- Tobler, W. (1970). A computer movie simulating urban growth in the detroit region. *Economic Geography*, 46(2):234–240.
- Török, K., Kisé Fodor, L., and Vácsi, O. (2007). Nemzeti biodiverzitás-monitorozó rendszer: Bevezető, történet, eredmények.
- Treitz, P. and Howarth, P. (2000). High spatial resolution remote sensing data for forest ecosystem classification: An examination of spatial scale. *Remote Sensing of Environment*, 72(3):268–289.
- Trimble, editor (2013). *eCognition Developer: Reference Book*. Trimble Germany GmbH.
- Tsai, F. and Chou, M.-J. (2006). Texture augmented analysis of high resolution satellite imagery in detecting invasive plant species. *Journal of the Chinese Institute of Engineers*, 29(4):581–592.
- Tuominen, S. and Pekkarinen, A. (2005). Performance of different spectral and textural aerial photograph features in multi-source forest inventory. *Remote Sensing of Environment*, 94(2):256–268.

- Vekerdy, Z. and Meijerink, A. (1998). Statistical and analytical study of the propagation of flood-induced groundwater rise in an alluvial aquifer. *Journal of Hydrology*, 205(1):112–125.
- Wezyk, P., Kok, R. d., and Zajaczkowski, G. (2004). The role of statistical and structural texture analysis in VHR image analysis for forest applications - A case study on Quickbird data in Niepolomice Forest. In Strobl, J., Blaschke, T., and Griesebner, G., editors, *Angewandte Geoinformatik*, pages 770–775, Heidelberg. Wichmann Verlag.
- Wood, E. M., Pidgeon, A. M., Radeloff, V. C., and Keuler, N. S. (2012). Image texture as a remotely sensed measure of vegetation structure. *Remote Sensing of Environment*, 121:516–526.
- Wulder, M., Hall, R. J., Coops, N. C., and Franklin, S. E. (2004). High spatial resolution remotely sensed data for ecosystem characterization. *BioScience*, 54(6):511–521.
- Wyatt, B. (2000). Vegetation mapping from ground, air and space - competitive or complementary techniques? In Millington, A. and Alexander, R., editors, *Vegetation Mapping: from Patch to Planet*, pages 3–18. John Wiley & Sons, Inc., Chichester.
- Xiao, X., Zhang, Q., Braswell, B., Urbanski, S., Boles, S., Wofsy, S., Moore, B., and Ojima, D. (2004). Modeling gross primary production of temperate deciduous broadleaf forest using satellite images and climate data. *Remote Sensing of Environment*, 91(2):256–270.
- Xie, Y., Sha, Z., and Yu, M. (2008). Remote sensing imagery in vegetation mapping: a review. *Journal of Plant Ecology*, 1(1):9–23.
- Yan, G., Mas, J. F., Maathuis, B. H. P., Xiangmin, Z., and van Dijk, P. M. (2006). Comparison of pixel-based and object-oriented image classification approaches—a case study in a coal fire area, Wuda, Inner Mongolia, China. *International Journal of Remote Sensing*, 27(18):4039–4055.
- Yu, Q., Gong, P., Clinton, N., Biging, G., Kelly, M., and Schirokauer, D. (2006). Object-based detailed vegetation classification with airborne high spatial resolution remote sensing imagery. *Photogrammetric Engineering & Remote Sensing*, 72(7):799–811.
- Zhang, Z. and Liu, X. (2013). Worldview-2 satellite imagery and airborne lidar data for object-based forest species classification in a cool temperate rainforest environment. In

- Rahman, A., Boguslawski, P., Gold, C., and Said, M., editors, *Developments in Multidimensional Spatial Data Models*, Lecture Notes in Geoinformation and Cartography, pages 103–122. Springer Berlin Heidelberg.
- Zólyomi, B. (1937). A Szigetköz növénytani kutatásának eredményei. (Results of botanical research in the Szigetköz.). *Botanikai Közlemények*, 34:169–192.